



An-Najah National University
Faculty of Graduate Studies

**MODELING AND ASSESSMENT OF INDUSTRIAL
WASTEWATER IMPACTS ON JENIN
INDUSTRIAL FREE ZONE WASTEWATER
TREATMENT PLANT**

By

Osama Harbi Omran

Supervisor

Dr. Abdulhaleem Khader

**This Thesis is Submitted in Partial Fulfillment of the Requirements for the Degree of
Master of Water & Environmental Engineering, Faculty of Graduate Studies, An-Najah
National University, Nablus - Palestine.**

2025

MODELING AND ASSESSMENT OF INDUSTRIAL WASTEWATER IMPACTS ON JENIN INDUSTRIAL FREE ZONE WASTEWATER TREATMENT PLANT

By

Osama Harbi Omran

This Thesis was Defended Successfully on 20/07/2025 and approved by

Dr. Abdulhaleem Khader

Supervisor

Dr. Subhi Samhan

External Examiner

Dr. Shadi Sawalha

Internal Examiner



Signature



Signature



Signature

Dedication

To my family, whose unwavering support and encouragement have been my cornerstone throughout this academic journey. To my parents, for their endless love and sacrifices, and to my siblings, for their constant motivation and belief in my aspirations. This work is also dedicated to the people of Palestine, whose resilience and commitment to sustainable development inspire my efforts to contribute to a better environmental future.

Acknowledgements

I express my deepest gratitude to my supervisor, Dr. Abdulhaleem Khader, for his invaluable guidance, expertise, and unwavering encouragement throughout this research journey. His insightful feedback and commitment to academic excellence profoundly shaped this thesis.

I am sincerely thankful to An-Najah National University and the Faculty of Graduate Studies for providing me with the opportunity to pursue this research and for their continuous support.

Special thanks go to the Palestinian Water Authority (PWA) for their valuable support and contributions, which significantly enhanced the quality and impact of this thesis.

Special thanks also go to the Middle East Desalination Research Center (MEDRC) for their sponsorship, which provided essential resources and support, enabling the successful completion of this work.

My appreciation extends to the Palestinian Industrial Estates and Free Zones Authority (PIEFZA) for their cooperation and provision of critical data that formed the foundation of this study.

I am grateful to Hydromantis GPS-X Co. for generously providing a student license, which was instrumental in facilitating my research.

I am deeply indebted to my late uncle, Dr. Mohamad Said, whose mentorship and encouragement from the beginning of my academic journey were pivotal in shaping my path. His memory continues to inspire my work.

I also extend my gratitude to my colleagues and friends for their support, shared ideas, and encouragement during challenging times. Their intellectual discussions and camaraderie greatly enriched my research experience.

Finally, I owe profound thanks to my family for their unconditional love, patience, and understanding. Their unwavering belief in me has been a constant source of strength and motivation.

Declaration

I, the undersigned, declared that I submitted the thesis entitled:

**MODELING AND ASSESSMENT OF INDUSTRIAL WASTEWATER
IMPACTS ON JENIN INDUSTRIAL FREE ZONE WASTEWATER
TREATMENT PLANT**

I declare that the work provided in this thesis, unless otherwise referenced, is the researcher's own work, and has not been submitted elsewhere for any other degree or qualification.

Student's Name: Osama Harbi Omran

Signature: 

Date: 20/7/2025

List of Contents

| | |
|--|-----|
| Dedication | III |
| Acknowledgements | IV |
| Declaration | V |
| List of Contents..... | VI |
| List of Tables | IX |
| List of Figures | X |
| List of Appendices | XI |
| Abstract | XII |
| Chapter One: Introduction and Theoretical Background | 1 |
| 1.1 Background..... | 1 |
| 1.2 Study Area..... | 3 |
| 1.3 Overview of (JIFZ-WWTP)..... | 6 |
| 1.4 Theoretical basis..... | 9 |
| 1.5 Problem statement..... | 9 |
| 1.6 Study hypothesis..... | 9 |
| 1.7 Importance of the Thesis..... | 9 |
| 1.8 Objectives..... | 10 |
| 1.9 Research Questions | 10 |
| 1.10 Literature review | 10 |
| Chapter Two : Methodology..... | 21 |
| 2.1 Data Collection and Analysis..... | 21 |
| 2.2 Modeling and Simulation Using GPS-X Software | 22 |
| 2.3 Data Collection | 23 |
| 2.4 Statistical Analysis Methods | 24 |

| | |
|--|----|
| 2.5 Model Calibration | 25 |
| Chapter Three: Results and Discussions | 36 |
| 3. General..... | 36 |
| 3.1 Probabilistic Design Using Monte Carlo Sensitivity Analysis | 41 |
| 3.2 Optimization of RAS and WAS for JIFZ-WWTP and Its Impact on Effluent Quality | 44 |
| 3.3 Analysis of Effluent Quality During Shock Load Event | 45 |
| 3.4 Breakdown of Key Effluent Parameters and Trends..... | 46 |
| 3.5 Interpretation of Trends and System Performance Impact | 48 |
| 3.6 Potential Causes of Effluent Deterioration..... | 48 |
| 3.7 Key Parameter Trends During the Shock Load | 49 |
| 3.8 Changes in Process Rates | 55 |
| 3.9 Biological Process Performance | 63 |
| 3.10 Other Process Impacts (Settling, Washout, Gas Transfer, Precipitation)..... | 68 |
| 3.11 System Resilience vs. Prolonged Instability | 72 |
| 3.12 Mitigation Strategies to Improve Resilience to Shock Loads..... | 75 |
| 3.13 Long-Term Process and Design Strategies..... | 77 |
| 3.14 Analyses of Final Clarifier Behavior during the shock load | 79 |
| 3.15 Clarifier Performance Failure & State Point Analysis | 81 |
| 3.16 Possible Causes of Clarifier Overloading | 82 |
| 3.17 Consequences of Clarifier Failure | 83 |
| 3.18 Strategies to Prevent Future Clarifier Failure | 83 |
| 3.19 Analysis of WWTP Operational Adjustments During Shock Load | 84 |
| 3.20 Comprehensive Risk Analysis of Non-Pretreated Wastewater | 88 |
| 3.21 Interpretation and System Performance Impact | 90 |
| Chapter Four: Conclusions | 91 |
| List of Abbreviations | 95 |

| | |
|--------------------|-----|
| Nomenclature | 97 |
| References | 99 |
| Appendices | 108 |
| الملخص | ب |

List of Tables

| | |
|--|----|
| Table 1: Key Details of JIFZ Project | 6 |
| Table 2: Pollutant loads and concentrations for the design of JIFZ-WWTP..... | 8 |
| Table 3: Effluent Quality Criteria – design criteria | 8 |
| Table 4: Influent Calibrated Characteristics | 30 |
| Table 5: Calibration of General Parameters | 32 |
| Table 6: Calibrated FSTs Parameters | 32 |
| Table 7: Checking the influent characteristics..... | 33 |
| Table 8: Effluent Simulation Results..... | 33 |
| Table 9: Removal Efficiency of JIFZ-WWTP..... | 38 |
| Table 10: Process Variables Prior to the Occurrence of the Shock Load..... | 51 |

List of Figures

| | |
|--|----|
| Figure 1 : General map for JIFZ's location..... | 5 |
| Figure 2 : Process Flow Diagram of JIFZ WWTP | 7 |
| Figure 3 : JIFZ Wastewater Treatment Plant 3D View | 8 |
| Figure 4 : Research Methodology..... | 21 |
| Figure 5 : Jericho-WWTP's Model | 29 |
| Figure 6 : Calibrated effluent total suspended solids..... | 34 |
| Figure 7 : Calibrated effluent total nitrogen. | 34 |
| Figure 8 : Calibrated effluent total COD. | 35 |
| Figure 9 : Calibrated effluent total cBOD5. | 35 |
| Figure 10 : Activated Sludge Model (Mulas,2006) | 13 |

List of Appendices

| | |
|--|-----|
| Appendix A: Jericho WWTP Lab Tests | 108 |
| Appendix B: Industrial WW Allowed Concentrations | 110 |
| Appendix C: Palestinian Specifications for reused treated WW | 111 |
| Appendix D: Conventional characterization of different industrial wastewaters | 113 |
| Appendix E: Aeration Tank Mantis 2 Rates Before the Shock Load | 114 |
| Appendix F: Aeration Tank Mantis 2 Rates During the Shock Load | 122 |
| Appendix G: JIFZ-WWTP's Influent Concentration | 130 |
| Appendix H: JIFZ-WWTP's Effluent Concentration | 131 |
| Appendix I: Diagram of the simulation model used during the research. | 132 |
| Appendix J: Effluent total COD, BoD, TSS and TN Vs. Influent Flow | 133 |
| Appendix K: Optimizing the RAS Vs. Effluent pollutants | 135 |
| Appendix L: Monte Carlo probability Distribution of Effluent pollutants | 136 |
| Appendix M: Optimized RAS and WAS Vs. Effluent pollutants | 138 |
| Appendix N: Effluent Concentrations during the Shock Load Scenario | 140 |
| Appendix O: Time-Series Simulation of Biological Processes in an Extended Aeration Wastewater Treatment Plant | 141 |
| Appendix P: Mechanistic Clarifier Model - The 1-D Flux Model | 142 |
| Appendix Q: Final Sedimentation Tank Solids Prior to and during the Shock Load... | 143 |
| Appendix R: FST State Point Analysis prior to and during the Shock Load | 144 |
| Appendix S: Effluent Concentration | 145 |
| Appendix T: Effluent Concentration Analysis and WWTP's Recovery Scheme During the Shock load | 146 |
| Appendix U: Effluent Concentration Analysis and WWTP's Recovery Scheme During the Shock after removing the Energy Drink Process | 148 |
| Appendix V: Changes in Key Variables (Before vs. During Shock Load) | 149 |
| Appendix W: FST Variables Prior to the Occurrence of the Shock Load | 150 |
| Appendix X: Recommended Pre-treatment Processes for Various Industries | 152 |
| Appendix Y: JIFZ-WWTP designed process | 153 |
| Appendix Z: Types of Clarifiers in GPS-X | 160 |

**MODELING AND ASSESSMENT OF INDUSTRIAL WASTEWATER
IMPACTS ON JENIN INDUSTRIAL FREE ZONE WASTEWATER
TREATMENT PLANT**

**By
Osama Harbi Omran
Supervisor
Dr. Abdulhaleem Khader**

Abstract

The Jenin Industrial Free Zone Wastewater Treatment Plant (JIFZ-WWTP), designed for domestic wastewater, faces challenges from unregulated industrial effluents, impacting its biological treatment and effluent quality. This study evaluates the plant's performance using a dynamic simulation model in GPS-X software (version 8.5) with the ASM1-based MANTIS framework. Calibrated with 2024 data from the Jericho WWTP, the model accounts for local temperature, elevation, and influent characteristics to reflect microbial behavior and oxygen dynamics in Jenin.

Simulations tested normal operations, high-load scenarios, and a shock event with 1,000 m³ of untreated industrial wastewater. Under optimal conditions, the JIFZ-WWTP achieved high pollutant removal: TSS (95.18%), VSS (93.62%), COD (89.5%), cBOD₅ (94.32%), PO₄³⁻ (99.88%), and TP (66.45%), limited by particulate phosphorus. TN removal was lower (33.8%) due to insufficient anoxic conditions and carbon availability. Suggested improvements include adding an anoxic reactor, external carbon dosing (e.g., methanol), and optimizing solids retention time.

The plant maintained reusable WW Class C effluent quality at influent flows up to 1000 m³/day of industrial wastewater by regulating return activated sludge (RAS) at 460 m³/day and waste activated sludge (WAS) at 60 m³/day, ensuring stability under peak loads. Monte Carlo simulations showed 68% of scenarios met nitrogen targets, 33% met cBOD₅ and COD standards, and 87% achieved TSS compliance, highlighting sensitivity to industrial discharge variations.

A shock-load scenario revealed vulnerabilities, with effluent concentrations of COD (8,000 mg/L), BOD₅ (3,500 mg/L), TP (63 mg/L), TKN (37 mg/L), and TSS (510 mg/L) exceeding Palestinian limits. Biomass activity declined, nitrification stopped, and

solids accumulated, with gradual recovery post-event. The study recommends stringent pretreatment (screening, pH correction, equalization, dissolved air flotation, anaerobic digestion, coagulation, flocculation, precipitation, filtration) and real-time influent monitoring. Operational strategies like increased WAS and chemical dosing during peak loads are vital. The JIFZ-WWTP supports sustainable water management in Jenin by enabling treated wastewater reuse for irrigation. Also, Israel's 100 million ILS annual deduction from Palestinian tax revenues because of the non-treated WW.

Keywords: Jenin Industrial Free Zone (JIFZ), Industrial Wastewater, GPS-X Simulation Software, Monte Carlo Sensitivity Analysis, Heterotrophic Biomass.

Chapter One

Introduction and Theoretical Background

1.1 Background

The Earth's water is in constant motion, driven by the hydrologic cycle, a natural process that governs the ongoing flow of water across, above, and beneath the planet's surface. Water continuously transitions between its forms: liquid, vapor, and ice as part of this dynamic cycle (1).

The primary goal of wastewater treatment has traditionally been to ensure safe disposal, protecting public health and avoiding pollution of water bodies or other environmental troubles. Additionally, there is a growing focus on recovering valuable resources from wastewater, such as energy, nutrients, water, and other reusable materials (2).

Sustainable enhancement of wastewater treatment is a widely recognized concept. It involves adopting appropriate treatment technologies that balance environmental, economic, and social factors. Environmental considerations include technology's ability to produce high-quality effluent and its energy requirements for operation. Economic factors incorporate the costs of installation, operation, and maintenance. Social aspects focus on community acceptance and the positive impact on the local environment (3).

In developing nations, costly and sophisticated technologies are often impractical, making it essential to select straightforward, cost-effective solutions that still deliver adequate effluent quality. This can be undertaken by employing a single treatment process or a combination of suitable processes tailored to specific needs (4).

Industrial activities are increasingly contributing to water pollution, posing significant environmental challenges, especially when industrial wastewater is discharged into municipal wastewater treatment plants (WWTPs). These effluents often contain high levels of organic and inorganic pollution, heavy metals, and toxic compounds, which can disrupt biological treatment processes, such as extended aeration systems (5).

In developing countries, the high cost of treating industrial wastewater often leads municipal wastewater treatment plants to process a combination of municipal sewage

and partially treated industrial effluents. This mixture increases the likelihood of shock loads with elevated pollutant concentrations (6).

Over 90% of municipal wastewater treatment plants (WWTPs) rely on Activated Sludge Systems (ASS) as a central element of their treatment processes, establishing these systems as a critical method for treating diverse types of wastewater (7).

The extended aeration system, an adaptation of the traditional activated sludge process, is commonly employed for its capacity to manage varying loads, enhance the biological breakdown of organic material, and generate low amounts of sludge (8).

However, the introduction of industrial wastewater into extended aeration WWTPs poses several operational challenges. Toxic compounds may inhibit microbial activity, leading to reduced treatment efficiency, fluctuations in pH, increased sludge production, and issues such as sludge bulking and foaming (9).

These challenges can result in deteriorating effluent quality, higher operational costs, and potential environmental risks if the treated wastewater does not meet discharge regulations (10).

Typically, wastewater treatment plants (WWTPs) are engineered to handle domestic wastewater. However, in Industrial Parks, industrial wastewater (IWW) differs significantly from sewage due to its distinct discharge patterns and chemical compositions. Despite these differences, many industrial wastewater treatment facilities, like sewage treatment plants, incorporate biological processes as essential components of their treatment sequence. Due to the diverse nature of wastewater characteristics, designing biological processes and their associated upstream and downstream unit processes effectively poses a significant challenge (5). To solve this problem, factories perform pre-treatment to deliver wastewater of similar quality to the domestic WW. However, this process poses a great danger if the factories do not adhere to the pre-treatment process required by them, or if there is a defect in the pre-treatment unit, which may lead to a defect in the central WWTP.

In this research, the influent of the industrial Estate will be modeled, and the expected factories and their pre-treatment processes will be linked with the central WWTP, studying the scenarios of any defect that occurs in the process which may lead to

complete failure in the operation. Thus, the study will suggest proper monitoring, warning, and controlling system to the factories' effects to avoid the expected risks and mitigate their effects on central WWTP, as well, as the future studies in this context will be recommended.

1.2 Study Area

The establishment of the Jenin Industrial Free Zone (JIFZ) represents a strategic initiative aimed at advancing the broader socioeconomic development of Palestine, with particular emphasis on the Jenin Governorate. Located in the northern region of the West Bank, JIFZ occupies a key geographic position along the Haifa–Amman corridor, thereby offering considerable logistical advantages. These include proximity to northern urban centers, access to regional transportation networks, and the availability of a skilled and motivated Palestinian workforce. The zone also presents attractive opportunities for both domestic and foreign investors, particularly in the agro-industrial and light manufacturing sectors.

The industrial development at JIFZ is designed to accommodate technologically advanced agro-food production facilities alongside light industrial operations. To support this vision, a comprehensive infrastructure package has been planned, encompassing: External and internal road networks, Potable water supply and storage systems, An activated sludge wastewater treatment facility employing extended aeration technology, Electrical infrastructure including 35 MW power transformers and a natural gas distribution network, A solid waste management system, Security and administrative structures, Logistical zones including healthcare units and parking facilities.

With technical and financial assistance from the German government, the Palestinian Industrial Estates and Free Zones Authority (PIEFZA) is overseeing the development of this 90-hectare industrial zone. The project places a strong emphasis on environmental protection and aims to integrate sustainable environmental management practices throughout its operational lifecycle. Given the scale and nature of the planned industrial activities, a comprehensive environmental and social assessment is essential to anticipate and address the potential impacts both positive and adverse that may arise (74).

A central component of the zone's infrastructure is the JIFZ Wastewater Treatment Plant (JIFZ-WWTP), which is among the largest facilities of its kind in Palestine. The treatment plant is based on extended aeration activated sludge technology and was originally designed for the treatment of municipal (domestic) wastewater. However, it is intended to serve the industrial park and must therefore accommodate wastewater characteristics that differ significantly from its original design specifications. This necessitates a detailed evaluation of the plant's treatment performance under industrial loading conditions and the development of strategies to ensure continued compliance with environmental standards (74).

This initiative represents a practical application of treated wastewater (TWW) reuse for agricultural irrigation. The potential benefits of this approach are particularly significant in the Jenin governorate, an area characterized by its expansive plains, most notably the Marj Ibn Amer plain, which is recognized as one of the most fertile agricultural zones within the West Bank. Jenin also holds the distinction of being the largest agricultural region in the area, contributing approximately 16.2% to Palestine's total agricultural output (11).

If the wastewater treatment plant (WWTP) is operated and maintained in accordance with design specifications and that all precautionary measures are effectively implemented, several positive environmental impacts are anticipated. Chief among these is the mitigation of groundwater contamination risks through the controlled treatment of wastewater prior to discharge. In addition, the treated effluent may contribute positively to the natural recharge of the underlying aquifer system, thereby enhancing local water sustainability. Moreover, the availability of adequately treated wastewater supports the potential for safe reuse in agricultural irrigation, aligning with water resource conservation strategies.

Nonetheless, certain adverse impacts may arise, particularly from the handling and storage of treatment chemicals and from noise emissions associated with the plant's operational activities. Of greater concern, however, is the risk posed by inadequate operation, maintenance, or oversight of industrial effluent pre-treatment processes. Failure in these areas could lead to the uncontrolled release or overflow of untreated or partially treated industrial discharges, many of which may contain hazardous

substances. Such events could pose significant threats to surface and groundwater quality, as well as broader ecological and public health systems.

Moreover, JIFZ-WWTP operates within a complex socioeconomic and political environment that poses both opportunities and challenges for sustainable wastewater management in Palestine. A critical external constraint is the annual deduction of approximately 100 million ILS from the Palestinian Authority's tax revenues by Israel, attributed to the costs of transboundary wastewater treatment (73). In this context, the implementation and proper operation of wastewater treatment plants (WWTPs), coupled with the reuse of treated wastewater, represent a crucial solution for addressing water scarcity and environmental sustainability in the region.

The present study focuses on a 90-hectare area designated as the Study Area, within which the WWTP and associated industrial activities are situated, as delineated in Figure 1 and Table 1.

Figure 1

General map for JIFZ's location

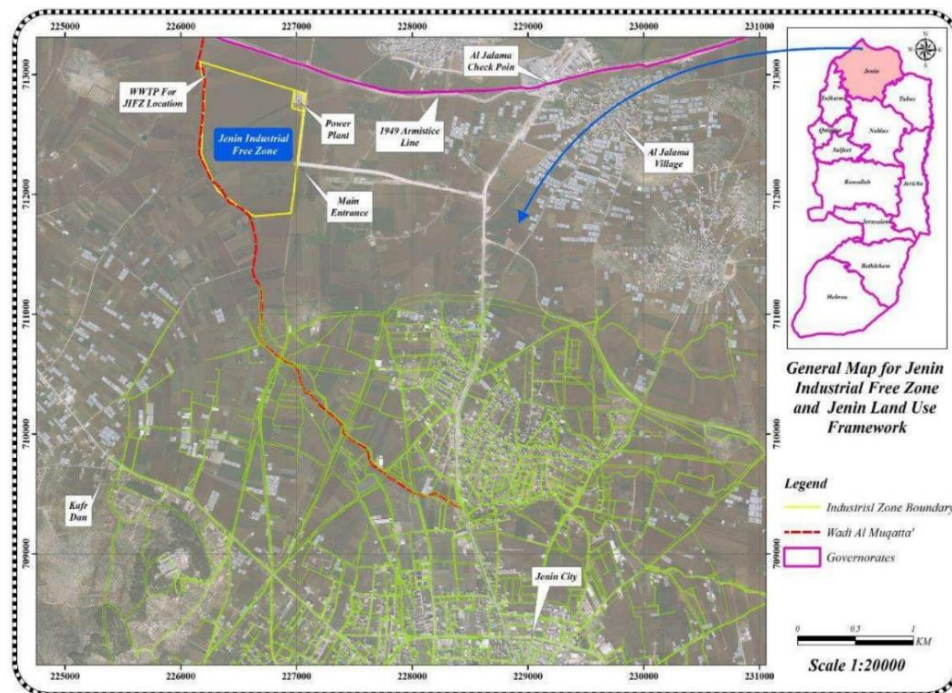


Table 1*Key Details of JIFZ Project*

| Parameter | Details |
|--|---|
| Region | West Bank- Palestine |
| Governorate | Jenin |
| Proposed Project Area (for the three phases) | - 86 hectares for industrial area - 4 hectares for administration/ logistic facilities |
| Near villages and city | - Jalame Village - Jenin City |
| Project Resident Population size | 5,500 (for work not for living purposes) |
| Employment | Direct jobs: 5,000 Indirect jobs: 45,000 |
| Water Demand | 2000 m ³ /d (information received from Palestinian Water Authority (PWA)) |
| Wastewater generated | 1,000 m ³ /day – 2000 m ³ /d |
| Wastewater Treatment Plant (JIFZ-WWTP) | 1000 m ³ /day – 2000 m ³ /d - activated sludge technology |
| Effluent Treatment Plant (ETP) | Individual industries to treat effluent up to domestic waste standards |

1.3 Overview of (JIFZ-WWTP)

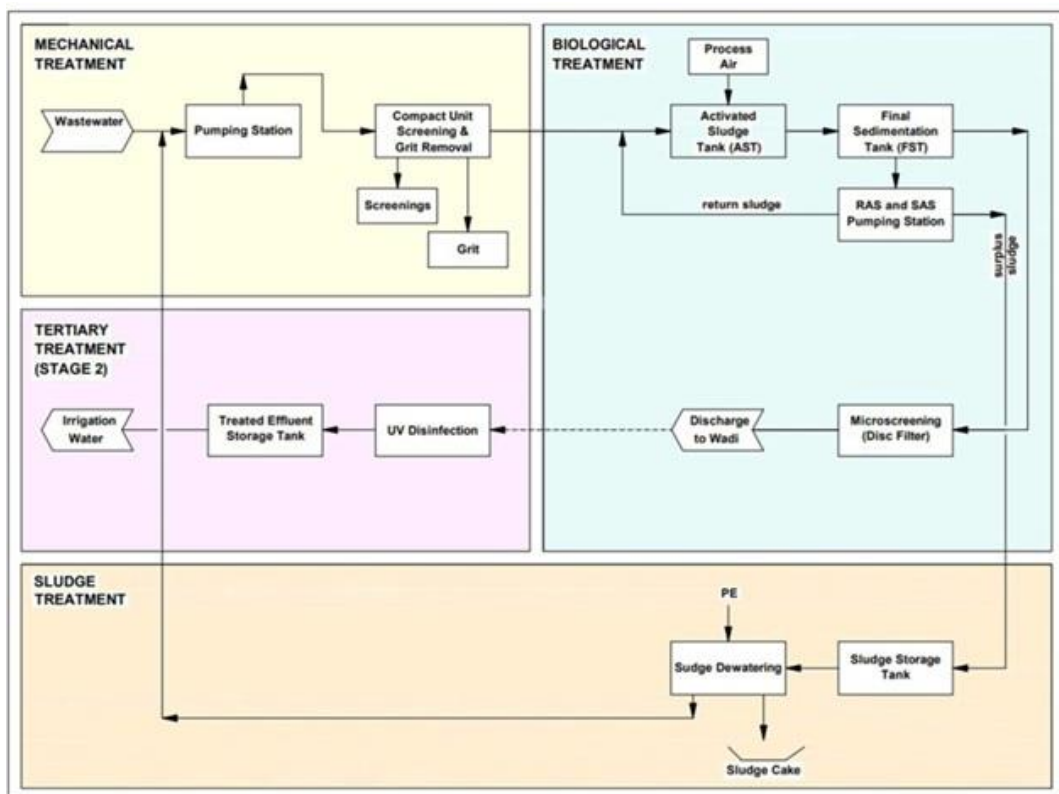
Since the nineties, the Palestinian Industrial Estate and Free Zone Authority (“PIEFZA”) has been responsible for Establishing industrial estates. In the case of Jenin with its favorable geographical position near the Green Line and proximity to Haifa Port and the border with Jordan, the proposed estate has "free zone" status. With signing of the memorandum of understanding, in October 2015 between PIEFZA, TOBB-BIS as the Developer and Operator, and KfW as the funding agency mandated by the German government the financing of the Project was ensured (74).

The Project area is located close to Jenin adjacent to the Green Line border. It covers the infrastructure for an industrial estate on a green-field site of about 890.000 m² together with the necessary off-site infrastructure.

All generated wastewater within the JIFZ will be collected by a sewerage system that will be discharged to a Waste Water Treatment Plant (WWTP). As identified in the Master Plan, the JIFZ-WWTP is located in the North Eastern corner of the JIFZ. The wastewater collection system in the JIFZ is connected to the sewage pumping station, from where the sewage is pumped to the WWTP. The location of the JIFZ WWTP site is at the North-West corner of the JIFZ. The JIFZ-WWTP process is explained in figure (2,3) and annex (Y).

Figure 2

Process Flow Diagram of JIFZ WWTP



Pollutant loads and concentrations for the design of JIFZ WWTP are given in the following tables (2 and 3).

Table 2

Pollutant loads and concentrations for the design of JIFZ-WWTP.

| Parameter | Unit | Stage 1 | Stage 2 |
|------------------|------|---------|---------|
| BOD ₅ | mg/l | 520 | 1040 |
| COD | mg/l | 1.04 | 2.08 |
| TSS | mg/l | 520 | 1040 |
| TKN | mg/l | 64 | 128 |

Table 3

Effluent Quality Criteria – design criteria

| Parameter | Unit | Stage 1 | Stage 2 |
|--|--------|---------|---------|
| Biological Oxygen Demand, BOD ₅ | mg/l | 10 | 10 |
| Total Suspended Solids, TSS | mg/l | 10 | 10 |
| Total-Nitrogen, T-N | mg/l | 10 | 10 |
| Nematodes | eggs/l | - | 1 |

Figure 3

JIFZ Wastewater Treatment Plant 3D View



1.4 Theoretical basis

The research builds principles of wastewater treatment, focusing on its environmental, economic, and social impacts. It emphasizes sustainable wastewater treatment, integrating proper technologies for energy efficiency and cost-effectiveness.

It also addresses the challenges posed by Industrial Wastewater (IWW), which differ significantly from domestic wastewater in composition and treatment needs, requiring pre-treatment by industries to ensure compatibility with wastewater treatment plants (WWTPs).

1.5 Problem statement

Jenin Industrial Free Zone Wastewater Treatment Plant (JIFZ-WWTP) is designed for domestic wastewater, yet it will receive industrial wastewater that may vary in characteristics and volume. Failures in pre-treatment units of factories could overwhelm the plant's capacity, may lead to operational failures, environmental pollution, and public health risks.

1.6 Study hypothesis

- The malfunction or inefficiency of factory pre-treatment units will set back on the operation and performance of JIFZ-WWTP. This can result in system failures or reduced treatment efficiency.
- Variations in the characteristics and volumes of industrial effluents will increase the likelihood of operational failures in the treatment plant.
- Implementing advanced monitoring and control systems can mitigate risks and enhance the plant's resilience to industrial wastewater challenges.

1.7 Importance of the Thesis

- The importance of this thesis that it will enhance the experience in the field of operating the Industrial Parks and WWTPs in Palestine especially under the expected challenges during the operational phase of JIFZ-WWTP since it has been designed to receive a domestic wastewater while it is dedicated for an industrial park.

- The study will put in our hands a numerical model, respective analysis, and results about the behavior of one of the domestic WWTPs dedicated to an industrial park.
- The findings of this study offer significant value to a wide range of stakeholders, including infrastructure planners, plant operators, environmental regulatory authorities, engineers, academic researchers, and other relevant professionals engaged in the field.
- Enhance the sustainability of domestic wastewater management systems.

1.8 Objectives

- To study the potential impact of industrial wastewater on JIFZ-Wastewater Treatment Plant in case of malfunction of the factory's pre-treatment units.
- To develop and confirm a framework for the permissible industrial pollution load at Domestic WWTPs. And propose enhancements to increase WWTP resilience.

1.9 Research Questions

- What is the maximum industrial pollution load that a domestic WWTP can manage without compromising operational efficiency?
- How do variations in effluent composition and environmental conditions (e.g., temperature, rainfall) impact WWTP performance?
- What adjustments in operational parameters are needed to optimize the integration of industrial effluents?

1.10 Literature review

A model serves as a representational framework designed to capture and simulate aspects of real-world phenomena, enabling both comprehension and forecasting of specific conditions or behaviors (12).

One thing to keep in mind while creating a model is that it is just a simplifying of reality and that no ideal model has ever been created.

A simulation model may be mathematical, conceptual, physical, or a mix of these.

The process of project resizing (smaller or bigger) is known as physical modeling. Typically, the important factors and the geometry scale. Bench and pilot scale procedures are also included (13).

Understanding the cause-and-effect links between the different parts of the system that may be expressed both qualitatively and quantitatively is represented by conceptual models (14).

A system's effectiveness performance, technical characteristics, and cost can often be quantitatively described using mathematical models (14).

Typically, a few requirements must be met for any model to be considered helpful. The following areas are related to these criteria:

- Model validation, which comprises three steps, is the appearance of a correlation between the outcome and the actual system. (15).
- Replicative: the model can replicate the system's input/output behavior.
- Predictive: a unique forecast of future behavior may be made by synchronizing the model with the system into a state.
- Structural: it can be demonstrated that the model accurately depicts the system's internal (structural) operations.
- Model verification: the model's state variables must, in some manner, be like quantifiable circumstances of the actual process, either directly or indirectly. This suggests a relationship between a model's complexity and the quantity of accurate data from the physical process. (16).

Modeling wastewater treatment plants is a helpful technique for evaluating plant capacity and enhancing plant operations, which lowers energy and chemical expenses (17).

Three steps were taken in the development of activated sludge modeling:

1. Initial period: empirical criteria.

2. Second period: steady-state interactions between the use of organic substrates and growth of microbes.
3. Complex dynamic models in the third phase.

"Empirical design, piloting, and guesswork" may be used to describe the initial set of empirical criteria, which spanned the process discovery period until the early 1950s (18).

One of the fundamental parameters considered at the outset was the duration of aeration, which was determined by factors such as the influent sewage strength and the desired level of treatment efficiency (19). Moreover, the required aeration duration increases proportionally with the extent of organic matter oxidation needed to achieve the treatment objectives (20).

"Sludge age" is defined as the proportion of mixed liquor suspended particles to the influent wastewater's daily suspended solids (SS) load (21). The phrase "mean cell residence time" (MCRT), introduced by Lawrence and McCarthy in 1970, is equivalent to "sludge age" (18).

According to Eckenfelder and O'Connor (1954), The efficiency of the activated sludge process in treating organic waste is influenced by factors such as the duration of aeration, the concentration of activated sludge solids, and the biochemical oxygen demand (BOD) loading rate (22). Lastly, a straightforward empirical equation was developed by Eckenfelder and Porges (1957) to calculate the tank's oxygen consumption and excess sludge production. This stage work is summed up in this equation (23).

The second phase, often referred to as the steady-state phase, involves microbial growth and the consumption of organic substrates, which can be formally described by applying chemical reaction kinetics to model the relationship between aerobic microbial proliferation and substrate utilization under steady-state conditions (24).

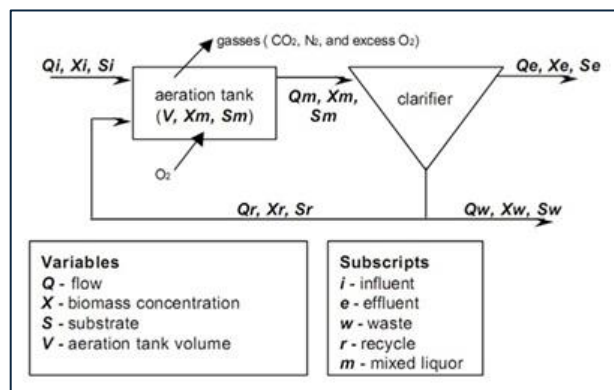
Monod (1942) investigated the connection between the concentration of substrate (carbohydrate) and growth rate for groups of *Bacillus subtilis* and *Escherichia coli* (25).

The development of the steady-state model for the activated sludge process was achieved through conducting a mass balance analysis on both the biomass and substrate components.

Figure (10) can be used to write the process's mass balance. It is crucial to write two mass balance equations: one for biomass along with one for substrate.

Figure 4

Activated Sludge Model (Mulas,2006)



The following presumptions should be made to simplify the equations (Hammer and Hammer, 2008):

- All flow rates are constant.
- The concentration of the influent substrate remains constant.
- The clarifier's solids storage remains unchanged.
- The concentration of influent biomass is zero.
- The reactor's mixed liquid and substrate concentrations remained unchanged.
- Only in the aeration tank does biological activity occur.

These assumptions are not considered by these assumptions, such as (Gall, 1999): Time varying influent flows and concentrations.

- Waste and recycling flows that change over time in response to process management requirements.

- Fluctuations in sludge settleability and the corresponding mass accumulation within the clarifier, as sludge blanket levels increase and decrease.
- Input biomass concentrations are not zero.
- Sophisticated flow streams, such as internal recycles and step feeds.
- Substrates that are too complex to be accurately represented as a single composite substrate.
- The simultaneous removal of nutrients from various biomass populations (such as nitrifiers).
- The equations do not contain kinetic coefficients that are influenced by factors, such as temperature or toxicity.

The usefulness of steady-state design flow equations is impacted by these factors in three ways (Gall, 1999):

- They result in transitory behaviors that steady-state models cannot predict.
- They make it impossible to find clear solutions to the mass balance equations because of their complexity.
- They do not take into consideration chemical and biological processes that could skew the reactions shown in earlier equations.

Complete models have been created because of the earlier issues.

The mathematical system models that exist as a collection of coupled differentials or transform equations are commonly referred to as dynamic models.

They are employed in both the subsequent reconfiguration of the system and controller design as well as the theoretical analysis of system behavior (25).

Basic understanding of the biology, chemistry, and physics of wastewater treatment processes is reflected in the current generation of dynamic activated sludge models.

The process of turning basic knowledge into mathematical form is known as model development.

Simulation: the process of solving models with computer hardware and numerical techniques.

The intersection of basic knowledge and model development has been illustrated by the IWAQ family of models. (13).

The International Water Association (IWA) formed a group to examine and create a model that describes the activated sludge process in order to encourage researchers to adopt AS models more widely (27).

The initial model created by that team is called ASM1, or Activated Sludge Process Model No.1, and it serves as the foundation for describing biological processes such as carbon oxidation, nitrification, and de-nitrification in suspended growth (activated sludge) systems (18).

Additionally, the model seeks to provide a clear explanation of sludge generation. The concentration of organic materials was measured using COD (Chemical Oxygen Demand) (28).

The ASM1 framework was subsequently extended by the development of ASM2d and other models to broaden its scope, specifically to incorporate the mechanisms of biological phosphorus removal and to account for the denitrification capabilities of polyphosphate-accumulating organisms (PAOs), respectively (18).

Developed with similar goals to ASM1, the Activated Sludge Model No. 3 (ASM3) was introduced specifically to enhance the representation of biological nitrogen removal processes. A key difference between ASM1 and ASM3 lies in the latter's incorporation of storage polymers, recognizing their significant function in the metabolic conversion pathways of heterotrophic activated sludge (28).

Numerous factors must be taken into consideration while simulating the behavior of an activated sludge system, including processes like carbon oxidation, nitrification, and de-nitrification. The response must be indicative of the most significant basic processes taking place within the system in order to be mathematically comprehensible and yield reasonable predictions (29).

Simulators are computer programs that solve IWA models, which forecast how an activated sludge system will react to changes in a variety of parameters. They can also forecast how the system will react in various scenarios, giving operators insight into how the physical system functions internally and assisting them in avoiding a number of undesirable circumstances before they become operational issues (30).

Simulators provide the operator with the means to understand the design engineer's proposal, assist in obtaining a permit under all circumstances, enhance the profitability of running an AS facility, and comprehend the precise nature of these procedures (31).

In a study by Semenova and Sergienko (2024), the treatment effectiveness of a multi-stage wastewater system under varied pollutant loads was simulated using GPS-X with the Mantis2 model. According to the study, when pollutant concentrations changed within $\pm 20\%$ of average values, the treatment plant was able to sustain high removal efficiency for BOD, COD, and TSS. However, when influent nitrogen beyond a threshold, total nitrogen accumulation in the activated sludge was noted (32).

In another study, the sedimentation basin in an extended aeration system at the Al-Hur WWTP was modeled using GPS-X. The study discovered that sedimentation performance decreased when mixed liquid suspended solids (MLSS) exceeded 3,000 mg/L, suggesting a threshold for ideal sludge concentration (33).

Using GPS-X simulations, Latif et al. (2020) investigated intermittent aeration cycles in extended aeration systems. Their results showed that when the Sludge Retention Time (SRT) was set at 10 days, the removal of COD, BOD, TSS, $\text{NH}_4\text{-N}$, and TN remained within allowable discharge limits, indicating an ideal operating range (34).

Cao et al. (2021) employed GPS-X in conjunction with response surface methodology (RSM) to optimize nitrogen removal in extended aeration plants. Sensitivity study showed that SRT and oxygen concentration were essential for reaching up to 97% nitrogen removal efficiency, indicating that appropriate aeration and sludge age control might be used to handle excessive nitrogen input (35).

The Al-Muamirah WWTP's capacity to manage different pollution loads was examined by a GPS-X simulation. TSS and COD in the effluent stayed below 40 and 100 mg/L,

respectively, suggesting that the plant successfully complied with environmental discharge regulations (36).

Because extended aeration wastewater treatment plants (WWTPs) are effective at decomposing organic pollutants and removing nutrients, they are frequently utilized for biological treatment (33) (37). However, pollutants frequently introduced by municipal and industrial discharges have the potential to inhibit with biological processes (38) (39). Determining the highest allowable pollutant concentrations in WWTPs is therefore essential for maximizing plant performance and guaranteeing adherence to environmental regulations (40). A robust wastewater treatment modeling program called GPS-X helps anticipate plant performance across a range of influent conditions and simulate various operational scenarios (9).

In wastewater management, mathematical modeling has emerged as a vital tool, research like that done by Moghaddam and Pirali (41) Hasan et al. have shown how well GPS-X works to replicate full-scale plant operations by adjusting important kinetic and stoichiometric parameters (33). demonstrated GPS-X's ability to forecast the effectiveness of pollutant removal by modeling secondary sedimentation basins. These models make it possible to evaluate how different pollution loads affect long-term aeration systems. Furthermore, GPS-X can manage uncertainty in wastewater treatment design, enabling engineers to use probabilistic techniques for more accurate forecasts (38).

Although industrial wastewater can be a useful supply of organic substrate, there are dangers involved if the pollutant load is more than what can be treated. Mikosz suggested a computer simulation approach that balances the availability of organic substrate with treatment capacity to calculate allowable industrial pollution loads for municipal WWTPs. His research demonstrated the need for real-time monitoring and model calibration by showing that COD loads exceeding 9,000 kg/day may be safely treated under particular biomass concentration conditions (39).

Treatment reliability must be systematically evaluated to evaluate WWTP performance. To assess daily performance fluctuations, Djedou et al. used reliability analysis with Niku's technique. Their results showed that total suspended solids (TSS) showed significant variability because of operational disturbances, while COD and BOD5 levels

stayed within compliance. This emphasizes the necessity of adaptive control techniques and ongoing monitoring (40).

Complex contaminants introduced by industrial discharges may have an impact on biological treatment. A multi-step procedure was created by Collivignarelli et al. to evaluate the suitability of industrial wastewater for municipal treatment facilities. To assess how industrial pollutants affect microbial activity, the procedure included respirometry testing. This showed that strict restrictions on pollutant concentrations are necessary to safeguard biological processes (9).

For reliable simulation results, WWTP models must be calibrated. By creating an effective calibration process for the ASM3 model, Simon-Várhelyi et al. increased the accuracy of simulations for the treatment of municipal wastewater. Their research highlights how crucial it is to choose the right kinetic and stoichiometric parameters when simulating extensive aeration systems in GPS-X (42). Furthermore, Várhelyi et al. investigated various optimization strategies for WWTP model calibration, contrasting Pareto multi-objective, hybrid, genetic, and classical algorithms to increase simulation accuracy (43).

Resource recovery from wastewater offers chances for sustainable management beyond limits on contaminant concentrations. Hao et al. promoted an integrated approach to WWTP management by highlighting the possibility of recovering organic chemicals, nitrogen, and phosphorus from wastewater. According to Libhaber and Orozco-Jaramillo, sustainable treatment approaches concentrate on incorporating suitable technology that optimize treatment effectiveness while lowering expenses (2) (4). Additionally, it has been demonstrated that improving extended aeration systems with more aerators and primary sedimentation tanks increases the effectiveness of pollution removal (8).

Likewise, a significant issue that may compromise the precision of pollutant concentration forecasts is uncertainty in wastewater treatment design and operation. The necessity of combining probabilistic modeling with conventional deterministic methods is emphasized by Belia et al. More accurate estimates of system performance under changing influent conditions are made possible by GPS-X's use of Monte Carlo simulations and scenario-based analysis (38).

The integration of machine learning approaches with conventional models has been a recent focus of wastewater treatment modeling developments. Because of this connectivity, treatment plans can be dynamically adjusted in response to operational data in real time. WWTPs can save operating costs and increase treatment efficiency by utilizing artificial intelligence (43).

Using GPS-X modeling software, research on how industrial wastewater affects activated sludge wastewater treatment plants (WWTPs) has shown several gaps that need to be filled (44).

a) Comprehensive Modeling of Diverse Industrial Effluents

Although GPS-X has been widely used for municipal wastewater scenarios, there has not been much use of it for industrial wastewater, which is distinguished by a high degree of compositional diversity and the presence of toxins. For example, GPS-X has been used in studies to analyze the capacity of municipal wastewater treatment plants; however, there is a lack of thorough modeling of this type for industrial effluents (37).

b) Dynamic Simulation of Industrial Load Variations

Wastewater from industrial facilities frequently has varying flow rates and levels of contaminants. Dynamic simulations that take these variances into consideration are lacking in current research, even though they are essential for creating robust treatment procedures. For instance, more targeted study on industrial load changes is required, even though some studies have employed GPS-X to model operating performance under various scenarios (39).

c) Integration of Advanced Treatment Processes

The utilization of GPS-X for evaluating the performance of integrating advanced treatment methods—such as membrane bioreactors or advanced oxidation processes—within existing activated sludge systems for industrial wastewater treatment has been limited. Exploring these combinations could potentially enhance overall treatment efficiency (41).

d) Long-Term Performance and Fouling Predictions

Current research does not adequately use long-term simulations to forecast problems such as membrane fouling or biomass inhibition brought on by certain industrial pollutants. For WWTP operation to be viable, this gap must be filled (42).

e) Economic and Environmental Assessments

To assess the viability and sustainability of treatment solutions for industrial wastewater, research combining GPS-X process simulations with economic analysis and environmental effect assessments is required.

Targeted study to fill these gaps will improve the use of GPS-X in WWTP optimization for industrial wastewater treatment, resulting in more sustainable and effective operations (44).

Chapter Two

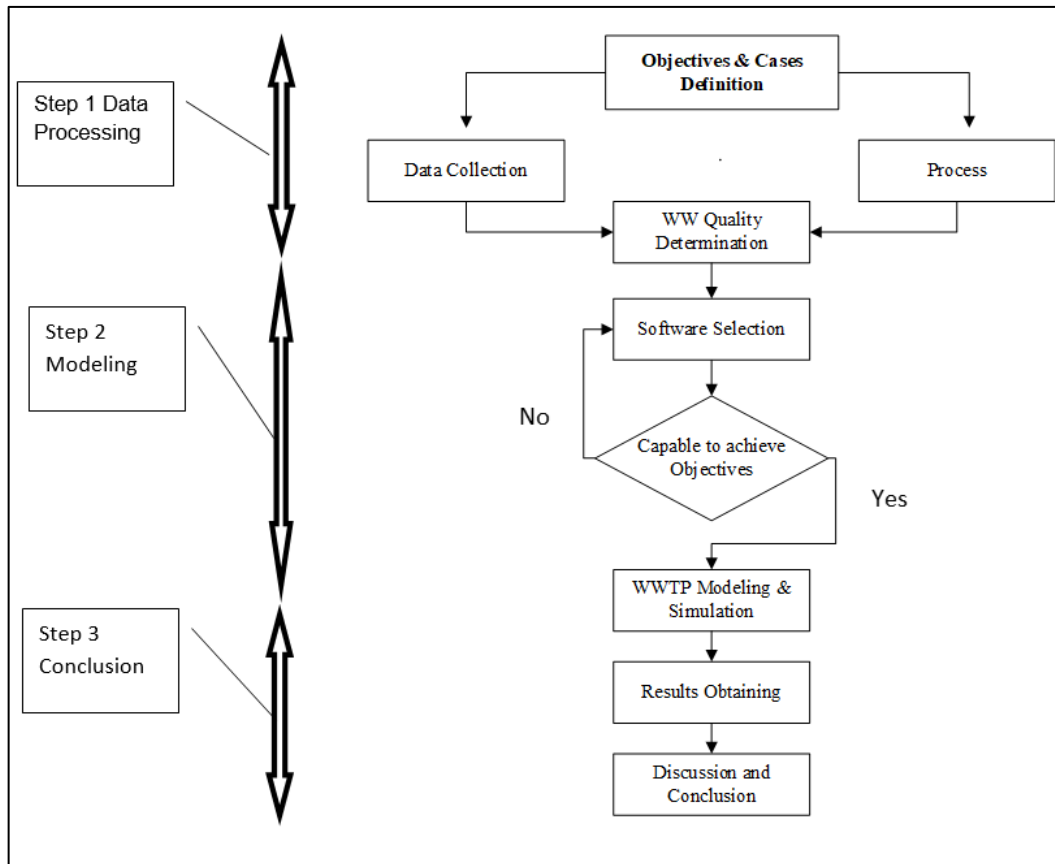
Methods

2. Methodology

The methodological approach is structured into three primary phases, which are outlined in the flowchart below in figure (4):

Figure 5

Research Methodology



The research methodology is designed to systematically address the challenges posed by industrial wastewater on the JIFZ-WWTP. It is structured into the following steps:

2.1 Data Collection and Analysis

Thorough data collecting will guarantee a strong simulation base. Details of the treatment procedure, influent characteristics, and any pollutant loads from industrial plants will all be included in the data.

Finding gaps, comprehending wastewater characteristics' fluctuation, and assessing WWTP's existing operating capability will be the main goals of the data analysis.

2.2 Modeling and Simulation Using GPS-X Software

The activated sludge treatment process under various operational scenarios was simulated using GPS-X version 8.5, an academic-licensed software developed by Hydromantis Environmental Software Solutions, Inc. This widely adopted standalone modeling tool integrates biological treatment processes for systems such as anaerobic digestion (ADS) and activated sludge processes (ASP), alongside multiple chemical and physical reaction modules. The widely recognized ASM1 framework was adapted through the incorporation of the Mantis model within GPS-X, which introduced modifications including additional growth mechanisms related to heterotrophic and autotrophic microorganisms. Notably, the Mantis model also encompasses aerobic denitrification as one of its components (35).

For the activated sludge process modeled in this study, the ASP framework was constructed within GPS-X using the MANTIS and simple1d clarifier modules, drawing upon a library of customized carbon and nitrogen components. The model includes over 60 composite and state variables, supported by extensive libraries of expressions that detail the processes via more than 30 stoichiometric and 24 kinetic parameters for inputs and outputs. This modeling approach primarily utilizes ASM1 to simulate nitrification, denitrification, and organic carbon degradation, focusing specifically on the removal efficiencies of chemical oxygen demand (COD), biochemical oxygen demand over five days (BOD_5), and nitrogen species, including nitrite and nitrate ($NO_2 + NO_3$), ammonia nitrogen (NH_3-N), and total nitrogen (TN).

Calibration The modeling process includes:

Finding the goals of the model (e.g., evaluating plant performance under stress scenarios).

Setting up the model using parameters such as tank dimensions, flow rates, pollution loads, and operating and validation of the model using real-world data to ensure its accuracy.

Multiple scenarios are simulated, including Hydraulic variations (e.g., dry weather, wet weather, and peak flow conditions). Pollution load variations (e.g., high BOD/COD, seasonal changes, and illegal discharges). Equipment failures (e.g., pump breakdowns, digester failures, and complete system failures) (36).

Discussion and Recommendations:

Based on simulation results, the study will identify operational risks and propose monitoring systems, pre-treatment enhancements, and control measures to mitigate these risks.

2.3 Data Collection

The data collection process is critical to ensuring the accuracy and reliability of the model and involves:

Operational Data:

Collect data on wastewater characteristics such as flow rates, pollutant concentrations (e.g., BOD, COD, suspended solids), and other influent parameters.

Gather details on the design and operation of the JIFZ-WWTP, including dimensions of tanks, equipment specifications, and sludge management processes.

Factory Data:

Obtain data on the types of industries expected in the JIFZ, their effluent characteristics, and pre-treatment measures in place.

Identify the variability in wastewater discharge patterns due to seasonal changes or factory operations.

Scientific Data:

Extract information from relevant literature to define parameters for modeling and simulation, such as pollutant decay rates, microbial growth rates, and sludge characteristics.

Scenario-Specific Data:

Collect information on potential abnormal conditions, such as illegal discharges or equipment malfunctions, to simulate worst-case scenarios.

Gather data on regional weather patterns and their influence on hydraulic loading.

Data Sources:

Palestinian Industrial Estates and Free Zones Authority (PIEFZA) is identified as a primary data source, along with scientific literature and laboratory experiments for supplementary data.

2.4 Statistical Analysis Methods

While the study focuses heavily on modeling and simulation, several statistical analysis methods are implicitly applied:

1. Data Validation and Calibration:

- Collected data is analyzed to check for completeness and consistency. Missing data will be supplemented using established scientific parameters or experimental results.
- The GPS-X software will be calibrated with real-world data to align the model's predictions with actual plant operations.

2. Simulation Scenarios:

- Simulations will run for various scenarios to assess plant performance under different conditions. These include:
 - Hydraulic Load Variations: Assessing the plant's ability to manage peak and low flow conditions.
 - Pollution Load Variations: Evaluating the impact of varying BOD, COD, and other pollutant concentrations.
 - Equipment Malfunctions: Simulating the effects of pump failures, sludge line disruptions, or complete system breakdowns.

3. Key Performance Metrics:

- Metrics like effluent quality (BOD/COD levels), sludge production, and treatment efficiency will be analyzed for each scenario.
- The impact of industrial effluent on the plant's biological processes, such as microbial activity in activated sludge, will also be evaluated.

4. Comparative Analysis:

- Results from various scenarios will be compared to determine the most critical factors affecting plant performance and identify thresholds for system failure.

5. Predictive Insights:

- Statistical insights gained from simulations will help predict future risks and guide the development of monitoring systems and pre-treatment standards for industries.

2.5 Model Calibration

1. The Necessity of Calibration

Complex systems can be simplified using mathematical models, which are intended to highlight essential functions while leaving out specifics. For example, just a few biomass types are usually used to mimic heterotrophic bacteria, which are remarkably diverse. Because of this innate simplification, calibration is necessary for:

Fill in the knowledge gaps on the biological, chemical, and physical mechanisms that control the system.

To guarantee correct forecasts, strike a balance between model simplicity and accuracy.

2. Definition and Scope of Calibration

Model calibration refers to the systematic process of adjusting model parameters to enhance the agreement between observed measurements and the model's simulated outcomes. According to the International Water Association's (IWA) 2012 Guidelines for Good Modeling Practice, calibration is defined as an iterative procedure whereby

model parameters are fine-tuned until the simulation outputs closely replicate a corresponding set of observed data.

Depending on the goal of the model and the data available, calibration can concentrate on biological, operational, or physical characteristics with modifications. Typical calibration parameters consist of:

- Characterization of influences (e.g., influent fractions)
- Behavior of settleability (such as relationships between sludge volume indexes)
- Aeration parameters (such as fouling factors and oxygen transfer efficiency)

3. Pre-Calibration: Data Analysis

To guarantee correct model inputs, a thorough data analysis is needed before calibration. Among the crucial actions are:

Data collection involves finding and choosing relevant datasets while taking equipment failures, plant improvements, and seasonal fluctuations into account.

Characterization of influent and typical ratios is one way to verify data.

Consistency is checked via mass balance.

Preparing the data for simulation involves formatting and importing it into GPS-X.

4. Methodology for Model Calibration

To improve model correctness, the calibration procedure employs a methodical approach:

Choice of a steady-state dataset to serve as the basis for dynamic simulations.

Model configuration, ensuring that physical and environmental specifications reflect actual plant conditions.

Selection of a proper influent model that accurately stands for wastewater characteristics.

Definition of calibration targets, including mixed liquor suspended solids (MLSS), sludge production, and effluent quality.

Calibration Process:

Running simulations to find discrepancies between modeled and observed data.

Adjusting key parameters, such as influent composition, settleability dynamics, microbial kinetics, and aeration.

Iterate the process until the best fit is achieved.

Model Validation: Using an independent dataset to confirm the accuracy of the calibrated model.

5. Key Calibration Parameters

The primary parameters influencing calibration outcomes include:

- Influent characterization: A critical factor in predicting treatment performance.
- settleability parameters: Typically adjusted using sludge volume index (SVI) correlations and clarifier specifications.
- Biological process adjustments: While widely used models such as Mantis2 and Mantis3 are well-calibrated, site-specific variations in microbial growth rates and half-saturation constants may necessitate minor modifications. However, parameters such as biomass yields, and inert fractions are well-established and rarely require adjustments.

More considerations for complex systems, including:

- Aeration efficiency (oxygen transfer efficiency, alpha factor, fouling).
- Solids managing performance (e.g., dewatering efficiency).
- Tertiary treatment processes (e.g., filtration, chlorination).
- Biofilm parameters (e.g., surface area, maximum thickness).

6. Settling Parameter Optimization

Clarifier performance significantly affects model accuracy, and adjustments typically focus on:

- Sludge volume index (SVI) correlations to characterize settling behavior.
- Clarification parameters, ensuring proper representation of sludge settling rates.
- Physical setup considerations, such as best feed point placement (preferably near the clarifier bottom rather than the surface).

7. Calibration Workflow

The calibration process is conducted in sequential steps to refine model predictions systematically:

- a) Initial Simulation: Finding uncalibrated parameters.
- b) Stepwise Calibration Approach (recommended order of adjustments):
 - Influent characterization
 - MLSS concentration
 - Dissolved oxygen (DO) concentration
 - Sludge production
 - Effluent concentration
 - Operational costs (e.g., airflow, pumping costs).

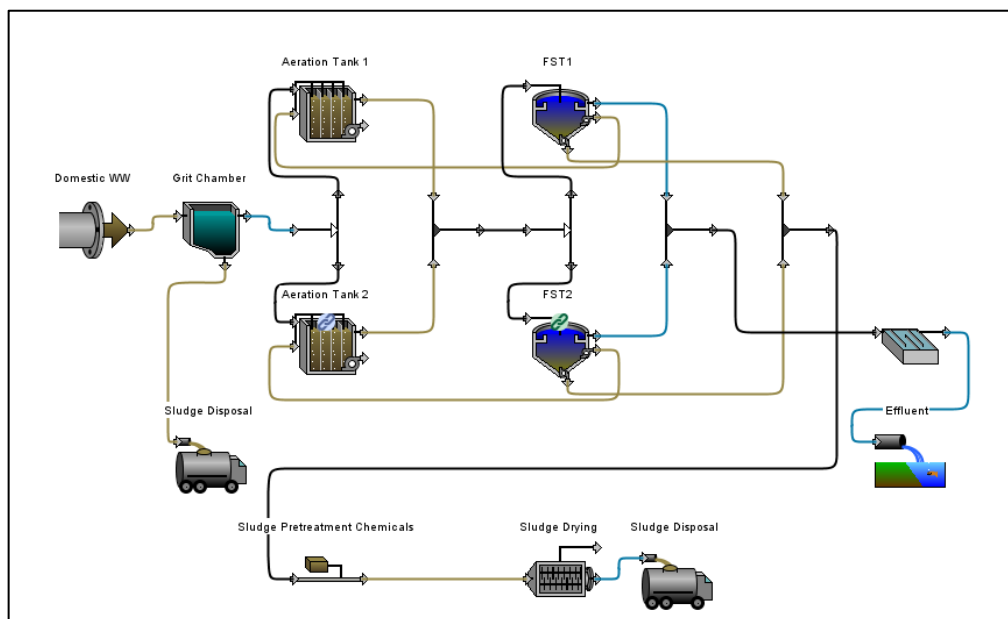
8. Case Study: Calibration of the JIFZ-WWTP Model Using Jericho WWTP Data

To ensure the accuracy of the JIFZ-WWTP model, calibration was conducted using real-world data from the Jericho Wastewater Treatment Plant (WWTP), which employs the same process technology: Extended Aeration Activated Sludge. A comparative analysis of influent and effluent characteristics facilitated optimization to reflect actual operating conditions as shown in Table (4).

The calibration process was informed by data collected from 728 tests conducted in November 2024 (Appendix 1) where reflected in the model as shown in Figure (5). Adjustments were made to account for site-specific factors, including:

- Altitude above mean sea level (AMSL), which influences oxygen solubility.
- Temperature variations, affecting microbial kinetics and aeration efficiency.
- Operational constraints, ensuring realistic representation of process performance.

Figure 6
Jericho-WWTP's Model



Key Findings and Adjustments

1. **Influent Characteristics** The influent parameters were modified to better align with the expected wastewater composition in Jericho. Notable adjustments included an increase in total COD (from 430 gCOD/m³ to 981 gCOD/m³), total TKN (from 40 gN/m³ to 57.4 gN/m³), and total phosphorus (from 10 gP/m³ to 17.3 gP/m³). These changes suggest a higher organic and nutrient load, necessitating careful monitoring of treatment efficiency.

Table 4*Influent Calibrated Characteristics*

| Variable | Unit | Default values in GPS-X software | Calibrated Value |
|--|---------------------|----------------------------------|------------------|
| total COD | gCOD/m ³ | 430.0 | 981.0 |
| total TKN | gN/m ³ | 40.0 | 57.4 |
| total phosphorus | gP/m ³ | 10.0 | 17.3 |
| ortho-phosphate | gP/m ³ | 8.0 | 3.0 |
| VSS/TSS ratio | gVSS/gTSS | 0.75 | 0.61 |
| Readily biodegradable fraction of total COD | - | 0.2 | 0.7 |
| particulate inert fraction of total COD | - | 0.13 | 0.055 |
| colloidal fraction of slowly biodegradable COD | - | 0.15 | 0.1 |
| P content of soluble inert material | gP/gCOD | 0.01 | 0.02 |
| pH | - | 7.0 | 7.4 |

2. **Aeration and Oxygen Transfer** The aeration system was recalibrated by modifying parameters such as the alpha factor and diffuser settings. The alpha factor for fine bubble aeration was increased to 0.7, reflecting site-specific conditions that influence oxygen transfer efficiency. Additionally, the height of the diffuser from the floor was slightly reduced to 0.25 m, potentially improving aeration performance.
3. **Clarification and Solids Separation** The calibration process included adjustments to the clarifiers' configuration. The first settling tank (FST1) and second settling tank (FST2) were altered from flat-bottom to sloping-bottom designs, with increased depth to 5.63 m at the sidewall and 8.73 m at the center. This modification improves sludge settling efficiency and enhances effluent quality.

4. **Sludge Management** The sludge volume index (SVI) was optimized at 189.531 mL/g, and changes in sludge underflow rates were implemented to maintain process stability. The return activated sludge (RAS) recycle ratio was set at 100%, ensuring adequate biomass recirculation to sustain microbial activity. Additionally, waste activated sludge (WAS) flow was adjusted to 60 m³/d, controlling sludge retention and minimizing excess biomass accumulation.
5. **Effluent Quality and Compliance** The model outputs indicate compliance with effluent standards, with final effluent characteristics showing reduced concentrations of total suspended solids (TSS) at 17.2 mg/L, COD at 33.6 mg/L, and BOD at 14.8 mg/L. However, soluble phosphate levels remained relatively high at 13.48 mgP/L, suggesting potential challenges in phosphorus removal that may require additional optimization.

Challenges and Future Considerations

- **Temperature Effects:** The liquid temperature was calibrated at 25.1°C to reflect the local climate, which impacts microbial kinetics and aeration efficiency. Future studies should assess seasonal variations in temperature and their implications for process stability.
- **Nutrient Removal:** While nitrification appears effective, with final ammonia concentrations at 0.119 mgN/L, further refinement of denitrification processes may be needed to optimize total nitrogen removal.

Conclusion

The calibration of the JIFZ-WWTP model using the Jericho WWTP data provided a robust basis for simulating operational performance under site-specific conditions. The adjusted parameters successfully aligned with anticipated wastewater characteristics and treatment objectives as shown in tables (5-8).

Table 5*Calibration of General Parameters*

| Variable | Unit | Default | Value |
|--------------------------------|------|---------|--------|
| liquid temperature | C | 20.0 | 25.1 |
| elevation above sea level | m | 0.0 | -490.0 |
| number of optimized parameters | | 1 | 6 |

Table 6*Calibrated FSTs Parameters*

| Variable | Unit | Value |
|---------------------------------------|----------------------|------------|
| maximum settling velocity | m/d | 315.457 |
| hindered zone settling parameter | m ³ /gTSS | 0.00044323 |
| flocculant zone settling parameter | m ³ /gTSS | 0.00275097 |
| maximum settling velocity | m/d | 315.457 |
| hindered zone settling parameter | m ³ /gTSS | 0.00044323 |
| flocculant zone settling parameter | m ³ /gTSS | 0.00275097 |
| rate constant for storage of PHA | gCOD/gPAO/d | 6.0 |
| saturation coefficient of PAO for Sac | mgCOD/L | 4.0 |
| saturation coefficient for Xpp/Xbp | gP/gCOD | 0.01 |
| maximum growth rate of PAO | 1/d | 1.0 |
| aerobic decay coefficient for PAO | 1/d | 0.2 |

Table 7*Checking the influent characteristics*

| Ratio | Units | Typical Range | Actual value from Calibrated model |
|------------------------|------------|---------------|------------------------------------|
| VSS/TSS | gVSS/gTSS | 0.6-0.85 | 0.61 |
| BoD5/COD | gBOD5/gCOD | 0.4-0.55 | 0.619 |
| NH4-N/TKN | -- | 0.65-0.9 | 0.436 |
| Filtered COD/Total COD | -- | 0.25-0.7 | -- |

Table 8*Effluent Simulation Results*

| | | |
|------------------|-----------|--------|
| Flow | m3/d | 709.8 |
| TSS | mg/L | 23.42 |
| VSS | mg/L | 20.69 |
| cBOD5 | mg/L | 8.274 |
| COD | mg/L | 32.22 |
| Ammonia N | mgN/L | 0.1192 |
| Nitrite N | mgN/L | 0.1644 |
| Nitrate N | mgN/L | 13.32 |
| TKN | mgN/L | 2.593 |
| TN | mgN/L | 16.08 |
| Soluble PO4-P | mgP/L | 13.48 |
| TP | mgP/L | 14.04 |
| Total Alkalinity | mgCaCO3/L | 68.49 |
| pH | - | 7.0 |
| DO | mgO2/L | 2.0 |

The Figures (6-9) provide a visual confirmation of the calibration process's success, illustrating how the JIFZ-WWTP model, after the adjustments that explained above, can reliably predict effluent quality under normal conditions.

Figure 7

Calibrated effluent total suspended solids.

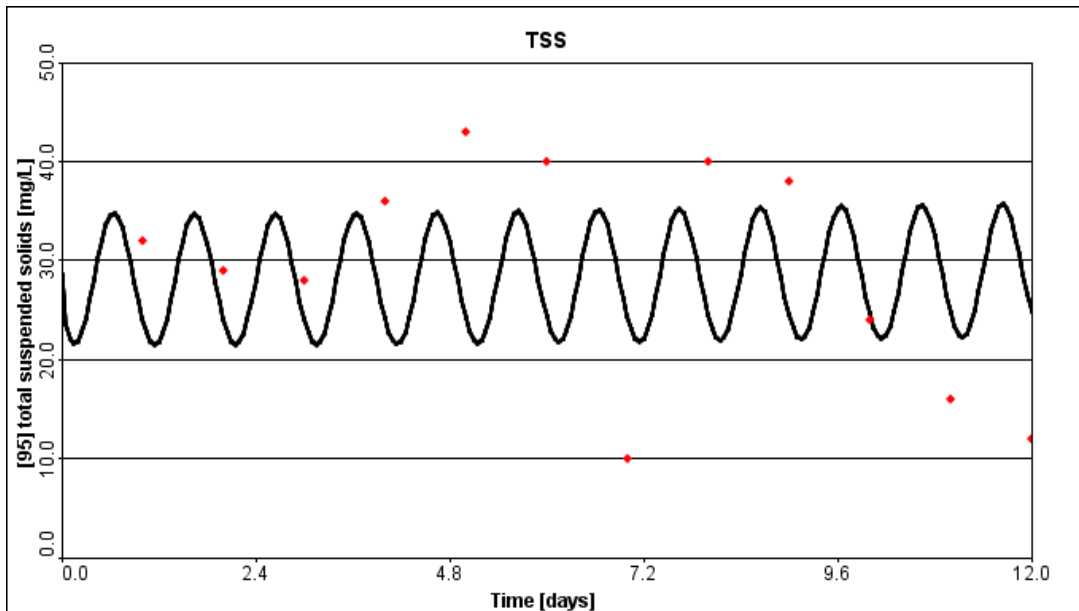


Figure 8

Calibrated effluent total nitrogen.

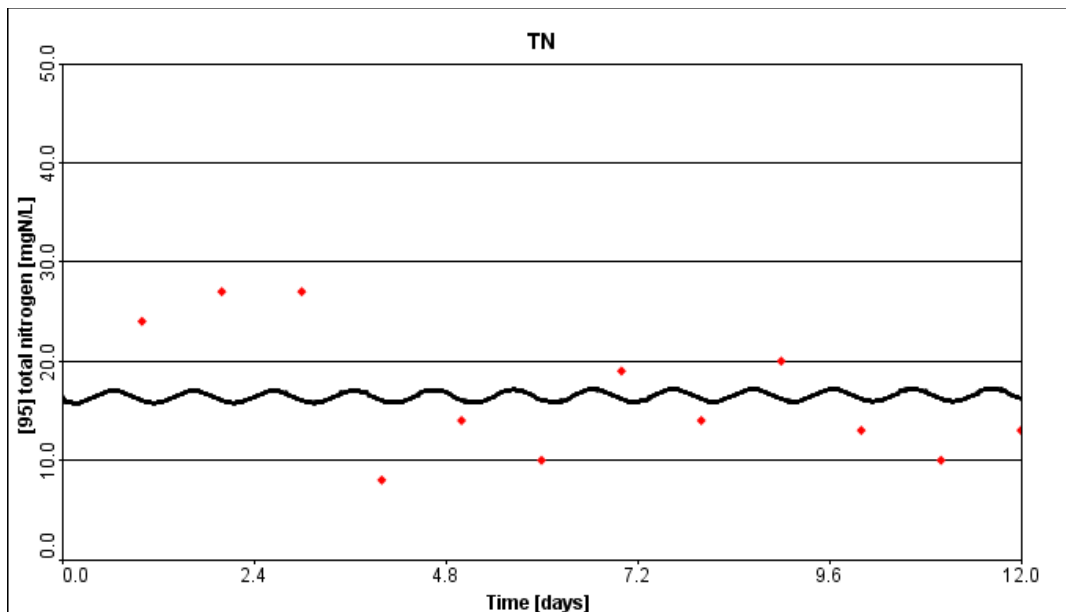


Figure 9

Calibrated effluent total COD.

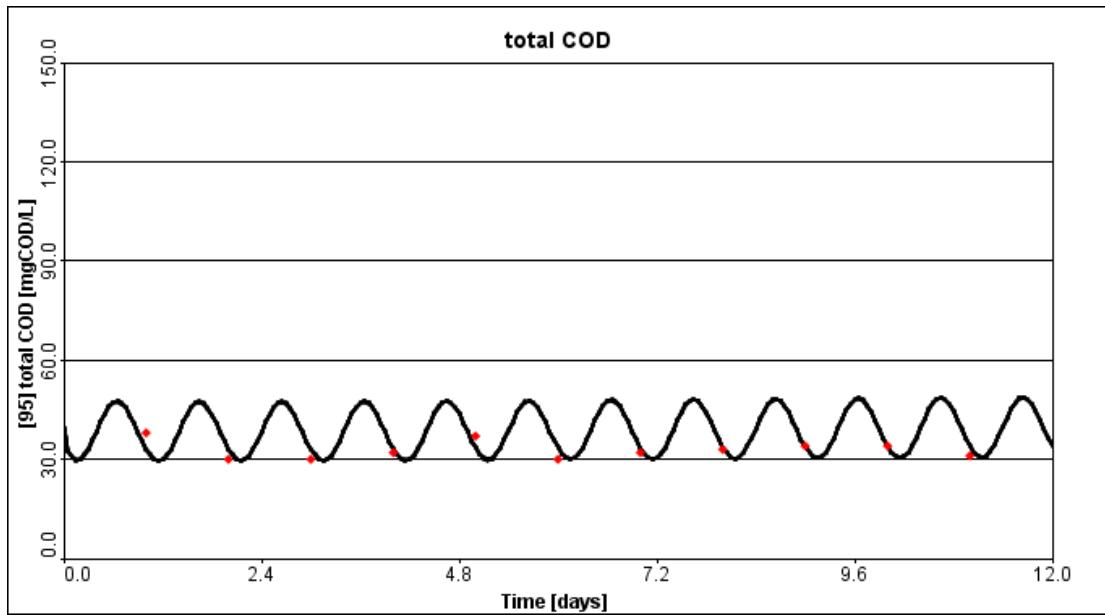
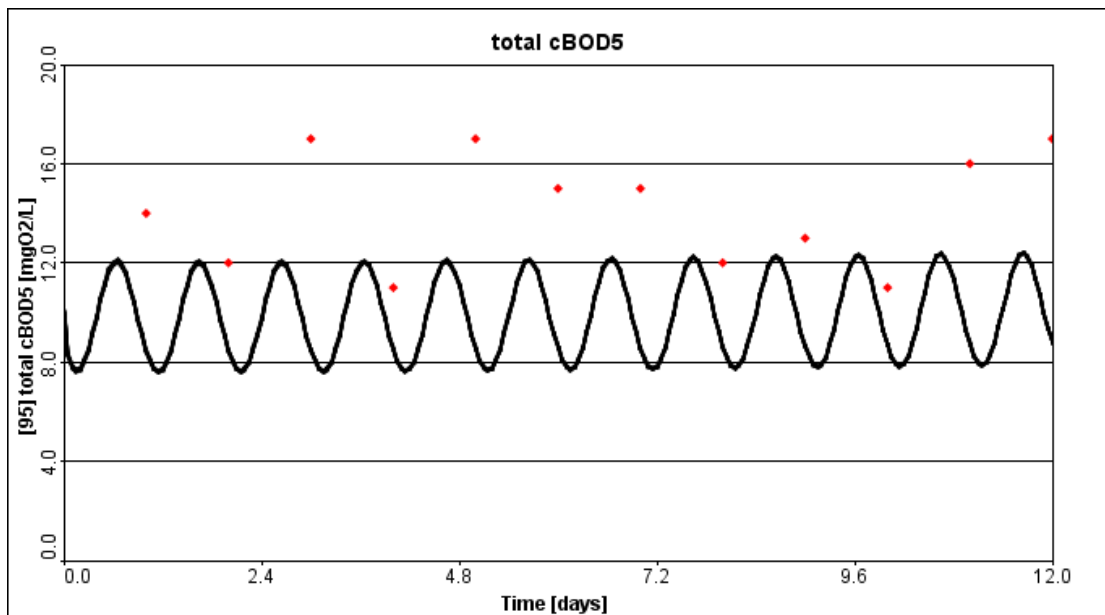


Figure 10

Calibrated effluent total cBOD5.



Chapter Three

Results and Discussions

3. General

The main objectives of this study are to study the impact of the non-pretreated IWW on JIFZ-WWTP (Activated Sludge Process) and to determine the maximum permissible pollutant concentration that an existing extended aeration JIFZ-WWTP can handle, as well as, to study the behavior of the treatment operations during the shock loads and possible operating emergency procedure to improve the treatment and recovery efficiency by optimizing certain influencing parameters as shown in Tables 4, 5 and 6.

Because the WWTP is new and not yet operational, influent parameters were estimated based on expected industrial effluent qualities provided by PIEFZA. The WWTP's design data and system configurations was collected in incorporated to the JIFZ-WWTP's model as shown in Appendix I, as well as, the calibrated parameters as shown in Table (4,5 and 6) were reflected and validated.

The following are key performance indicators (KPIs):

Removal Efficiency Calculation

$$\text{Removal Efficiency (\%)} = \frac{\text{Influent} - \text{Effluent}}{\text{Influent}} \times 100$$

The removal efficiencies of crucial parameters may be used to assess the extended aeration wastewater treatment plant's (WWTP) performance that shown in Table 9 as the following:

a) Removal of Suspended Solids

- Removal of TSS: 95.18%
- Removal of VSS: 93.62%

The great effectiveness of the sedimentation and biological processes is indicated by the high removal efficiency of suspended particles. Solids are being effectively separated from the treated effluent by the combination of biological treatment and final clarifying.

b) Removal of Organic Matter

- Removal of COD: 89.50%
- Removal of cBOD5: 94.32%

Excellent biological degradation of organic pollutants is shown by the cBOD5 elimination efficiency (>90%), which is to be expected in prolonged aeration systems because of their lengthy retention duration and increased microbial activity.

It is possible that some non-biodegradable organic compounds are present in the influent since the COD removal efficiency is decreased but still within acceptable bounds.

c) Phosphorus Removal

Removal of Phosphorus and Soluble Orthophosphate (S_PO4): 99.88%

Removal of Total Phosphorus (TP): 66.45%

The high phosphate removal efficiency indicates that chemical precipitation may be used in addition to biological phosphorus absorption. Particulate phosphorus may not be settling effectively or may be returning to the effluent, as seen by the much lower total phosphorus removal (66.45%).

d) Total Nitrogen Removal

Influent TN: 64 mg/L

TN in the effluent: 42.39 mg/L

Efficiency of Removal: 33.8%

This comparatively low nitrogen removal indicates that the prolonged aeration system's denitrification is not operating at its best. Potential problems might consist of:

1. Since prolonged aeration mostly concentrates on nitrification, there are insufficient anoxic conditions for denitrification.

2. Low carbon availability restricts the amount of nitrogen gas that can be produced from nitrates by denitrifying bacteria.
3. The effluent's high nitrate content (37.31 mg/L) suggests that denitrification is not yet complete, but nitrification is proceeding effectively.

Ways to Enhance TN Removal:

- Prior to aerobic treatment, provide an anoxic zone to improve anoxic conditions.
- Add an external carbon source, such as methanol or acetate, to increase the availability of carbon sources.
- Sludge retention time (SRT) should be optimized to balance denitrification and nitrification.

Table 9

Removal Efficiency of JIFZ-WWTP

| Parameter | Influent (mg/L) | Effluent (mg/L) | Removal Efficiency (%) |
|---------------------------------|-----------------|-----------------|------------------------|
| Total Suspended Solids (TSS) | 284.7 | 13.72 | 95.2 |
| Volatile Suspended Solids (VSS) | 173.7 | 11.09 | 93.62 |
| COD | 1040 | 109.2 | 89.5 |
| cBOD5 | 642.4 | 36.51 | 94.32 |
| Ammonia Nitrogen (S_NH3) | 25 | 0.3272 | 98.7 |
| Total Kjeldahl Nitrogen (TKN) | 64 | 4.816 | 92.5 |
| Total Nitrogen (TN) | 64 | 42.39 | 33.8 |
| Soluble Orthophosphate (S_PO4) | 3 | 0.003748 | 99.9 |
| Total Phosphorus (TP) | 4 | 1.342 | 66.45 |

According to research, the JIFZ-WWTP has high removal efficiency for TSS (95.18%), COD (89.50%), and BOD (94.32%) under typical operating circumstances.

Given that the JIFZ-WWTP's HRT of 29.07 hours and SRT of 20 days fit within the usual norms, it is probable that it is an extended aeration system.

Given its performance and design, the evidence points to the plant being completely classed as extended aeration; nonetheless, nutrient removal, such as nitrogen (33.8%), might be enhanced.

Comparing Performance under Typical Circumstances

Under typical circumstances, the JIFZ-WWTP performs admirably, efficiently treating household wastewater. It accomplishes:

- BOD Removal: 94.32%, which guarantees clean effluent by eliminating all organic materials that bacteria may decompose.
- COD Removal: 89.50%, which is a little less than BOD but still quite successful, shows that some non-biodegradable organics are still present.
- Excellent solids separation, which is essential for producing pure water, is demonstrated by the TSS Removal of 95.18%.

As anticipated for a long-term aeration system intended for comprehensive treatment, these measures demonstrate the plant's capacity to manage normal loads while eliminating contaminants with high efficiency.

How Much of an Extended Aeration System It Is

As an extended aeration activated sludge system, the JIFZ-WWTP has the following features:

- Longer contact time for biological treatment is possible with HRT of 29.07 hours, which falls within the usual range of 18 to 36 hours for extended aeration.
- A stable microbial population for improved treatment is supported by an SRT of 20 days, which is at the lower end of the (20–40) day range.

The plant is completely classed as extended aeration given these metrics and its strong performance; nevertheless, its nutrient removal, particularly nitrogen at 33.8%, indicates potential for optimization in comparison to ideal extended aeration systems.

Limitations in Nutrient Removal

Remarkably, nitrogen removal is only 33.8%, which is lower than predicted for certain extended aeration systems, probably because of restricted denitrification processes, even though organic and solid removal is excellent. This may have an impact on adherence to more stringent environmental regulations.

The design identifies the activated sludge process used by the JIFZ-WWTP as an expanded aeration system. Longer solids retention periods (SRT) and hydraulic retention times (HRT) are characteristics of extended aeration, a variation of the traditional activated sludge method that improves biological treatment and stabilizes sludge while lowering the creation of extra sludge. Smaller or variable load applications, including industrial zones with home wastewater inputs, are best suited for this system.

The JIFZ-WWTP's designation as an extended aeration system is supported by the table below:

Extent of Being an Extended Aeration System

| Parameter | JIFZ-WWTP Value | Typical Extended Aeration Range |
|-----------------|-----------------|--|
| HRT (hours) | 29.07 | 18 - 36 hours |
| SRT (days) | 20 | 20 - 40 days |
| BOD Removal (%) | 94.32 | 88 - 98% (based on literature) |
| COD Removal (%) | 89.5 | 89 - 95% (based on literature) |
| TSS Removal (%) | 95.18 | 90 - 95% (based on literature) |
| TN Removal (%) | 33.8 | Variable, often 30-60% with optimization |

Which demonstrates that its parameters fall within or are near the usual ranges. The elimination of lower TN points to an area for improvement, which is not out of the ordinary and may be fixed with better design.

The JIFZ-WWTP is completely categorized as an extended aeration system based on the analysis, with performance metrics (high BOD, COD, and TSS elimination) and design parameters (HRT 29.07 hours, SRT 20 days) matching standard criteria. Under typical circumstances, its efficacy in treating household wastewater illustrates the advantages of prolonged aeration, including stability and little sludge formation. The low nitrogen removal, however, raises the possibility that further procedures would be required for applications with strict nutrient requirements, which is a prevalent factor in wastewater treatment design.

This thorough assessment serves as a basis for comprehending the plant's capabilities and improvement areas, especially in industrial settings where performance may be troubled by fluctuating loads.

The maximum influent flow (Q) is optimized using RAS and WAS based on the sensitivity analyses that were performed for several regulating factors. where the WWTP design specifies that the RAS and WAS are 320 m³/d and 50 m³/d, respectively. The WWTP can only treat 900 m³/d without compromising the effluent criteria for reusable WW in agriculture class (C), as shown in Annex (C), as can be seen in the appendix (J).

The optimal operating parameters for FST have been determined through numerous optimizations; as illustrated in Annex (K), the Q of WAS is 60 m³/d, and the Q of RAS is 460 m³/d.

3.1 Probabilistic Design Using Monte Carlo Sensitivity Analysis

The timing, flow rates, and concentrations of industrial waste feeds can vary greatly. To obtain fair characterization, sampling is necessary.

To find out what might occur in various scenarios, sensitivity analysis will be employed if valuable information (such as flow rate) is absent. Additionally helpful is Monte Carlo analysis.

Benefits:

- Make it possible to examine several inputs at once.

- Offers not only correlations (direct/indirect, for example), but also the likelihood of reaching performance standards.
- An outstanding uncertainty analysis tool that enables users to evaluate the effects of variables with insufficient data.

Drawbacks:

- Needs input distributions, which may not always be available.
- Requiring a lot of computation, thousands of simulations.

Evaluating the Resilience of Wastewater Treatment Systems to Industrial Effluent Variability

1. Change in the Composition of Industrial Wastewater

- Situations with elevated levels of nutrients, BOD, and COD.
- Situations involving sharp changes in pH (alkaline or acidic inputs).
- Various levels of biodegradability according to industry effluents (dairy, food processing, pulp, and paper sectors, for example).

2. Variable Flow Rates

- Regular flow rates as opposed to irregular and intermittent flow rates.
- The effect of peak flows during cleanup or production cycles.
- The simulation of surges or breaks in flow brought on by manufacturing schedules.

3. Modifications to the Environment

- Changes in the surrounding temperature and how they affect biological functions.
- Dilution or overflow situations are caused by rainfall events.

- Seasonal variations impact treatment effectiveness and influent features.

4. Operational parameters of treatment plants

- Situations where reactor layouts, sludge retention durations, and aeration levels vary.
- How plant performance is affected when primary sedimentation is absent.

5. Pretreatment's Effect on the Source

- Cases where industries properly pretreated vs those that did not.
- Incomplete or Missing Input Data: Monte Carlo analysis can be used to model situations when influent composition or flow rates are not fully known.
- Assessing the range of potential results based on probable data distributions.

6. Extreme Circumstances

- High-strength wastewater that contains inhibiting substances, such as nitrous acid or free ammonia.
- The unexpected appearance of pollutants that are not biodegradable.

To assess the impact of changes in influent characteristics on WWTP performance, a Monte Carlo analysis was conducted for many unknown factors as following:

- The range of total COD is 800–1500 mg/L.
- The range of TKN is 40–80 mg/L.
- The rapidly biodegradable fraction of total COD ranges from 0.4 to 0.8.
- Range of orthophosphate: 1–5 mg/L.

Probabilistic insights into important effluent quality parameters were obtained from the Monte Carlo simulations:

Total suspended solids (TSS): The probability distribution shows that solid-liquid separation is often successful since 87% of the effluent TSS values are less than 50

mg/L as shown in appendix (L). However, increases of more than 50 mg/L occasionally indicate potential sludge thickening events.

The fact that approximately 33% of effluent cBOD measurements are below 40 mgO₂/L highlights a significant degree of uncertainty in the efficiency of organic matter removal. The substantial range suggests that some influent circumstances may lead to elevated cBOD levels as shown in appendix (L).

Total COD: According to the Monte Carlo study, 33% of effluent COD levels fall below 100 mgCOD/L, which is comparable to cBOD. This emphasizes how important it is to have robust organic load control to ensure discharge restrictions are fulfilled as shown in appendix (L).

Total Nitrogen (TN): The probability analysis indicates that 68% of effluent TN values are below 45 mgN/L, indicating a moderate level of nitrogen removal efficiency. The fluctuation illustrates how WWTP performance is impacted by significant TKN fluctuations as shown in appendix (L).

3.2 Optimization of RAS and WAS for JIFZ-WWTP and Its Impact on Effluent Quality

After thorough optimization processes, the flow rates for Return Activated Sludge (RAS) and Waste Activated Sludge (WAS) were determined at 480 m³/d and 60 m³/d, respectively. To guarantee efficient sludge management and ideal process performance, these parameters were chosen based on simulations and operational restrictions.

The RAS flow rate is essential for preserving adequate biomass concentration in the aeration tank, which keeps the microbial populations in charge of nitrification and organic matter decomposition at the proper levels. In the meantime, excessive sludge accumulation that might result in process inefficiencies like decreased oxygen transfer or increased sludge age is prevented by the WAS flow rate, which regulates the amount of surplus biomass removed from the system.

The JIFZ Wastewater Treatment Plant (JIFZ-WWTP) was able to manage a maximum influent flow rate (Q_{max}) of 1000 m³/d without sacrificing the final effluent quality due to the adjusted RAS and WAS values. The constancy of important effluent metrics, as displayed in the accompanying appendix (M), provides confirmation of this:

Total COD (Chemical Oxygen Demand): The removal of organic materials is effective when the effluent COD content stays within allowable bounds.

The carbonaceous biochemical oxygen demand cBOD, is steady, indicating that biodegradable organic molecules are effectively broken down by heterotrophic bacteria.

Total Nitrogen (TN): The levels of TN show that the processes of nitrification and denitrification are operating correctly, limiting the amount of nitrogen released into the atmosphere.

The concentration of total suspended solids (TSS) is still low, indicating effective solid-liquid separation and appropriate settling in the secondary clarifier.

It appears that the aeration, sludge management, and clearing processes are well-balanced under these operating conditions since $Q_{max} = 1000 \text{ m}^3/\text{d}$ may be operated at without going beyond discharge limitations as shown in appendix (M). This makes the plant a strong and dependable prolonged aeration WWTP by guaranteeing that it can manage peak flow conditions without failing.

3.3 Analysis of Effluent Quality During Shock Load Event

This thesis section examines the effects of industrial shock loading during (Days 3–13) on wastewater treatment plant (WWTP) effluent quality as shown in annex (D). To evaluate the system's response to extreme conditions and recovery from the event, the following important effluent characteristics were analyzed: Total Phosphorus (TP), Total Kjeldahl Nitrogen (TKN), Biochemical Oxygen Demand (BOD₅), Chemical Oxygen Demand (COD), and Total Suspended Solids (TSS).

A shock load scenario has been studied, the WWTP was exposed to an immediate shock load of $1000 \text{ m}^3/\text{day}$ on Day 3. This shock load was directly caused by the non-pretreated wastewater produced by energy drink, meat and dairy processing, textile, and tannery industries, the characteristics was modeled according to annex (D). The substantial increase in organic and inorganic pollutants brought on by this shock load was evident from a detectable peak in pollutant concentrations. Elevated COD, ammonia, and total suspended solids (TSS) not only delayed the nitrification and breakdown of the substrate, but they also temporarily hindered microbial activity.

3.4 Breakdown of Key Effluent Parameters and Trends

Biochemical Oxygen Demand (BOD5) and Chemical Oxygen Demand (COD)

Prior to day 3 (before the shock load): The concentrations of BOD5 and COD were low, showing that good biological treatment performance is stable. The microbial community effectively degrades organic matter.

Days 3–13 (during the Shock load): When the influent peaks for BOD5 and COD, with COD peaking around 8000 mg/L and BOD5 peaking above 3500 mg/L, the effluent BOD5 and COD also increase significantly. This shows that:

- A remarkably high organic load was present in the influent, which was beyond the biological degradation capacity of the system.
- Influent may include some non-biodegradable or toxic organic matter, which limit the efficiency of the microbes.

A temporary decline in treatment effectiveness seems to have been caused by stress on the biological community, because of inhibitory chemicals.

As the system was restored after day 13, BOD5 and COD gradually decreased, but not immediately. The COD and BOD5 elimination delay suggests that the microbial population had to adapt and resupply.

However, organic molecules known as refractories - which decompose slowly - remained in the system.

Sludge washout or biomass degradation were cited as the causes of the residual organic materials in the effluent.

Total Kjeldahl Nitrogen (TKN) and Nitrification Performance

Prior to Day 3, TKN was low in effluent, demonstrating that nitrogen was effectively removed by biomass absorption and nitrification.

The content of TKN in the wastewater rose dramatically between Days 3 and 13, indicating that ammonia and organic nitrogen were not efficiently converted to nitrate.

Heterotrophs consuming the high organic load were destroyed or outcompeted with the nitrifying bacteria (ammonia-oxidizing and nitrite-oxidizing bacteria). High BOD limited nitrification by causing oxygen competition.

Following Day 13, TKN steadily decreased, although it recovered more slowly than BOD/COD. This is consistent with nitrifiers' gradual regeneration, which takes weeks to recover after inhibition or washout.

Total Phosphorus (TP)

Throughout the shock period, there was fluctuation in the effluent phosphorus content, with occasional peaks that corresponded to sludge instability.

Potential reasons for variations in TP:

Phosphorus was released from lysed cells due to the high organic load that inhibited the Enhanced Biological Phosphorus Removal (EBPR) microorganisms.

Stored phosphorus may have been absorbed into the effluent due to increased sludge waste caused by system overloading.

Higher TP in the effluent may have resulted from problems with secondary clarifier performance (poor settling).

Although TP remained moderately increased after the shock, the system progressively recovered, suggesting potential long-term consequences for phosphorus elimination mechanisms.

Total Suspended Solids (TSS)

Prior to Day 3, the effluent had a low TSS, which suggested good sludge settleability.

The sharp increase in TSS from Days 3–13 indicated either toxic effects or biomass deflocculation brought on by stress and/or increased clarifier sludge washout.

A significant percentage of immature scattered microbial cells or filamentous development causes poor sludge settling.

Following Day 13, TSS decreased but took longer to stabilize, indicating continued difficulties with settling and sludge compaction.

3.5 Interpretation of Trends and System Performance Impact

The patterns in effluent quality show that the biological processes of WWTP have been clearly disrupted.

The following are the main interpretations:

1. The significant increase in BOD5 and COD indicates that the influent's quantity of organic materials, both biodegradable and potentially non-biodegradable, exceeded the system's metabolic capability.
2. Nitrification Collapse: The rise in TKN indicates a considerable influence on nitrifying bacteria, because of washout, oxygen competition, or inhibitory chemicals. The slow post-shock recovery results in a considerable decline in nitrifier numbers.
3. Sludge Instability and Washout: The elevated TSS concentrations suggest that the shock resulted in poor settling, clarifier washout, and sludge deflocculation. This caused high effluent turbidity and solids residue.
4. The phosphorus swinging of Biomass Decay indicate that either microbial stress or the physical death of organisms that store phosphorus caused a disruption in biological phosphorus removal.

3.6 Potential Causes of Effluent Deterioration

The observed degradation of the effluent was caused by several underlying mechanisms:

a) Overloading of Organic Materials (High F/M Ratio)

A significant rise in the food-to-microorganism (F/M) ratio was caused by the influence of abnormally high BOD and COD levels.

Nitrogen depletion and consequent nitrification failure resulted from heterotrophic bacteria outcompeting nitrifiers.

b) Inhibition of Biomass and Toxic Shock

Microbial activity may have been suppressed by some components of industrial waste, such as solvents, heavy metals, or extremely high or low pH values.

Because of their toxicity, some bacteria lysed, releasing internal components into the effluent, such as organic nitrogen and phosphorus.

c) Limitations of Dissolved Oxygen (DO)

The rapid BOD jump caused a transient oxygen deficit due to increased oxygen demand, which further hindered microbial metabolism and nitrification.

Low DO conditions may have resulted from the aeration system's inability to promptly compensate for the elevated oxygen demand.

d) Poor Settleability and Sludge Washout

Stress-induced deflocculation increased the amount of solids that were carried over into the effluent. It is possible that inadequate sludge compaction or overloading of secondary clarifiers have had an impact. Recovery was further slowed down by excessive sludge loss since the system had to develop its microbial populations again.

In conclusion, the effluent patterns during days 3–13 of the shock load event demonstrate how high-strength industrial waste can seriously harm WWTP operation. High effluent concentrations of BOD, COD, TKN, phosphorus, and TSS were the result of many main consequences, including sludge washout, enhanced phosphorus release, nitrification failure, and hindered organic breakdown. Even while the system recovered progressively after the shock, the lag in some parameters particularly nitrogen removal highlights the damage to biomass's long-term effects. Stable effluent quality and regulatory compliance may be ensured by reducing the impacts of future shock loads using process optimizations, industrial pretreatment, and improved monitoring systems as shown in appendix (N).

3.7 Key Parameter Trends During the Shock Load

Extended aeration wastewater treatment facilities (WWTPs) depend on microbial populations to break down organic pollutants and recover nutrients. Effective microbial

activity monitoring is essential for maximizing treatment performance, preventing process interruptions, and ensuring compliance with effluent quality standards. Computational modeling software such as GPS-X provides a solid basis for simulating microbial kinetics, substrate use, and system responses to varying operating circumstances. In this section, microbial activity and its impact on key water quality indicators are evaluated using GPS-X as shown in table (10).

Table 10*Process Variables Prior to the Occurrence of the Shock Load*

| | Unit | AT1 | AT2 | FST1 | FST2 |
|--------------------|----------------------------|---------|---------|-------|-------|
| Volume | m ³ | 1209 | 1209 | 168.7 | 168.7 |
| HRT | h | 29.07 | 29.07 | 4.057 | 4.057 |
| F to M Ratio | kgBOD5/(kg MLVSS.d) | 0.3369 | 0.3317 | - | - |
| Vol. Org. Loading | kgBOD5/(m ³ .d) | 0.2647 | 0.2647 | - | - |
| Nitrification Rate | mgN/(L.h) | 1.048 | 1.056 | - | - |
| Nitrate Util. Rate | mgN/(L.h) | 0.09636 | 0.09757 | - | - |
| Total OUR | mgO ₂ /(L.h) | 14.32 | 14.47 | - | - |

Process Variables During the Occurrence of the Shock Load

| | | | | | |
|--------------------|----------------------------|-----------|-----------|-------|-------|
| Volume | m ³ | 1209 | 1209 | 168.7 | 168.7 |
| HRT | h | 29.07 | 29.07 | 4.057 | 4.057 |
| F to M Ratio | kgBOD5/(kg MLVSS.d) | 1.599 | 1.578 | - | - |
| Vol. Org. Loading | kgBOD5/(m ³ .d) | 1.595 | 1.595 | - | - |
| Nitrification Rate | mgN/(L.h) | 0.0004434 | 0.0004556 | - | - |
| Nitrate Util. Rate | mgN/(L.h) | 0.0 | 0.0 | - | - |
| Total OUR | mgO ₂ /(L.h) | 9.073 | 9.182 | - | - |

The biomass growth in a wastewater treatment process, especially in systems that use biofilm or activated sludge. It is an illustration of the Monod-based kinetic model, which states that microbial growth is determined by several limiting substrates (Equation 4.2).

$$growth = \mu h * Xbh * ((SO/(KO + SO)) * (SS/(KS + SS)) * (SNH/(KNH + SNH)) * (SP/(KP + SP)))$$

Where:

| | |
|---------------------|------------|
| $SO / (KO + SO)$ | Oxygen |
| $SS / (KS + SS)$ | Substrate |
| $SNH / (KNH + SNH)$ | Nitrogen |
| $SP / (KP + SP)$ | Phosphorus |

F/M, or food-to-microorganism Ratio

During the shock period as shown in appendix (O), the F/M ratio experienced a significant rise. F/M was in the usual range (~0.2–0.5, a common ideal range for complete-mix systems) under normal conditions (Days 0–3) (45). F/M rose because of the introduction of untreated industrial waste, which started around Day 3 and significantly increased the "food" (organic load) without immediately increasing biomass. The biomass was receiving significantly more substrate per unit mass than typical, as seen by the high F/M that lasted until Day 13. As the extra substrate was eaten up and the microbial community grew or changed to cope with the load, F/M started to decline back toward pre-shock values by Days 14–15 (after the shock). A slightly lower than initial F/M ratio had a prolonged impact after the shock, because of biomass growing during the shock (raising the denominator) and the influent load returning to normal. In summary, the shock load caused a temporary overload in terms of substrate relative to biomass, evidenced by the elevated F/M ratio during Days 3–13.

Active vs Inactive Volatile Suspended Solids (VSS)

During the shock as shown in appendix (O), there was a noticeable change in the mixed liquid solids' composition. A higher proportion of active VSS made up most of the biomass before Day 3, whereas a minor portion consisted of inactive or inert solids (cell debris, non-biodegradable materials). After the shock load was applied, the proportion of active biomass decreased while the percentage of inactive VSS rose. This indicates that more inert organic matter was left behind after some of the biomass was

overloaded, destroyed, or inactivated by the sudden load (or any hazardous substances in the industrial influent). Toxic shock or a lack of vital nutrients may have caused certain cells to lyse, resulting in inert substances.

The data clearly indicates that the fraction of inactive VSS increased over the mid-shock period, reaching its high around Day 13. via the conclusion of the shock (Day 13 onward), the tendency reverses: the active VSS percentage rises once again as the system heals, new biomass grows, and dead cells are gradually eliminated (via sludge waste or microbial consumption). However, flushing out all the inert accumulation can take some time. The important thing to remember is that waste decomposition is only facilitated by active biomass (46). Therefore, decreased treatment activity in the aeration tank is directly correlated with an increase in inactive VSS during the shock.

Oxygen Uptake Rate (OUR)

The OUR changed in response to the shock load, indicating variations in the respiration of microorganisms. OUR was comparatively constant prior to the shock, suggesting a consistent rate of oxygen consumption for nitrification and carbon oxidation. Two consequences happened when the shock load first arrived (Day 3):

- a. **Initial inhibition:** The bacteria's respiration may have quickly slowed or stopped if the industrial waste included hazardous substances or depleted oxygen, which would have resulted in a drop in OUR just before the shock started. This is consistent with observations that biological activity, particularly that of sensitive microorganisms, is initially inhibited by toxic shocks (47).
- b. **Subsequent spike:** the OUR dramatically rose when adapted heterotrophic bacteria started to eat the abundant new substrate (47).

Given the abundance of BOD available during Days 3–13, heterotrophs entered a period of fast development and increased their oxygen consumption. Since microorganisms oxidized the organics spike, the peak OUR at this time shows the highest metabolic activity (the data may reveal a substantial OUR peak corresponding to maximum COD/BOD consumption). The high carbonaceous oxygen demand from heterotrophs exceeded any decrease in oxygen nitrification (caused by the loss of nitrifiers, which is

covered below). As the stress load decreased after Day 13, OUR would progressively return to normal levels.

If a significant amount of biomass that was accumulated during the shock is now going hungry (endogenous respiration phase), OUR may even fall below the initial baseline by Days 15–20. The microbial community's struggle and subsequent aggressive metabolism in reaction to the shock load are reflected in the OUR trend, which shows a dip followed by a surge during the shock.

Heterotrophic vs. Autotrophic Biomass (Nitrifiers)

These two important microbial groups were affected by the shock load as shown in appendix (O) in different ways:

- a) **Heterotrophic Biomass:** In general, heterotrophs - which consume organic carbon or BOD - do well as the food supply rises. The heterotrophic population expanded to exploit the rich organic substrate during the shock after overcoming any early inhibitory effects. The F/M spike caused rapid growth to bacteria. We see an increase in the concentration of total biomass by the latter stages of the shock, which is mostly caused by heterotrophic growth and is also attributed to higher mixed liquor VSS. This extra biomass may be young and dispersed since fast growth under high F/M usually produces smaller flocs or even filamentous organisms, which restrict settleability. However, heterotrophs indeed comprised the dominant component of biomass during the shock, given that they may double in a matter of hours to days when provided with an abundance of food.
- b) **Autotrophic Biomass (Nitrifiers):** The shock had a harmful effect on nitrifying bacteria, which include ammonia and nitrite oxidizers. There were several contributing factors:
 - 1) A shock load can rapidly blockade or kill a considerable number of nitrifiers, and many industrial waste components are toxic to nitrifiers or pH-altering.
 - 2) Because heterotrophs develop more faster than nitrifiers, they outcompete nitrifiers for oxygen and space when a high BOD load occurs. Since the slow-growing nitrifiers are unable to multiply quickly enough to keep up with the increased wasting or dilution brought on by the shock, they can be repressed or washed out.

- 3) As faster-growing carbonaceous organisms replace nitrifiers and are lost in wasted sludge, a prolonged high BOD event will actually ultimately cause nitrification to stop (48).

The findings indicate a decrease in nitrifier indicators (such as ammonia-oxidizing activity or nitrifier biomass fraction) throughout Days 3–13, which might lead to almost 0% nitrification by the shock's peak.

Only after the shock load is eliminated, and even then, there may be a lag in the autotrophic population's recovery. Nitrifiers would start to recover by Day 20 (one week following the shock), but because of their slow development, it would take several weeks for nitrification to fully recover.

In conclusion, the shock loading from Day 3 to Day 13 increased the inactive biomass percentage and devastated nitrifier populations, while also causing high F/M ratios and high OUR (after an initial fall) because of rising heterotrophic activity. The overall variations in treatment performance during the event are supported by these interrelated parameter modifications.

3.8 Changes in Process Rates

COD Removal and Hydrolysis

It is evident that a spike in COD processing rates was caused by the shock load. Colloidal COD adsorption increased from 8.3 to 21.2 mg COD/L·d, and the aerobic hydrolysis of particulate/enmeshed COD quadrupled from 465 to 931 mg COD/L·d, as indicated in Appendix (G). This hints that during the event, many organic materials were broken down and absorbed. After the shock, the net intake of slowly biodegradable COD increased by about ten times, from around 73 to 629 mg COD/L·d consumed. Put another way, the biomass was exerting a lot more effort to break down the influx of particulate matter and slow down COD. However, the model indicates that not all the newly created soluble COD could be absorbed right once. During the shock, the easily biodegradable COD increased at a net +258 mg COD/L·d, whereas under normal load it was being depleted (net –282 mg COD/L·d). During the shock load, this transient accumulation of soluble organics suggests a decrease in COD removal efficiency since substrates were being created (by hydrolysis) more quickly than

heterotrophs could consume them. Such a shock frequently results in an increase in intermediate metabolites or effluent COD in actual plants until biomass growth catches up. However, given a little extra time, well-acclimated biomass may frequently still oxidize the excess COD if aeration and mixing are enough. In this case, the system did react by producing additional heterotrophs (explained below), indicating that it was able to consume the extra COD and demonstrating some resistance.

Ammonia Release and Ammonification

The ammonification rate (conversion of organic N to NH_4^+) increased from 40.8 to 56.1 mg N/L·d when more organic nitrogen entered the system. This indicates that a greater amount of nitrogen (such as proteins, urea, etc.) was introduced by the shock load and quickly mineralized to ammonia. The breakdown of organic matter resulted in a surge in ammonia being released into the aeration tank. This increases the nitrifier's substrate, but if nitrification is initially unable to keep up, it may also result in quickly higher ammonia levels in the reactor.

During the shock, nitrifiers absorbed more NH_4^+ , which indicates that ammonia was originally greater, and that nitrification went into overdrive to compensate. In fact, the model's "rate for total ammonia" increased more negative (from -10.17 to -11.64 mg N/L·d).

Nitrification (Ammonia & Nitrite Oxidation)

The increased ammonia triggered an increase in nitrification activity. Nitrite oxidizing bacteria (NOB) growth about doubled from 1.17 to 2.14 mg COD/L·d, whereas ammonia-oxidizing bacteria (AOB) growth increased from 4.47 to 6.86 mg COD/L·d. Similarly, the tank's net nitrate creation more than doubled; according to the model, nitrate production increased from around 15.4 to 33.2 mg N/L·d. This suggests that to convert the excess ammonia into nitrate, the nitrifiers were replicating and working harder. Crucially, the net nitrite production rate increased from a negligible $+0.109$ to $+0.542$ mg N/L·d, indicating that some nitrite buildup had place during shock. To put it another way, nitrite accumulated five times greater than previously because not every NO_2^- was instantly changed to NO_3^- . When a shock load occurs, nitrification becomes imbalanced, which is a typical warning. This is usually caused by AOB producing nitrite at a little slower rate when NOB is under stress. One reason is because nitrifiers

are outcompeted by heterotrophic bacteria (which feed on the plentiful COD) for dissolved oxygen, which essentially makes oxygen more limiting for the slower NOB process (49). Nitrite conversion to nitrate may become a rate-limiting phase when there is a short rise in BOD because it raises the DO needed to maintain nitrite oxidation at a steady pace. Therefore, there was a transient oxygen deficit for nitrifiers in the aeration tank during the shock, which resulted in residual nitrite in the mixed liquid. The fact that nitrate output really rose significantly despite this indicates that nitrifiers continued to function, although under stress.

Denitrification

Anoxic denitrification is affected by the shock load in two ways. For denitrifying heterotrophs, the additional COD offers more electron donors; however, the surge of nitrate from accelerated nitrification necessitates reduction. The model's N₂ gas output (from NO_x reduction) increased from 1.93 to 2.27 mg N/L·d being stripped as N₂, indicating that denitrification did occur at a greater rate. Additionally, COD's anoxic hydrolysis quadrupled (much like aerobic hydrolysis), suggesting that the anoxic zone, assuming it existed, had an abundance of substrate for fermentation and use. Nevertheless, nitrogen removal efficiency decreased overall even with increased denitrification; nitrate was still existing in the aerobic zone more quickly than previously (33 vs. 15 mg N/L·d produced, as mentioned).

This suggests that the higher nitrate load during the shock was not entirely reduced by the anoxic zone (or anoxic pockets). Since heterotrophs have more food for NO₃⁻ reduction, high influent COD can promote denitrification to a certain extent. However, excess nitrate will persist if the system's anoxic capacity or carbon dose is exceeded.

Increased residual nitrate and some nitrites are shown in the data, which is consistent with denitrification failing to maintain 100%. It is likely that a substantial portion of the COD was aerobically oxidized rather than accessible for denitrification in the anoxic stage since the shock load was mostly supplied to the aerobic zone (for instance, surge right in aeration). Furthermore, the anoxic retention duration or volume may have effectively decreased, lowering overall denitrification, if aeration had increased in response to the shock (to manage the COD). This is consistent with research showing that even when COD removal remains high, temporary high organic loads typically

reduce overall N removal efficiency (50). In conclusion, there was a short-term buildup of NO_x (particularly NO_3^- and possibly NO_2^-) in the reactor/effluent because the system probably converted a lot of ammonia to nitrate (high nitrification) during the shock but was unable to convert all that nitrate to N_2 in time.

Oxygen Uptake and Aeration Efficiency

The oxygen requirement increased because of the shock load. Over the course of the event, the model's total O_2 consumption rate went from -343.7 to -389.1 $\text{mg O}_2/\text{L}\cdot\text{d}$, which indicates that the biomass had an almost 13% greater oxygen uptake rate (OUR). This makes sense since both increased nitrification and increased COD oxidation use more oxygen. This meant that to maintain dissolved oxygen levels, the blowers had to supply a lot more O_2 to the plant's aeration system. The DO concentration decreased during the first shock phase if the aeration system was full or unable to ramp up rapidly. Reduced DO would worsen the previously mentioned nitrifier competition problem, further delaying nitrite oxidation (49). Additionally, because aerators operating at full efficiency supply O_2 less effectively and at greater energy costs, it reduces total aeration efficiency. The aeration pump was forced to its limits by the shock load. When a shock occurs in actual operations, operators may notice a sudden reduction in tank DO until the aeration is increased. While a greater OUR during shock indicates strong microbial activity, it also serves as a signal that aeration must continue to prevent the formation of oxygen-starved zones. We may even observe isolated anoxic conditions developing in what ought to be an aerobic zone if the overload caused portions of the aeration tank to become oxygen depleted. Simultaneous nitrification-denitrification (some N removal in the aerobic zone) may result from this, but there is also a chance that NO_2^- or even soluble ferrous iron may be produced if anaerobic pockets arise (not shown here, but possible with extreme oxygen drop). In conclusion, the shock strained the aeration efficiency and significantly increased oxygen consumption, necessitating more airflow to sustain performance. Given that nitrification continued to progress smoothly, the system's ability to mostly fulfill this demand indicates that it had some aeration capacity in reserve, which added to its resilience.

Microbial Population Dynamics (Heterotrophs, Nitrifiers, PAOs, etc.)

Heterotrophic Biomass Surge

The aeration tank's heterotrophic bacteria population rise steeply because of the heavy organic loading. Ordinary heterotrophs' net growth rate more than doubled, rising from around 67.3 to 140.4 mg COD/L·d. This illustrates how BOD-consuming microorganisms quickly increase in response to the plentiful food (high F/M ratio). The heterotrophs were fed by the shock load, which accelerated their growth significantly compared to steady-state conditions. Shock events often result in such a biomass spike, as the microbial population moves toward high-rate feeders that can take advantage of the quick substrate abundance.

Young, active cells (lower than average sludge age) made the mixed liquid more concentrated. There are two sides to this: on one hand, more heterotrophs imply a higher ability to consume COD, which is how the system adjusts to the shock. However, fast development can also increase the demand for respiration (as shown by OUR) and disrupt floc structure (many new cells can produce lighter flocs or stay scattered). Crucially, when food is abundant, heterotrophs outcompete other organisms for oxygen and substrates. Most of the easily accessible COD (and even some oxygen that nitrifiers also need) would have been overwhelmed by the heterotrophs during the shock. The data clearly shows the dominance of heterotrophs, whose growth rate throughout the event was orders of magnitude larger than that of any specialist bacteria. The system's attempt to self-correct by directing more biomass into rapidly developing degraders is demonstrated by this type of community shift, which is a natural adaptation to an organic overload.

Nitrifier Population – Maintained but Diluted

As slower-growing autotrophs, nitrifying bacteria (AOB and NOB) did enhance their activity, but they were unable to short-term reproduce as quickly as heterotrophs. The model indicates that during the shock, the net growth of ammonia-oxidizer biomass increased from 1.66 to 4.27 mg COD/L·d, whereas that of nitrite-oxidizer biomass increased from 0.44 to 1.35 mg COD/L·d. These encouraging growth rates indicate that the nitrifier populations were thriving rather than collapsing, which is a favorable

indication that they withstood the shock. However, because heterotrophs increased, nitrifiers made up a lower portion of the biomass during and just after the shock.

This can temporarily reduce the effective nitrification capacity per unit biomass in a mixed culture until the nitrifiers increase in number. The data does not reveal net deterioration; in fact, nitrifier net growth remained positive, suggesting no significant loss. However, there is a chance of some washout or loss of nitrifiers if the shock caused some sludge to be wasted or washed (more on that later). However, the higher nitrifier decay rates (NOB decay rose slightly from 0.733 to 0.790 mg COD/L·d) suggest that certain nitrifiers could have been subjected to stress or endogenous respiration because of the more severe circumstances. The important thing is that the nitrifying community seems to have been mostly unaffected by stress. They continued to function, although at their highest level, rather than vanishing, which would demonstrate negative net growth. This indicates a lack of significant toxic inhibition on nitrifiers; rather than poison, the impact is more likely to be one of competition and environmental stress (low DO, high ammonia). In many shock events, nitrifiers are the first to be knocked out if a toxic material is present (51). Their continuous development in this case suggests that the shock was primarily biological, or at the very least, not immediately harmful to nitrifiers. As substrate levels stabilize over a longer recovery time, the heterotroph population boom may diminish, allowing nitrifiers to recover their required portion of the biomass (particularly if the sludge age is maintained). However, nitrifiers were outnumbered and exerted a lot of effort during the shock, which is consistent with the nitrite accumulation (they were unable to completely remove all ammonia/nitrite during the peak loading).

Phosphate-Accumulating Organisms (PAOs) and Phosphorus Cycling

The results demonstrate that the shock load had a significant effect on PAOs, the bacteria that provide increased biological phosphorus elimination. Normal (pre-shock) circumstances showed some poly-P uptake and a little amount of PHA storage by PAOs (on acetate), but at incredibly low rates ($\sim 10^{-8}$ to 10^{-7} range). Those rates fell to two orders of magnitude (to zero) during the shock. For instance, PAOs' acetate-based substrate (PHA) storage decreased from 3.38×10^{-8} to 3.23×10^{-10} mg COD/L·d, which is insignificant. throughout the shock, PAOs' growth and uptake activities were at zero (no anoxic P uptake, no aerobic P uptake, both were zero before and throughout the

shock). In the meanwhile, PAO degradation persisted at around 10^{-9} mg COD/L·d. This suggests that throughout the shock event, the PAO population stagnated or even decreased. The biological P elimination process was either overpowered or suppressed. This might be explained by a few factors: (1) Substrate competition: Although the shock brought in a lot of carbon, PAOs cannot store that carbon as PHA unless the anaerobic zone contains VFAs like acetate. The easily degradable COD may have been consumed by common heterotrophs and GAOs (glycogen-accumulating organisms that compete with PAOs) before PAOs could use it. PAOs are frequently outcompeted by GAOs that do not contribute to P removal if the influent C:P ratio rises significantly. (2) Modified anaerobic/aerobic regime: The biological phosphorus release/uptake cycle's timing and environment can be disrupted by a shock load. For example, PAOs would not release P appropriately if the shock resulted in any oxygen spill into the anaerobic zone (because of excessive airflow).

Alternatively, PAOs in the anaerobic zone could not receive the substrate they anticipate if the shock were sent straight into the aerobic zone. This would result in less PHA storage and less P uptake. (3) Inhibition: PAOs can be vulnerable to certain toxins or extremes (pH swings, etc.), even though heterotrophs and nitrifiers were unaffected. PAOs may have been temporally disadvantaged by the drastic chemical changes (such as pH brought on by CO₂ removal). (4) Dilution or washout: PAOs usually require longer SRT and develop more slowly. The PAO component may have been diluted by the massive increase in regular biomass, and PAOs may have been unreasonably eliminated since they were not actively developing if any sludge was lost or wasted during the event (either intentionally or by washout). Phosphorus release behavior has one effect. When PAOs absorb VFAs, they typically release orthophosphate in the anaerobic phase and subsequently absorb more P in the aerobic phase. Any phosphorus that PAOs released anaerobically would stay in solution until it was eliminated by another mechanism if they did not absorb almost any phosphorus during the shock, as the data indicates. In fact, the model indicates that the tank's ortho-phosphate (PO₄³⁻) removal rate decreased from -1.235 to -2.602 mg P/L·d (the negative sign indicates that PO₄ was being removed from the liquid).

Given that PAOs were not active, it is interesting that P was removed from solution more quickly following shock; this suggests that chemical precipitation is the P sink

(described under "Other Impacts"). The extra phosphate either remained in the water or was abiotically precipitated by the metals present since PAOs were not performing their function. Additionally, some PAO cell lysis may have taken place, causing dying PAOs to release their stored poly-P as orthophosphate, which would temporarily raise the amount of soluble P. If pH increased, any such release along with the shock's high NH_4^+ might cause struvite precipitation. In summary, the shock load caused the EBPR to become unbalanced; as a result, the system had to address phosphorus through physicochemical pathways because the specialized P-removers were asleep. When a toxic impact or high organic load occurs, biological P removal effectiveness decreases and effluent P levels might rise unless chemical P removal takes place (52).

Microbial Inhibition or Toxicity Signs

The alterations seen are compatible with an organic overload rather than a toxic shock, and the results show no obvious signs of acute toxicity altering the biomass. We would anticipate considerable biomass degradation and nitrification loss (often >50% inhibition) under a toxic shock situation (53), and maybe floc breakdown (with protozoa vanishing and cells dying) (54). The fact that nitrifiers are still growing and heterotrophs are flourishing here indicates that the substrate was non-toxic and easily biodegradable. For certain groups (such as fermenters and nitrifiers), the tiny increases in decay rates are negligible and the result of regular endogenous respiration at larger biomass levels rather than a toxic impact. Additionally, after an initial surge in oxygen uptake, toxic shock frequently results in an immediate decline (as microorganisms are destroyed); in contrast, our OUR climbed and remained high, suggesting that bacteria remained active. We may thus assume that the shock was a high-organic event that lacked inhibitory chemicals; in other words, it was more of a "food shock" than a "toxic shock".

This divergence is significant because it indicates that the microbial community did not collapse or die out but rather saw a change in structure that favored fast growers.

Biomass Washout Potential

One danger of a shock load is that biomass may be washed out of the system by the increased flow or turbulence (if the shock also included hydraulic surges). Washout might not be severe in the short run if the shock was only a concentration rise at normal

flow. The model indicates increased biomass output rather than a decline in total biomass. However, some biomass loss may result from settling issues or clarifier stress (see below). We may observe a net negative "rate for heterotrophic biomass" (meaning losing biomass) or something like for nitrifiers, which we do not, if there had been substantial washout.

Therefore, rather than being flushed out, the biomass mostly remained in the reactor and was able to grow inside. This demonstrates resilience once more since the biomass was simply redistributed among the many sorts of organisms rather than being lost forever.

To summarize, the microbial ecology was altered by the shock load: PAOs were freezing out, nitrifiers persisted (although under stress), heterotrophs and de-nitrifiers grown. There is no proof of a significant harmful hit; instead, it was a case of "feast conditions" that favored some populations. These dynamics are consistent with well-known competitive principles: typical heterotrophs (and GAOs) will predominate with high carbon loading, frequently at the expense of PAOs (which need a balance of anaerobic/carbon and aerobic conditions) and nitrifiers (which prefer slower, low-C settings). A degree of biological resilience is demonstrated by the system's capacity to sustain nitrification (although with some nitrite accumulation) and develop again, however the suppression of PAOs indicates a change in community function that may have longer-term effects on nutrient removal.

3.9 Biological Process Performance

Aerobic Oxidation and Respiration

The shock caused the aerobic processes in the tank to speed up. The aerobic heterotrophs switched to a high-rate respiration mode, consuming substrate, and oxygen as quickly as possible, in response to the increase in rapidly biodegradable COD. Intense aerobic metabolism was confirmed by the spike in the dissolved oxygen uptake rate, which was more negative. If aeration had been temporarily inadequate, this rapid respiration may have resulted in localized oxygen depletion in some areas of the tank, therefore generating micro-anoxic zones. Heterotrophs may use nitrate or nitrite as electron acceptors in these areas (simultaneous denitrification).

Even in assumed aerobic portions, the results do demonstrate a slight increase in anoxic activity. For example, heterotrophs' anoxic growth on nitrite increased (3.30 → 3.96 mg COD/L·d), indicating that some denitrification utilizing NO_2^- may have taken place, maybe because of oxygen constraint pockets. Overall, the BOD removal aerobic response rates successfully maintained up with the shock (no significant COD buildup other than the intermediates seen), indicating that aerobic functioning was deducted but not broken.

Acid/base changes and the generation of CO_2 are two consequences of severe aerobic oxidation. According to the model, CO_2 stripping quadrupled (more CO_2 was driven off, as CO_2 gas transfer increased from -109 to -248 g C/m³·d). Since eliminating CO_2 lowers carbonic acid, blowing out that much CO_2 increased the pH in the aeration tank. Although free ammonia inhibition is often an issue at high pH (>8.5), an increase in the aerobic zone's pH might alter the ammonium balance, boosting free NH_3 . Although we do not know the precise pH, the precipitation data - which will be covered later - confirms that the pH did rise sufficiently to cause mineral precipitation.

Thus, the aerobic processes changed the mixed liquor's chemistry (pH and gas balance) in addition to consuming organics and ammonia.

Anoxic/Denitrification Performance

There were two effects on the anoxic responses. On the advantage side, de-nitrifiers have lots of fuel because of the availability of COD. On the other hand, the anoxic zone may get less carbon than anticipated if any of the COD stayed in the aerobic zone (because of prolonged aeration or DO surplus). Assuming a conventional process structure (e.g., an anoxic zone followed by the aeration), the shock would have delivered a large COD to the anoxic region initially. A short-term nitrate deficit in the anoxic zone may result from the heterotrophs' expected quick consumption of most of the available nitrate (assuming they ran out of NO_3^- before consuming all the substrate). In such case, any remaining COD would go into the aerobic zone, where it might either oxidize to CO_2 or result in the above-mentioned aerobic denitrification. The results indicates that denitrification was exerting more effort because nitrate absorption did rise (not just nitrate production but also N_2 gas). Without process adjustments, the anoxic zone would have to quadruple its performance to keep up with the twofold increase in

nitrate output. Consequently, during the shock, more nitrate than normal left the anoxic zone and ended up in the aerobic effluent or the final effluent. This supports the concept that shock reduced the effectiveness of nitrogen removal (52).

Furthermore, anoxic pathways may be impacted by a larger nitrite presence because some de-nitrifiers prefer or degrade nitrite more quickly than nitrate. According to the model, heterotrophic growth on nitrite (as an electron acceptor) increased. Thus, denitrification may have happened in two stages: first, the nitrate was rapidly removed, and then the nitrite reduction was conducted. The modest amount of nitrite that accumulated indicates that the de-nitrifiers were unable to do the task in the allocated detention period.

If things go out of balance, another potential consequence in anoxic zones during shock is the production of intermediate chemicals such as nitrous oxide (N_2O). Although we do not have any data on N_2O here, if nitrate is low and nitrite is high, excessive COD can occasionally induce de-nitrifiers to create N_2O , a powerful greenhouse gas. This is hypothetical, but worth noting as a potential consequence in real facilities.

Anaerobic Reactions and Fermentation

The shock load would have a major effect in the anaerobic zone of the treatment train, which is typical for enhanced biological phosphorus removal EBPR. Intense fermentation would result from a rush of soluble and particulate COD into an anaerobic basin; common fermentative bacteria and acidogens would then turn the surplus COD into volatile fatty acids (VFAs) such as propionate and acetate. Acetate production/accumulation increased, according to the model (rate increased from +0.0219 to +0.0156 mg COD/L·d). However, net production decreased slightly, because of certain organisms rapidly consuming any VFAs that were created.

PAOs (and GAOs) may have quickly absorbed the generated VFAs in the anaerobic zone. While doing so, PAOs would typically release phosphate; but, as we saw, PAOs seem to have been inactive or outcompeted. Some VFAs could have been eaten by GAOs, which do not eliminate P. Additionally, some VFAs may have been transferred to the anoxic zone or absorbed onto biomass. The propionate rate was constant, indicating that whatever propionate that did develop was either utilized right away or

remained low. Overall, the anaerobic reactor produced a lot of VFA and released a lot of phosphate, but since PAOs were disrupted, the phosphate was not completely reabsorbed later, which resulted in a large amount of soluble P downstream (which was later alleviated by precipitation).

Although traditionally activated sludge is not made for methanogenesis, another anaerobic feature is that fermenters and methanogens in the mixed liquor may begin to exhibit activity if pockets become anaerobic under large loads. It is excellent that the methanogen model rates stayed at zero, meaning that no methane was produced; this indicates that the system did not become completely anaerobic for an extended period. Nothing noteworthy, though, since we see extraordinarily little methane gas and hydrogen gas transfer values in both situations. The shock prevented the aeration tank from producing anaerobic gas, which is to be expected because any anoxic pockets were temporary and swiftly re-aerated, preventing the occurrence of actual anaerobic digestion.

Intermediate Metabolites Build-up

Nitrite has been mentioned as a crucial intermediary that accumulated. In addition, the buildup of soluble biodegradable COD (readily degradable substrate) in the reactor during shock is a transitional phenomenon that indicates the presence of partly decomposed organic or metabolic wastes. Volatile fatty acids, soluble microbial products (SMPs), and fermentation byproducts that were not immediately eaten are a few examples.

A portion of the particulate COD was hydrolyzed to soluble organics more quickly than those organics could be oxidized or absorbed, according to the model's positive RBCOD production rate during shock. If microorganisms do not have the enzymes to break it down completely right away, the shock load may also appear temporarily as an intermediate if it includes any molecules (such as an industrial solvent surge or an uncommon substrate). Although there is not any proof of a particular intermediate here (all COD appears to be worked on eventually), it is something to think about in actual situations because shock loads can occasionally contain chemicals that are not anticipated and can build up. Eps (extracellular polymeric substances) are an additional intermediary to consider. Bacteria can create more Eps (slime) in high substrate

conditions, which can alter the floc's characteristics. According to studies, shock loads frequently raise EPS, especially polysaccharides, which might have an impact on settling and nutrient elimination (52). Although Eps is not specifically mentioned in our data, the quick growth and low DO may cause organisms to exude more viscous substances, which might portend a minor slime bulking.

Toxic or Inhibitory Compounds

As previously stated, there is no obvious indication of harmful intermediates (for example, a quick decrease in activity may be observed if the shock contained a poisonous consequence). For completeness, we would anticipate nitrification and suppression of COD absorption if the shock had contained anything like a significant dosage of heavy metals or phenols (53), and perhaps the buildup of organic acids due to the freezing of beta-oxidation or other processes. None of it is shown; rather, everything accelerated, which is a sign of an excess that is mostly organic and that bacteria may break down. Therefore, we can state with confidence that the data shows no signs of toxic shock.

Overall Process Function

The biological process continued to operate during the shock, although at its limitations, despite certain imbalances. Aerobic oxidation persisted (no oxygen depletion collapse, only a decrease in DO), nitrification persisted, even though with some restriction at the nitrite stage, and denitrification persisted, although incompletely. The function that was most severely affected was the anaerobic/EBPR function (with P removal changing from biological to chemical). These modifications are consistent with well-known shock loading wastewater processes. Research has shown that a surge in BOD may be managed in terms of carbon removal, but nitrogen and phosphorus removals frequently drop during the event. High organic loads usually result in a transient overload of aerobic treatment and a change in nutrient removal routes (52). Our data agrees that nitrates accumulated, and biological P removal paused, whereas carbon removal was maintained (no significant effluent COD loss other than temporary).

Lastly, it is important to remember that these results might be influenced by operator's reactions during a shock. In a practical plant, operators can react by adding an external alkalinity source to buffer pH, boosting aeration (to oversee COD and nitrification), etc.

These reactions can avoid a DO crash or pH decrease, for example, but they can also cause other problems, such as over-aeration that lowers denitrification. According to the data we have, the system's inherent capability was put to the test during an uncontrolled or naturally occurring shock. In full nutrient polishing, it did not perform as well as it did in COD and ammonia oxidation.

3.10 Other Process Impacts (Settling, Washout, Gas Transfer, Precipitation)

Sludge Settleability and Bulking Tendencies

The settling behavior and bulking risk of the sludge itself are important consequences of shock loading. Heterotrophs that develop quickly (high F/M conditions) typically generate younger, lighter flocs. New biomass can generate "fluffy" flocs that settle poorly because it frequently contains more water. Furthermore, because filamentous bacteria like *Sphaerotilus natans* flourish in high organic, low DO conditions (typically at the intake end of aeration tanks), they could multiply if the shock resulted in any DO deficiency. After shock events or toxic upsets, when F/M is high and competition is weakened, filamentous bulking may occur (54).

The parameters (high BOD, locally low DO) were favorable for filament development in our situation during the shock. Although filamentous creatures may have flowered, this is not directly measured by the data. If so, sludge thickening (increased sludge volume index, inflated slow-settling sludge) might be seen in the days after the shock. The secondary clarifier may momentarily become overloaded because of the abrupt rise in biomass content, even in the absence of filaments. If some biomass in the aeration was sheared off or if there was increased bacterial production, a shock load may convey more solids to the clarifier, increasing the risk of washout or turbidity.

The clarifier would experience more particles removal due to hydraulic stress if the shock were accompanied by strong flow, such as a slug of high-strength wastewater volume. Although our analysis primarily assumes a concentration shock, it is important to remember that solids can be lifted by any increase in flow or gas generation. For instance, the "de-nit rising sludge" problem occurs when sludge particles rise and float due to increased N₂ gas produced by the enhanced denitrification inside the sludge (either in the aeration or in the clarifier blankets). There is a minor increase in the likelihood of bubbles forming in sludge because of the moderate rise in N₂ gas

generation. The additional N_2 might cause some sludge buoyancy and overflow if the clarifier held onto nitrate-laden sludge during a quiet phase.

Furthermore, according to published research, the shock altered the amount of EPS (extracellular polymer), which most likely increased polysaccharides (52)). Excess EPS can cause "slime bulking," which is a slimy sludge that does not compress effectively. In contrast to filamentous bulking, this also leads to poor settling. It is possible that the sludge temporarily got overwhelmed with bound water and EPS due to the heterotroph surge, which reduced the effectiveness of settling.

In conclusion, even though the data is centered on reaction speeds, it is likely that settling performance deteriorated after the shock. Higher SVI would result from more biomass and potential filament/EPS production. The plant may have to slow down flow to allow sludge to settle or incur some solids loss in the effluent if it is not effectively managed (for example, by using a selector or modifying wasting). If the sludge could resume normal settling following the shock (e.g., filaments die back when F/M decreases again, flocs are restabilized), it would demonstrate the system's robustness in this aspect. Bulking problems might not go away if the shock caused a long-term alteration, such as the loss of a sizable percentage of excellent floc formers. Bulking, however, was a temporary instability rather than a long-term issue because the microbial community mostly survived.

Transfer of Gas and Foaming

The transference of oxygen and CO_2 has previously been covered. Notable is the rising stripping of CO_2 ; as more CO_2 was forced out, the aeration's pH most likely increased ($-248 \text{ gC/m}^3\cdot\text{d}$). A higher pH can sometimes lead to improved foaming because filamentous organisms, such *Nocardia*, can generate stable foams in high F/M events and specific surfactants in wastewater bubbles more at a particular pH. Operators commonly notice foamy sludge during or after a shock, even if foaming is not visible here (especially if the shock contains fats, oils, or surfactants). Tiny bubbles may form in the aerator because of the rise in nitrogen gas production (denitrification gas) that we discussed; typically, these just release into the atmosphere (as caught in the gas transfer) until they become stuck in flocs. We do see that N_2 gas transfer got more negative, indicating that more N_2 was exiting the liquid, causing more bubbles to develop and be

released. Although this is excellent since it indicates the elimination of nitrogen, those bubbles may raise sludge if they were trapped behind a layer of biomass in a clarifier. Changes in gas transport therefore relate to the settling problem mentioned above.

The model also demonstrates zero changes in methane and hydrogen gas (CH_4 transfer remained at around 8.99×10^{-5} mg COD/L·d, while H_2 changed from -0.0164 to -0.0078 mg COD/L·d). Therefore, there will not be any problems with odor or flammable gases. Both before and throughout, there was no ammonia stripping, which is normal at normal pH and temperatures since ammonia remains in solution as ammonium.

Chemical Precipitation Reactions

The shock load has a very noticeable effect on the rates of mineral precipitation. The model forecasts a massive rise in scaling reactions during the shock: for example, calcium carbonate (CaCO_3) precipitation increased by 860×, from almost nothing (0.000424 g/m³·d) to 0.3673 g/m³·d. The precipitation of magnesium ammonium phosphate (struvite) increased by approximately 100×, from 3.6×10^{-7} to 3.6×10^{-5} g/m³·d. It even reversed from a minor dissolution (-2×10^{-8} g/m³·d) to a precipitation of 3.57×10^{-6} g/m³·d for amorphous calcium phosphate [$\text{Ca}_3(\text{PO}_4)_2$]. Magnesium carbonate (MgCO_3) was the most striking, rising from zero to 9.139 g/m³·d. These figures show the circumstances brought on by the shock load, which encourage the development of mineral solids in the mixed liquor.

The pH shift and supersaturation brought on by increased CO_2 stripping, as well as variations in ion concentrations, are the most reasonable causes. As said, aeration elevates pH by removing CO_2 (55). The solubility of carbonates and phosphates would be reduced by a higher pH (entering the mid-sevens or higher). When the solution surpasses their solubility, calcium and magnesium that are present in the water (due to hardness or upstream dosage) will precipitate out as CaCO_3 or MgCO_3 (particularly when CO_2 is eliminated, forcing the carbonate equilibrium toward solid formation). The model depicts CaCO_3 and MgCO_3 scaling, which means that carbonate scaling may have occurred in the biomass or on the surfaces of the aeration tank. Similarly, when Mg^{2+} , NH_4^+ , and PO_4^{3-} are present in adequate amounts and the pH is normally above ~7.5, struvite ($\text{MgNH}_4\text{PO}_4 \cdot 6\text{H}_2\text{O}$) develops (56). We had high PO_4^{3-} due in part to

PAOs not taking it up and high NH_4^+ from ammonification during the shock. The circumstances were favorable for struvite when the pH rose due to CO_2 outgassing. The model verifies a significant increase in struvite precipitation. This has two benefits: on the one hand, it purges the water of phosphate and ammonia, improving the effluent quality for those nutrients. Uncontrolled struvite, on the other hand, can build up in the system where you do not want it to and block pipes and pumps. This chemical treatment may have preserved the effluent phosphate levels by turning it into a solid, as PAOs were not actively removing P. The shock caused the system to "switch" to chemical phosphorus elimination mode. In order to precipitate struvite for P recovery, many plants purposefully raise the pH in their side streams (55), here, it happened in the mainstream by accident. A certain amount of ammonium is also used by the struvite precipitation (1 mol NH_4 per mol struvite). However, it would not significantly lower the total N-load because the amount of precipitation was little in absolute nutritional terms (3.6×10^{-5} g/ m^3 is tiny). The significant MgCO_3 precipitation indicates that there was a significant amount of magnesium in the wastewater (from groundwater or specific industrial inputs), and that MgCO_3 separated from the solution when CO_2 was removed. This may have consequences, like scaling on walls or aerator diffusers.

To summarize, a series of inorganic processes were triggered by the shock: Significant mineral scaling and the production of struvite were generated by the pH being elevated by CO_2 stripping (56).

Thus, in addition to the biological reaction, the system also exhibited a chemical response, which successfully precipitated out part of the surplus nutrients. A rapid rise in precipitate (white coatings or crystals) in the aeration tank may be noticed by operators. If left unchecked, this can eventually lower the efficiency of the equipment (e.g., fouling aeration membranes from CaCO_3). However, it had the short-term benefit of buffering the phosphate release brought on by PAO disruption.

Solids Production and Wastage

Unless more biomass is wasted, the system's total suspended solids (TSS) would rise as biomass growth increased. As the yield coefficients at high loading create slightly less inert percentage per unit COD eliminated, the model indicates an increase in the generation of unbiodegradable cell products from 27.97 to 23.13 mg COD/L·d. This is

an intriguing minor decline. In any event, more biomass is released (either as endogenous residue or as new cells) when more organic substrate is ingested. If no additional waste were conducted, the plant would experience a rise in MLSS following the shock.

To keep the system from being overwhelmed with young sludge during an extended shock, operators frequently increase sludge waste. Given that this is an acute occurrence, they may wait and let the biomass eat up the remaining COD. However, to restore the target SRT, it might be necessary to eliminate extra biomass once the shock has passed. Otherwise, the system can briefly switch to a lower SRT (because the mean age is diluted due to the increased biomass). The results indicate an increase in heterotrophic biomass followed by its requirement to decompose or be wasted suggests that the shock caused a rise in sludge formation.

Summary of Other Impacts

The shock load affected the physical and chemical parts of the process in addition to challenging biology. The chemistry of the tank changed to encourage mineral precipitation, gas emissions (CO₂, N₂) rose, and sludge settleability deteriorated (risk of bulking or washout). All these phenomena in high-load situations are widely recognized. For example, according to EPA studies, increased BOD loading may increase the DO needed to prevent bulking (49), and uncontrolled pH fluctuations might lead to aeration tank scaling. Our findings align with such trends.

3.11 System Resilience vs. Prolonged Instability

Overall, the system displayed a combination of robust performance and transient instability when subjected to the shock load. Positively, the biomass was able to rapidly increase activity, preventing a total treatment failure, and the core treatment (COD and ammonia elimination) was maintained. Heterotrophs reduced demand in certain areas (producing soluble COD that they would later consume), and nitrification was slowed but still functioning. There were no signs of a complete breakdown. This implies that the system was capable of withstanding the shock. The microbial community dynamically changed rather than collapsing, as demonstrated by the fact that heterotrophs doubled in growth rate over the interval while nitrifiers continued to develop (not die). In the context of wastewater treatment, resilience is characterized by the ability to manage an

unexpected input by increasing biomass and process rates. Furthermore, as the shock decreased and regular loading began, any adverse effects (such as nitrite buildup or increased effluent nitrate or phosphate) were reversible. For instance, if the heterotrophs ceased to take over oxygen, the accumulated nitrite would be converted to nitrate, and if normal anaerobic/aerobic circumstances were restored, PAO activity may resume in later cycles. Nonetheless, the shock undoubtedly created certain instability, some of which may have persisted if left unchecked. The biggest effect is the disturbance of nutrient removal; elevated levels of phosphate and nitrate may remain in the effluent for a while after the shock until the biological cycles have stabilized. PAO function loss may not be instantly restored; it may take days for PAOs to regenerate from the residual population. During such period, the system may have higher effluent P or, if circumstances permit, rely on chemical precipitation. This is a temporary decrease in phosphorus removal performance, a sign of instability in that process step. In a similar line, any filamentous bulking brought on by the incident may result in settling issues that persist after the high loading phase. Once they have multiplied, filaments frequently need to be reduced by intervention (such as selectors, chlorination, or simply waiting out many sludge ages). Therefore, even when influent conditions return to normal, the shock's subsequent consequences (such as thickening sludge or a change in the structure of the microbial population) may cause ongoing instability in operations. For example, sludge settleability may have stayed low for a few days, which would have complicated sludge retention management and kept effluent TSS high. In terms of data, we would anticipate that after the shock conditions decrease, the heterotrophic growth rate would decrease (less substrate means that some of the excess biomass would go into endogenous respiration or die-off). Additionally, the nitrifiers, which now have a lot of ammonia converted to nitrate, might see a decrease in substrate (since ammonia input would return to normal), which could result in a temporary excess of nitrate that gradually gets denitrified. With some extra biomass that was not there previously, the system would progressively revert to its prior steady state.

That could exceed the system's requirements, increasing the need for oxygen long after the shock has passed until the biomass is depleted or dies. Burning off the excess biomass and restoring population balance, including allowing PAOs to recover are the main components of the recovery. The system's ability to continue processing

wastewater in a modified manner is proof of its resilience. There was no fundamental breakdown, such as a large biomass washout or total nitrification failure.

It is also possible to see the chemical precipitation that occurred as the system's natural physicochemical buffers absorbing part of the damage (a sort of self-healing aspect: excess P and alkalinity precipitated, preventing an even worse consequence for effluent P or pH).

This type of resilience is present in many well-designed activated sludge systems; they can withstand brief shocks up to a certain point, with performance dropping but not falling. On the other hand, if this shock had been poisonous or beyond the system's capability, we would have seen long-term instability, such as the need to reseed the biomass or nitrification requiring weeks to recover due to the nitrifiers being killed. Fortunately, that degree of disruption is not shown by the statistics. The system was shaken (as evidenced by intermediate accumulations and changed paths), but it adapted and will settle down with time, suggesting that it is temporary instability. Operational response is another face of resilience. The damage would be lessened if the operators had identified the shock and taken prompt action (increasing aeration, adding alkali to counteract the pH decrease from nitrification, dosing a precipitant or polymer to aid settling). True resilience would be demonstrated by those rates returning to normal and the system regaining their pre-shock removal efficiency. The data we evaluated represents a snapshot taken "during the shock." For example, once normal conditions return, we would expect to see the nitrite rate revert to almost zero, the phosphate removal by PAOs to resume, etc. In summary, the aeration tank experienced major but mostly controllable changes during the shock load event: the microbial balance significantly shifted toward heterotrophs (while nitrifiers and PAOs were under pressure), nitrification was stressed (with nitrite buildup), COD degradation rates increased, and oxygen demand rose steeply. These modifications resulted in short-term reductions in nitrogen and phosphorus removal performance as well as some operational bothers such mineral scaling and worse settling.

Crucially, the system demonstrated an adaptive response (increased biomass growth and alternate removal mechanisms like precipitation) rather than catastrophic collapse. This implies that the plant was resistant to shock loading. The observed instability was

temporary; given the strong microbial reaction and supporting measures, it is anticipated that the system would regain equilibrium following the shock rather than experiencing a prolonged collapse.

The shock load was a stress test of the plant's capabilities as it briefly upset the treatment balance. When biodegradable organics are introduced, the main alterations (increased COD hydrolysis, DO consumption, nitrite buildup, and PAO inactivity) all occur as expected. While regions like EBPR and settling show where instability might demonstrate, the system's continuous operation (although in a modified form) at that time shows resilience. By connecting these observations to well-known phenomena, such as oxygen competition in nitrification, the effects of carbon overloading on nutrient removal, and bulking following high F/M shocks, we can see that, despite being disruptive, the shock load event was managed as well as the biological process could have predicted, with recovery probably occurring quickly after conditions returned to normal.

3.12 Mitigation Strategies to Improve Resilience to Shock Loads

Several methods may be used in plant design and operation to stop or mitigate the effects of similar shock loads in the future:

Operational Adjustments During and Before Shocks:

1. Equalization and Controlled Feeding

Use surge basins or flow and load equalization tanks to catch unexpected industrial wastewater inputs (57). The WWTP may prevent the abrupt increase in F/M by holding and releasing the influent gradually. In this instance, the biomass would have had more opportunity to adapt and prevent severe inhibition if the Day 3–13 load had been gradually metered into the biological process over a longer time span. One of the best defenses against both hydraulic and biological shock loads is an equalization tank.

2. Dilution and Diversion

Operators can reduce the impact on the primary process by redirecting a portion of the incoming shock load for instance, to a holding lagoon or an underutilized tank if an equalization basin is not available. Toxicology and severe F/M fluctuations can also be

decreased by mixing industrial waste with municipal wastewater, if available, prior to entering the bioreactor.

3. Increase Aeration Capacity

At the start of a shock load, operators should increase aeration rates (e.g., turn on more blowers) in anticipation of increasing oxygen demand. For heterotrophs to utilize the extra BOD without becoming anaerobic and to give any remaining nitrifiers a shot at survival, it is vital that proper DO be maintained. If volatile toxins are present, further aeration aids in their removal. High-range automatic DO control devices or oxygen supplements (such as pure oxygen infusion in an emergency) may be helpful.

4. Modify Sludge waste (Increase SRT)

To extend the solids retention time during shock loading, it might be advantageous to temporarily decrease sludge waste. To sustain slow-growing nitrifiers and manage a greater load, a higher SRT retains more biomass in the system. Although MLSS will rise, preserving biomass can stop the washout of the very populations required for recovery if the clarifier can manage it or if it is used in conjunction with a selector to preserve proper settling. Basically, by retaining excess biomass, the plant may purposefully operate at a lower F/M as a buffer against high feed circumstances (58).

5. Bypass and Step-Feed

A portion of the flow can be divided among many feed points or directed straight to subsequent stages (avoiding the first aerobic tank) in certain plants with bypass lines or step-feed arrangements. Step-feeding can lower the initial shock to any one reactor zone and more uniformly distribute the load across the bioreactor capacity. Additionally, this can prevent nitrifiers from being overloaded with carbon by directing more BOD to a different area, protecting nitrification zones.

6. pH and Nutrient Control

Dosing neutralizing agents or nutrients can assist stabilizing conditions if industrial wastewater has an undesirable pH or is lacking in nutrients (industrial wastes may be lacking in nitrogen or phosphorus essential for biomass development). For instance, if a low pH shock is noticed, add alkali; if the BOD: N:P ratio is out of equilibrium, add diammonium phosphate. In an environment with an abundance of carbon, biomass can

grow to consume the extra BOD instead of starving to death when nutrition levels are appropriate.

3.13 Long-Term Process and Design Strategies

1. Industrial Pretreatment

Require the industry to build or enhance pretreatment for its effluent since it is the best mitigation strategy. For example, industry might equalize and partially treat (e.g., neutralize pH, remove heavy metals, or lower peak organics) prior to discharge if high COD is a problem. This keeps WWTP from first experiencing so strong shocks. This is enforced by industrial wastewater permits procedures at several municipal facilities.

Robust Biomass and Diversified Microbial Community: Preserve a resilient, diversified microbial community.

Bioaugmentation, or seeding the system with certain strains, is one method. Toxic substances can be rapidly consumed by introducing a bacillus blend or degraders before an expected shock. According to studies, bioaugmentation can mitigate the effects of toxic shocks and expedite the process' recovery (59).

Resilience can also be increased by ensuring that a certain percentage of the biomass get acclimated to industrial waste (via gradual exposure).

2. Integrated Fixed-Film Activated Sludge (IFAS) or Biofilm Systems

A refuge for biomass during high flows or harmful events can be created by upgrading the system to incorporate attached-growth medium (such as plastic carriers in IFAS or trickling filter/roughing biofilter pretreatment). Because of the extracellular matrix's ability to protect microorganisms and the greater diversity found therein, biofilms are often more resistant to shock loads. For example, IFAS systems have demonstrated a greater working range for MLSS and F/M and improved recovery from toxic shocks compared to traditional suspended growth (60). Because they stick to the media and do not wash off readily, these systems are better at retaining nitrifiers, allowing for some nitrification even at high throughput.

3. Multiple Stages and Redundancy

The shock effects can be localized by designing the WWTP with numerous treatment stages (for example, a secondary polishing step after a separate high-rate primary treatment for high BOD). The primary nitrification step might be shielded from the full force of an industrial load by an anaerobic pretreatment unit or high rate activated sludge. The ability to isolate and take one reactor offline, as well as redundant basins, might be helpful. For example, one overloaded basin could be brought offline to recover while others manage the flow.

4. Real-Time Monitoring and Early Warning

Invest in monitoring technologies that can identify unusual load surges. An increase in loading or hazardous circumstances can be detected early with the use of online COD/BOD sensors, ammonia analyzers, and respirometers (OUR sensors). For instance, operators would be notified to act (divert flow, modify aeration, etc.) even before traditional lab findings catch up if there was a significant increase in OUR or a decrease in DO. Proactive management actions and the activation of backup plans are made possible by early identification (57).

5. Emergency Protocols and Training

Create a well-defined shock-load response strategy. Predetermined actions include alerting plant personnel and the industry discharge, increasing aeration, stopping sludge wastage, introducing chemical neutralizers if known toxins are present, and increasing the frequency of monitoring. Employees should be taught to spot shock load indicators (such as foam, abrupt DO decrease, etc.) and act quickly. After the occurrence, nitrification can be recovered more quickly if there is an on-site supply of nitrifier seed culture or if transported seed sludge is available (some facilities retain a side stream nitrifying bioreactor or medium that can be used to reseed the main plant).

To sum up, the shock loading event that occurred between Days 3 and 13 gave WWTP a stress test. The system first degraded under the high and potentially harmful load, but once conditions stabilized, it progressively adapted and recovered, according to the examination of the F/M ratio, VSS composition, OUR, and microbial populations. The core of wastewater treatment performance is microbial ecology; when the equilibrium is

upset (high F/M, toxin input, DO depletion), treatment efficiency directly suffers. Fortunately, the system's partial recovery shows its natural resilience while also pointing up areas that need work. Through operational and design strategies, we may strengthen the plant's defenses by comprehending the trends and reasons for this incident. This guarantees that the WWTP can remain stable in the face of upcoming shock loads, safeguarding the plant's microbial "engine" as well as the quality of the water discharged into the environment.

3.14 Analyses of Final Clarifier Behavior during the shock load

By separating biomass (sludge) from treated effluent, a secondary clarifier is essential to the activated sludge process. The internal hydrodynamic processes that take place within a clarifier are seen in Appendix (P) and they are divided into three primary layers:

Analyses of Final Clarifier Behavior during the shock load

By separating biomass (sludge) from treated effluent, a secondary clarifier is essential to the activated sludge process. The internal hydrodynamic processes that take place within a clarifier are seen in Appendix (P) and they are divided into three primary layers:

Top Layer: Consists of mostly suspended solids-free cleared effluent. After flowing upward, the liquid leaves through an overflow weir for disposal or additional processing.

Feed Layer: This is where the influent wastewater enters, containing biological flocs and suspended particles. Because the clarifier is built to reduce turbulence, flocculation and early settling can take place.

Bottom Layer: Denser sludge particles gather in the sludge blanket when they settle owing to gravity. A part of this sludge is returned to maintain the biomass concentration in the aeration tank (Return Activated Sludge, or RAS), while the remainder is regularly removed by Waste Activated Sludge (WAS) pumping.

Solids concentration, sludge settling properties, and hydraulic loading all affect the clarifier's performance. Solids washout can deteriorate effluent quality if the concentration of sludge rises too much or if hydraulic overloading takes place.

1. Settling Velocity and the 1-D Flux Model in Our Research

In wastewater process simulations (such as GPS-X and BioWin), the Takács model and the 1-D flux model as described below in (equation 11 and Annex) are frequently used to optimize clarifier design and operating strategies. These models are essential for:

- maintaining optimal sludge blanket levels by optimizing RAS and WAS rates.
- forecasting clarifier overloading and sludge blanket rising at periods of high flow.
- striking a balance between hydraulic retention duration and influent solids loading to increase secondary clarifier efficiency.

1. Changes in Key Variables (Before vs. During Shock Load)

a) High Suspended Solids Overload.

As shown in appendix (Q) and appendix (R), TSS in the FST influent was 1047 mg/L before the shock load, however it was only 50.98 mg/L in the effluent, showing a strong solids removal efficiency (~95.1%).

Input TSS increased to 2582 mg/L (+146%) and effluent TSS increased to 1659 mg/L (+3156%) during the Shock Load.

This indicates that the clarifier was unable to efficiently settle solids, most often because of overloading, inadequate sludge settling, or growing sludge problems.

b) Extremely elevated levels of BOD and COD in wastewater.

In the FST effluent, BOD increased from 49.22 mg/L to 3586 mg/L (+7100%) and COD increased from 151.6 mg/L to 8788 mg/L (+5700%).

This indicates that solids and a lot of organic materials were fleeing the clarifier improperly separated. There is an excess of sludge in the effluent because the clarifier does not retain biomass.

c) Nitrite accumulation and nitrification failure.

Nitrification ceased or washed out entirely when the nitrate concentration dropped (from 37.32 mg/L to 0.004 mg/L).

The increase in nitrite concentrations from 0.26 mg/L to 81.9 mg/L indicates partial nitrification, in which nitrite oxidizers failed while ammonia oxidizers were active. Ammonia quadrupled, indicating that nitrifiers were using less.

d) Phosphorus & Alkalinity Effects

Because of probable chemical precipitation reactions (a pH rise may have caused calcium phosphate precipitation), total phosphorus decreased from 21.92 mg/L to 11.31 mg/L.

From 30.7 mg/L to 524.4 mg/L, alkalinity rose dramatically, suggesting chemical processes (such as the generation of struvite or the precipitation of CO_3^{2-}).

Increases in pH from 7.73 to 8.46 are consistent with substantial aeration-induced off-gassing and CO_2 stripping.

3.15 Clarifier Performance Failure & State Point Analysis

How successfully the final clarifier managed the shock load is shown by the state point analysis as explained below.

The state point was within the optimal clarifier operating range prior to the shock load appendix (R), suggesting satisfactory solids-liquid separation and sludge settling.

The COD was within acceptable limits (151.6 mg/L), whereas the TSS in the wastewater stayed low (~51 mg/L).

Overloading and Washout of the Clarifier During the Shock Load

- The clarifier was receiving more solids than it could settle because the state point moved over the intended solids loading curve as shown in appendix (R).

- The effluent TSS increased to 1659 mg/L, indicating a massive sludge washout; the clarifier's inability to separate solids efficiently led to a large discharge of BOD, COD, and suspended particles.

3.16 Possible Causes of Clarifier Overloading

a) High Organic and Hydraulic Load

The shock load caused a sharp rise in biomass and organic materials.

It is possible that the sludge blanket escalated too high, shortening the retention period and letting biomass leak into the effluent as shown in figures (16 & 17).

b) Bulking of Sludge or Disintegration of Floc

Without proportionate settling, the rise in TSS and VSS indicates a degradation in the floc structure of the sludge.

Slime bulking may have resulted from the abrupt rise in microbial activity (heterotrophs outcompeting nitrifiers), which created an oversupply of extracellular polymers.

c) Denitrification-Induced Rising Sludge

Nitrate levels were high (~37.3 mg/L) before the shock, indicating that denitrification was proceeding as usual.

Nitrate fell to 0.004 mg/L during the shock, indicating that the denitrification process had ended.

Rapid nitrate loss may have led to the formation of gas bubbles (N₂) in the sludge, which would have made it buoyant and exacerbated rising sludge problems.

d) Elevated pH and Chemical Deposition

The significant rise in pH (from 7.73 to 8.46) points to CO₂ stripping and the potential precipitation of phosphates or carbonates.

This may change the floc's characteristics, causing it to settle poorly or become more buoyant.

3.17 Consequences of Clarifier Failure

a) Infractions of Regulations

TSS (1659 mg/L) in the effluent is 3200% more than the legal limit of 50 mg/L.

This indicates that very turbid water discharged by WWTP might violate environmental discharge regulations as shown in appendix (W).

b) Depletion of oxygen in receiving water sources.

The effluent's elevated levels of BOD (3586 mg/L) and COD (8788 mg/L) would severely reduce the amount of oxygen in rivers. Hypoxia, fish deaths, and ecological harm might result from this.

c) Nitrification and Effluent Loss the Toxicity of Nitrite

The release of partly oxidized nitrogen is suggested by the decrease in nitrate (37.3 → 0.004 mg/L) and the rise in nitrite (0.26 → 81.9 mg/L).

Since nitrite is extremely harmful to aquatic life, habitats downstream would be seriously endangered if it were found in effluent at 81.9 mg/L.

d) Settling & Sludge Age Disruption

Slow-growing nitrifiers may be lost because of solids and biomass washout, which would lengthen the recovery time.

It might take weeks for the system to regain full biological activity if too much activated sludge was lost.

3.18 Strategies to Prevent Future Clarifier Failure

a) Increase Waste Activated Sludge (WAS) Removal

By lowering surplus biomass, higher WAS rates can avoid overloading the clarifier.

As a result, the FST input's TSS concentration would decrease.

b) Enhance Settling with a Coagulant

Adding ferric chloride or aluminum sulfate (alum) may assist in decreasing effluent solids and enhance settling of the sludge.

c) Increase Return Activated Sludge (RAS) Flow

By keeping more biomass in the system, higher RAS rates can lower the likelihood of sludge washout.

d) Reduce excessive DO and pH fluctuations by optimizing aeration.

CO₂ stripping brought on by high aeration increased pH and could have exacerbated precipitation or sludge thickening.

Proper microbial activity can be maintained, and pH spikes can be avoided with improved DO management.

e) Monitor and Control Nitrite Accumulation

Future shock loads should be controlled by slow load increases rather than abrupt surges because of the severe nitrite building (81.9 mg/L). Supplementing alkalinity may also assist in preserving nitrifier stability.

3.19 Analysis of WWTP Operational Adjustments During Shock Load

Ineffectiveness of Increased Airflow and RAS: Efforts to increase the flow rate of return activated sludge (RAS) and airflow to the aerators in an attempt at minimizing the effects of the shock load did not yield a substantial improvement in WWTP performance. Microbial efficiency and oxygen uptake were still below desirable. The air flow into the aeration tank increased from (500 m³/h to 1000 m³/h) in each of the ATs during the shock load from day 25.8 till day 34.4 without any improvements in the WWTP's efficiency as shown in figure (20).

Even in the presence of abundant oxygen, nitrification might collapse due to shock loads of toxic or inhibitory compounds (such as heavy metals, solvents, or certain organics) (61). Because the nitrifiers are biochemically hindered or killed in these situations, even adding aeration (DO) won't restore nitrification until the microbial population recovers (62). Kelly et al. (2004) shown, for instance, that single-pulse

shocks of toxins (such as cyanide, cadmium, and solvents) resulted in an instantaneous loss of nitrification and a gradual recovery over the course of days to weeks under normal aeration (61). Similarly, a recent research in Water (Tsai, 2022) discovered that nitrification only began after the inhibitory circumstances subsided and biomass expanded again, indicating that additional aeration had minimal effect on recovery in a shocked reactor since DO was already adequate (63).

While raising the RAS rate can temporarily retain particles in the system, it only serves to recirculate compromised sludge, making it an ineffectual solution on its own. Actually, by hydraulically overloading clarifiers and forcing additional solids out with the effluent, a too high RAS in an upset plant can exacerbate sludge settling (64).

According to field manuals, you must remove particles from bulking conditions more quickly than they collect; increasing RAS beyond a certain point just speeds up overflow and exacerbates effluent TSS (64). Furthermore, the biomass frequently deflocculates or bulks following a toxic shock because stressed or dead cells are unable to form dense flocs, which results in high SVI and poor settling (65). Bulking and filamentous bacteria can spread if this sludge (high RAS) is simply recirculated without being treated for its poor health. Since a sizable portion of the biomass is inert, toxic disturbances frequently produce an overgrowth of filaments like *Sphalerites natans* in the high-F/M outcome. This situation cannot be resolved by aeration or RAS correction alone (64). According to the research, aeration and RAS adjustments seldom restore nitrification on their own since they only address the symptoms (low DO or solids loss) while microbial inhibition is the underlying reason. They neither eliminate the inhibitory agent nor replace the lost nitrifiers (63). An aerated basin may have normal BOD removal but no ammonia oxidation until the nitrifier population recovers because, as one review states, "nitrifiers are excellent indicators of toxic shock" they are blocked at quantities that still let heterotrophs to operate (66).

Minor improvement with increased WAS: The effluent quality significantly improved when the flow rate of waste activated sludge (WAS) was raised from 60 m³/d to 300 m³/d at day 34.4, with COD, BOD, and ammonia concentrations decreasing more efficiently, the system quite recovered quickly, proving that removing excess sludge can successfully restore microbial equilibrium as shown in figure (20).

In contrast, recovery following a shock load frequently benefits from raising the waste activated sludge (WAS) rate. A percentage of the accumulated biomass is eliminated by wasting; crucially, this includes the dormant, injured, or toxic cells that are no longer in use. By removing this "dead weight" from the system, the operator reduces the age of the sludge and increases the amount of incoming substrate and nutrients that the surviving, healthier microorganisms may use to promote their development. This procedure facilitates the quicker restoration of an active microbial balance. To "keep the MLSS refreshed," technical experts stress that frequent or increased sludge waste is essential to avoiding the accumulation of contaminants and inert materials in the biomass (67). After a toxic shock, such toxins can stay adsorbed to floc and keep suppressing bacteria if no sludge is discarded. Many plants that escape waste have a gradual buildup of inorganic and non-biodegradable organics in the mixed liquor, which finally reaches hazardous levels that hinder microbial activity, according to a blog post by Christian (2023) (67). This situation results in a low percentage of active biomass and increases the sludge's vulnerability to bulking and subsequent disturbances. Conversely, higher WAS draws these harmful and inert substances out of the system, reducing their concentration. Waste also reduces the "false biomass" that was inflating the total solids but not aiding in treatment by decreasing the inventory of sludge (64). Consequently, the food-to-microorganism (F/M) ratio is reset to a more typical range, which inhibits excessive filaments and promotes the growth of floc-forming bacteria. It also results in a greater effective proportion of active microorganisms. Waste sludge removal is a crucial phase in recovering from an upset, according to textbooks on activated sludge operation. For example, a deliberate sludge waste to remove the decomposing floc is frequently followed by a toxic shock that kills nitrifiers. Fresh biomass can then re-colonize and reestablish nitrification, either naturally or by seeding (65). In lab reactors shocked with hazardous chemicals, floc recovery (re-flocculation) only happened after fresh biomass development, not only by discontinuing the toxin. This method was experimentally verified by Henriques et al. (2004).

The return to stable treatment can be accelerated by removing a portion of the damaged sludge and creating an environment that encourages recovery. Given the circumstances, raising the WAS rate is a useful maneuver to get rid of leftover pollutants and inert material, thus "making space" for the growth of a renewed microbial population.

Impacts of Sludge Management on Recovery (Case Studies): Laboratory research and extensive case reports show that post-shock sludge management has a significant impact on recovery effluent quality. Love and colleagues'-controlled tests provide a good illustration of the impact. In one research, reactors that received a toxic shock had a surge in effluent ammonia and a collapse in biomass settleability. Nitrification and flocculation only returned to baseline after two to three solids retention periods (with normal waste permitting old biomass turnover) (65).

This suggests that biomass turnover, or the amount of time required to remove or replace the inhibited organisms, correlates with the natural recovery timeline. Recovery can be sped up if operators step in to modify the sludge age. A stepwise feeding strategy (lower initial loading and gradual increase) combined with appropriate wasting allowed the fastest restoration of nitrification, while simply increasing aeration had little effect, according to Tsai et al.'s (2022) comparison of various recovery stimulation techniques in SBRs following a shock (salinity upsets in this case). In a different case study, a nitrification inhibitor (thiourea) disturbed an industrial WWTP, causing a nitrification breakdown and significant bulking. In response, the operators bioaugmented with a robust nitrifying culture after discarding away a significant amount of sludge. This method rapidly restored ammonia removal in the thiourea-shocked plant, according to Deng et al. (2022), whereas the unaugment control (without sludge replacement) remained nitrification-deficient and displayed continuous filament development (68). This practical illustration shows how removing the contaminated sludge and adding new biomass may significantly enhance recovery results. Maintaining an ideal sludge age and waste strategy is known to increase shock resistance even in the absence of bioaugmentation. According to operating data from municipal plants, systems that attempt to hold all solids (low WAS) experience lingering effects (high effluent NH_4^+ , TSS, etc.) for a longer period of time, while systems with shorter sludge ages (higher WAS rates) typically recover from toxic influent episodes more quickly because the community is younger and more resilient (67). In conclusion, case examples continuously show how important sludge control is to shock recovery: As the microbial population recovers, aggressive waste of damaged sludge and careful RAS/WAS management can aid in the removal of inhibitory residuals and excess biomass, enhancing settling and effluent quality. However, inadequate management frequently

results in prolonged periods of bad effluent (high ammonia or solids). One example of this is recirculating hazardous sludge (high RAS, low WAS) to "catch up." Adjusting sludge waste rates (and, when necessary, adding new biomass) is therefore supported by both experimental and field data as an efficient way to recover treatment performance following an industrial shock load as shown in appendix (S).

3.20 Comprehensive Risk Analysis of Non-Pretreated Wastewater

Several sensitivity tests revealed that the non-pretreated WW from the energy drink industry had the greatest impact on WWTP's facilities to reduce the shock load effect. One of the possibilities under investigation is JIFZ-WWTP experiencing a sudden discharge of 1000 m³/d from the energy drink industry's untreated WW on day three, which lasts for ten days, as seen in the appendix (T).

Impact of Removing "Energy Drink Processing" Flow and Optimizing WAS.

Key Observations from the Effluent Trends

1. COD and BOD Reduction

Effluent COD and BOD reached before the energy drink processing flow was removed, suggesting a high organic load that was more than the capacity of microbes to decompose.

The post-shock COD and BOD concentrations sharply decreased after this flow was stopped as shown in appendix (U), indicating that industrial wastewater from the production of energy drinks contained high-strength biodegradable and non-biodegradable organics that overloaded the biological treatment system.

By eliminating this source, the excessive food-to-microorganism (F/M) ratio decreased, which enhanced organic elimination and stabilized microbial metabolism.

The plant had entirely regained its treatment efficiency under the improved WAS method, as evidenced by the COD and BOD levels stabilizing at a much lower concentration after the shock.

2. Total Kjeldahl Nitrogen (TKN) and Ammonia Removal

Due to microbial inhibition brought on by the high-strength industrial waste, TKN was raised prior to the intervention, suggesting inadequate nitrification.

struggle for oxygen between nitrifiers (which oxidize ammonia) and heterotrophic bacteria (which consume BOD).

Following removal, TKN sharply decreased, indicating: Nitrifier recovery, perhaps because of less organic input and a better oxygen balance.

WAS optimization's efficiency in removing aged or inhibited biomass and encouraging the development of active nitrifiers.

The trend in nitrogen removal is consistent with research demonstrating that high WAS rates can hasten nitrifier regeneration and reinstate ammonia oxidation following a shock load incident (69).

3. Phosphorus Stabilization

The levels of total phosphorus (TP) showed very slight fluctuations.

The elimination of energy drink effluent avoided the possibility of phosphorus buildup in the system since it may include phosphorus-rich chemicals.

The sustained TP levels after removal indicate that the activated sludge system was able to prevent excessive phosphorus release from lysed microbial cells and restore biological phosphorus removal (EBPR) efficiency.

By repeatedly eliminating old biomass before cell lysis could release stored phosphorus, the enhanced WAS approach stopped phosphorus release (70).

1. Improved Suspended Solids (TSS) and Clarification

TSS was higher before the energy drink manufacturing effluent was removed, because of floc disintegration, biomass stress, or sludge thickening from an excessive organic load.

2. High F/M conditions, which encourage filamentous development and distributed flocs, result in poor sludge settleability.

3. TSS concentrations quickly decreased after removal, suggesting: Better clarifier performance and biomass settleability. Maintaining favorable sludge properties and avoiding excessive solids carryover were made possible by the higher WAS rate (71).

3.21 Interpretation and System Performance Impact

Why Was the Effluent Quality Improved by Eliminating the "Energy Drink Processing" Flow?

Organic Overload Reduction (COD/BOD)

Highly soluble carbohydrates and organic acids are probably present in the energy drink manufacturing influent, which leads to microbial proliferation and quick oxygen depletion.

After removal, the F/M ratio in the biological system was balanced, preventing heterotrophic bacterial excess and bringing the system back to steady-state conditions.

Why Was Maintaining WAS at 300 m³/d Effective?

By removing outdated, dormant biomass, active microbes were able to flourish, and treatment effectiveness was preserved.

Stabilizing treatment performance and regulating oxygen demand were made possible by preventing the buildup of extra sludge.

Research indicates that by decreasing inert biomass and encouraging active microbial growth, greater WAS rates aid in the recovery process following organic shocks (72).

Chapter Four

4. Conclusions

This study evaluated the treatment performance and resilience of the Jenin Industrial Free Zone Wastewater Treatment Plant (JIFZ-WWTP) under varying operational and loading scenarios, particularly focusing on its ability to manage industrial wastewater. The plant, which was originally engineered for domestic sewage using an extended aeration activated sludge process, faces substantial challenges as it transitions to serve a growing industrial catchment. A dynamic simulation model was developed using GPS-X software, incorporating the ASM1-based MANTIS framework. It was calibrated using 728 laboratory results from Jericho WWTP, with site-specific adjustments for climate and elevation to ensure realism in biological and hydraulic behavior.

Under baseline, steady-state conditions, the plant achieved high removal efficiencies for key pollutants. Simulations predicted an average reduction of total suspended solids (TSS) by 95.18%, volatile suspended solids (VSS) by 93.62%, chemical oxygen demand (COD) by 89.5%, and carbonaceous biochemical oxygen demand (cBOD₅) by 94.32%. Orthophosphate removal reached 99.88%, while total phosphorus (TP) was reduced by 66.45% likely constrained by the particulate bound fraction of phosphorus. Ammonia nitrogen removal was notably high at 98.7%, and total Kjeldahl nitrogen (TKN) removal reached 92.5%. However, total nitrogen (TN) removal remained relatively modest at 33.8%, limited by the absence of a dedicated anoxic stage and insufficient carbon for effective denitrification.

The plant's capacity to handle flow and pollutant load was further tested under shock loading conditions simulating an industrial discharge of 1,000 m³/day of untreated effluent. The system response was critical: COD spiked to 8,000 mg/L, BOD₅ rose above 3,500 mg/L, TP reached 63 mg/L, TKN climbed to 37 mg/L, and TSS exceeded 510 mg/L each far surpassing permissible discharge limits. These extreme values coincided with floc destabilization, biomass washout, and near-complete nitrification failure. Biological recovery, though gradual, highlighted the operational fragility of the system under unregulated industrial inputs.

The simulation identified a reliable operational flow limit of approximately 900 m³/day. Within this threshold, the system maintained effluent quality in accordance with Class C reuse or discharge standards. Beyond this range, the risk of treatment failure increased markedly. Sensitivity analysis further revealed that optimal process performance was sustained at a return activated sludge (RAS) rate of 460 m³/day and a waste activated sludge (WAS) rate of 60 m³/day. These setpoints preserved sludge age and mixed liquor balance, contributing to biological stability and minimizing the risk of clarifier overload or biomass loss.

To understand the variability of system performance under fluctuating influent quality, a Monte Carlo probabilistic simulation was conducted. The results were revealed: only 68% of scenarios achieved compliance for TN, while just 33% met COD and cBOD₅ standards. In contrast, TSS compliance was achieved in 87% of cases, reflecting the system's generally strong nitrification capacity but underscoring its sensitivity to organic load surges. These outcomes emphasize the operational risk posed by inconsistent or unregulated industrial discharges.

Considering these findings, it is evident that the current configuration of the JIFZ-WWTP is insufficiently robust to manage high-strength industrial wastewater without intervention. The biological processes, while effective under steady loads, lack the buffering capacity to absorb sharp fluctuations in pollutant concentration or flow volume. Therefore, the following recommendations are proposed to ensure long-term reliability and compliance with the treatment system:

- a) **Enforce comprehensive industrial pretreatment:** All industrial contributors to the JIFZ should be required to install and operate pretreatment systems tailored to their effluent characteristics. These may include pH adjustment, screening, equalization tanks, dissolved air flotation (DAF), anaerobic digestion, coagulation-flocculation units, chemical precipitation, and fine filtration stages.
- b) **Install real-time influent monitoring and early warning systems:** Continuous sensors for flow, COD, TSS, and pH should be integrated at the headworks to detect surges or anomalies before they compromise the biological process.

- c) **Maintain and dynamically adjust RAS and WAS flows:** Regular monitoring of sludge volume index (SVI), mixed liquor suspended solids (MLSS), and sludge age should inform RAS and WAS adjustments—particularly during periods of industrial variability.
- d) **Upgrade nutrient removal capabilities:** To improve TN removal, the introduction of an anoxic reactor with external carbon dosing (e.g., methanol) or operation in intermittent aeration cycles should be considered.
- e) **Develop contingency plans for overflow events:** Emergency protocols, including bypass or temporary storage options, should be established to handle extraordinary loading events while minimizing environmental harm.
- f) **Coordinate effluent reuse with quality assurance:** If the treated water is intended for irrigation, continuous compliance with reuse standards must be verified, and reuse must be suspended during any operational upsetting.

Future Research Areas

This thesis has advanced understanding of the JIFZ-WWTP's performance under variable and industrial wastewater conditions. However, further investigation is essential to improve the plant's resilience, efficiency, and regulatory integration. Key areas for future research include:

1. Shock Load Resilience

Future studies should evaluate design and operational improvements that enhance the WWTP's ability to absorb high-strength industrial discharges. This includes adding equalization tanks, emergency bypass systems, and implementing adaptive control strategies (e.g., variable aeration and recirculation). Scenario-based modeling of extreme events will help identify thresholds and preemptive actions to prevent system failure.

2. Sector-Specific Pretreatment

Strengthening industrial pretreatment is critical. Research should focus on customizing pretreatment systems for different industries in the JIFZ—such as DAF or anaerobic digestion for food processing, and chemical precipitation or filtration for textile or

tannery effluents. Installing real-time sensors at discharge points (monitoring pH, COD, and toxicity) can support compliance and early warning.

3. Advanced Modeling and Predictive Control

Building on the current GPS-X model, future work can integrate real-time data and AI to create a predictive “digital twin” of the plant. These tools could optimize aeration, sludge handling, and chemical dosing before a crisis occurs. Expanded uncertainty modeling (e.g., Monte Carlo) should also be used to design control systems with built-in safety margins.

4. Efficiency and Resource Recovery

Research can explore energy-saving strategies such as anaerobic pretreatment for biogas generation or phosphorus recovery from sludge. Further, optimizing aeration under variable loads and evaluating polishing technologies (e.g., wetlands or ozonation) will support safe effluent reuse and reduce operational costs.

5. Regulatory and Policy Frameworks

To complement technical advances, future studies should examine governance mechanisms that support compliance and risk management. This includes analyzing discharge regulation impacts, benchmarking international practices, and developing legal tools (e.g., contractual penalties or emergency holding ponds) to safeguard WWTP from industrial violations.

List of Abbreviations

| Symbol | Meaning |
|-----------|---|
| ASM1 | Activated Sludge Model no. 1 |
| ASS | Activated Sludge System |
| ADS | Anaerobic digestion system |
| AST | Activated sludge tank |
| AOB | Ammonia Oxidizing Biomass |
| BOD | Biochemical oxygen demand |
| BOD5 | Biochemical Oxygen Demand in a 5-day incubation |
| COD | Chemical Oxygen Demand in mgO ₂ /L |
| bCOD | Biodegradable COD |
| nbCOD | Non-biodegradable COD |
| sbCOD | Slowly Biodegradable COD in mgO ₂ /L |
| rbCOD | Readily Biodegradable COD mgO ₂ /L |
| MLSS | Mixed liquor suspended solids |
| TN | Total nitrogen |
| TP | Total phosphorus |
| TSS | Total suspended solids |
| VSS | Volatile suspended solids |
| JIFZ-WWTP | Jenin Industrial Free Zone – Wastewater Treatment Plant |
| AST | Activated Sludge Tank |
| FST | Final Sedimentation Tank |
| MCRT | Mean Cell Residence Time |
| PCBS | Palestinian Central Bureau of Statistics |
| PWA | Palestinian Water Authority |
| RAS | Recirculated Activated Sludge |
| WAS | Waste Activated Sludge |
| SRT | Sludge/solids retention time |
| SVI | Sludge volume index |
| TIC | Total inorganic carbon |
| VSS | Volatile suspended solids |
| DO | Dissolved oxygen |
| CSTR | Continuously stirred tank reactor |

| | |
|------|------------------------------------|
| HB | Heterotrophic bacteria |
| HRT | Hydraulic retention time |
| MC | Monte Carlo |
| MFC | Mass flow controller |
| PAO | Phosphor accumulating organism |
| SBR | Sequencing batch reactor |
| TAN | Total ammonium nitrogen |
| VSS | Volatile suspended solids |
| TKN | Total Kjeldahl Nitrogen |
| NOB | Nitrite Oxidizing Biomass |
| Eps | extracellular polymeric substances |
| VFAs | volatile fatty acids |

Nomenclature

| Symbol | Parameter | Unit |
|--------------------------|---|---------------------|
| X_{COD} | Particulate COD | mgO ₂ /L |
| S_s | Readily biodegradable soluble fraction of COD | - |
| S_i | Soluble inert fraction of COD | - |
| X_s | Soluble Biodegradable particulate fraction of COD | - |
| X_i | Particulate inert fraction of COD | - |
| X_{BH} | Heterotrophic biomass fraction of total COD | - |
| X_{BA} | Autotrophic biomass fraction of total COD | - |
| X_p | Inert materials fraction | - |
| S_{nh} | Ammonium fraction of soluble TKN | - |
| S_o | Dissolved oxygen | mgO ₂ /L |
| NO_2^- | Nitrite | mgN/L |
| NO_3^- | Nitrate | mgN/L |
| $\text{NH}_3 - \text{N}$ | Total ammonia (free NH ₃ -N and ionized NH ₄ ⁺ -N ammonia) | mgN/L |
| f_p | Particulate products fraction of biomass | - |
| i_{vt} | VSS/TSS | gVSS/gTSS |
| i_{cv} | $X_{\text{COD}}/\text{VSS}$ | - |
| f_{bod} | BOD ₅ /BOD ultimate ratio | gCOD/gVSS |
| i_{XB} | N content of active biomass | gN/gCOD |
| i_{XP} | N content of endogenous/inert mass | gN/gCOD |
| Y_H | Heterotrophic yield | gCOD/gCOD |
| Y_A | Autotrophic yield | gCOD/gN |
| U_A | Autotrophic endogenous fraction | - |
| $\mu_{\text{max,H}}$ | Heterotrophic maximum specific growth rate | 1/d |
| $K_{\text{S,S}}$ | Readily biodegradable substrate half-saturation coefficient | mgCOD/L |
| $K_{\text{O,H}}$ | Aerobic oxygen half-saturation coefficient | mgO ₂ /L |
| $K_{\text{A,H}}$ | Anoxic oxygen half-saturation coefficient | mgO ₂ /L |
| η_g | Anoxic growth factor | - |
| K_{NO} | Nitrate half-saturation coefficient | mgN/L |
| K_{NH_4} | Ammonia (as NH ₄ ⁺) half-saturation coefficient | mgN/L |

| | | |
|----------------|---|------------------------|
| b_H | Heterotrophic decay rate | 1/d |
| $K_{ALK, H}$ | Alkalinity half-saturation coefficient for heterotrophic growth | mgCaCO ₃ /L |
| $\mu_{max, A}$ | Autotrophic maximum specific growth rate | 1/d |
| K_{NH} | Ammonia (as substrate) half-saturation coefficient | mgN/L |
| $K_{O, A}$ | Oxygen half-saturation coefficient | mgO ₂ /L |
| $K_{ALK, A}$ | Alkalinity half-saturation coefficient for autotrophic growth | mgCaCO ₃ /L |
| K_h | Maximum specific hydrolysis rate | 1/d |
| K_X | Slowly biodegradable substrate half-saturation coefficient | gCOD/gCOD |
| η_h | Anoxic hydrolysis factor | - |
| K_A | Ammonification rate | mgN/L |
| Q | Inflow rate | m ³ /d |
| V | Volume of tank or reactor | m ³ |

References

1. How the Urban Water Cycle Works [Internet]. [cited 2025 Feb 16]. Available from: <https://www.sehinc.com/insights/how-urban-water-cycle-works>
2. Hao X, Li J, Liu R, Van Loosdrecht MCM. Resource Recovery from Wastewater: What, Why, and Where? *Environ Sci Technol*. 2024 Aug 13;58(32):14065–7.
3. Milenković L, Rađenović T, Baljošević A. The importance of wastewater treatment plants for sustainable development. *Econ Sustain Dev*. 2021;5(2):49–60.
4. Libhaber M, Orozco-Jaramillo Á. Sustainable Treatment and Reuse of Municipal Wastewater: For Decision Makers and Practicing Engineers [Internet]. IWA Publishing; 2012 [cited 2025 Feb 15]. Available from: <https://iwaponline.com/ebooks/book/468/sustainable-treatment-and-reuse-of-municipal>
5. Metcalf and Eddy, AECOM - Wastewater Engineering_ Treatment and Resource Recovery-McGraw-Hill (2014).
6. Elawwad A, Zaghoul M, Abdel-Halim H. Simulation of municipal-industrial full scale WWTP in an arid climate by application of ASM3. *J Water Reuse Desalination*. 2017 Mar 1;7(1):37–44.
7. Alagha O, Allazem A, Bukhari AA, Anil I, Mu'azu ND. Suitability of SBR for Wastewater Treatment and Reuse: Pilot-Scale Reactor Operated in Different Anoxic Conditions. *Int J Environ Res Public Health*. 2020 Mar 2;17(5):1617.
8. Ayoub M, El-Morsy A. Upgrading of an Extended Aeration System to Improve Wastewater Treatment. 2021;81(1).
9. Collivignarelli MC, Caccamo FM, Bellazzi S, Abbà A, Bertanza G. Assessment of the Impact of a New Industrial Discharge on an Urban Wastewater Treatment Plant: Proposal for an Experimental Protocol. *Environments*. 2023 Jun 22;10(7):108.
10. Orhon D, Germirli-Babuna Fatos, Karahan O. Industrial wastewater treatment by activated sludge. London ; New York: IWA Pub; 2009. 387 p.

11. Anera [Internet]. [cited 2025 Feb 15]. Jenin, Palestine: Securing a Productive Future. Available from: <https://www.anera.org/stories/jenin-palestine-securing-productive-future/>
12. Meijer, S. C. F. (2004). Theoretical and practical aspects of modelling activated sludge processes [Doctoral dissertation, Delft University of Technology]. Delft University Repository.
13. Gall, B. (1999, April 18–21). Review of activated sludge modelling. 1999 TAPPI International Environmental Conference and Exhibit, Nashville, TN, United States. Hydromantis, Inc.
14. Sedmak G, Bina D, MacDonald J, Couillard L. Nine-Year Study of the Occurrence of Culturable Viruses in Source Water for Two Drinking Water Treatment Plants and the Influent and Effluent of a Wastewater Treatment Plant in Milwaukee, Wisconsin (August 1994 through July 2003). *Appl Environ Microbiol.* 2005 Feb;71(2):1042–50.
15. Kops S, Vangheluwe H, Claeys F, Vanrolleghem P, Yuan Z, Vansteenkiste G. The Process of Model Building and Simulation of Ill-Defined Systems: Application to Wastewater Treatment. *Math Comput Model Dyn Syst.* 1999 Dec 1;5(4):298–312.
16. Corominas L, Flores-Alsina X, Muschalla D, Neumann MB, Vanrolleghem PA. Verification of WWTP Design Guidelines with Activated Sludge Process Models. *Proc Water Environ Fed.* 2010 Jan 1;2010(18):137–46.
17. Vanrolleghem PA, Jeppsson U, Carstensen J, Carlsson B, Olsson G. Integration of wastewater treatment plant design and operation — a systematic approach using cost functions. *Water Sci Technol.* 1996 Jan 1;34(3):159–71.
18. Makinia J, Zaborowska E. *Mathematical Modelling and Computer Simulation of Activated Sludge Systems.* IWA Publishing; 2020. 682 p.
19. Nelson, M. (2016). The biological treatment of wastewater. MI Lecture Note Series, 67, 34–39. Kyushu University, Institute for Advanced Study. <https://hdl.handle.net/2324/1566258>.

20. Hargrave BT. AEROBIC DECOMPOSITION OF SEDIMENT AND DETRITUS AS A FUNCTION OF PARTICLE SURFACE AREA AND ORGANIC CONTENT. *Limnol Oceanogr.* 1972 Jul;17(4):583–6.
21. Andrews, J. F. (1972). Control systems for wastewater treatment plants. *Water Research*, 6(4-5), 575–582. [https://doi.org/10.1016/0043-1354\(72\)90183-0](https://doi.org/10.1016/0043-1354(72)90183-0)
22. Atwater, J. W. (1973). A laboratory study on aerated stabilization basin operation at 3°C (Publication No. UBC_1973_A7 A88_3) [Master's thesis, University of British Columbia]. UBC Library. <https://open.library.ubc.ca/collections/ubctheses/831/items/1.0058497>.
23. Eckenfelder, W. W., Jr. (2000). *Industrial water pollution control* (3rd ed.). McGraw-Hill..
24. Wanner J. The development in biological wastewater treatment over the last 50 years. *Water Sci Technol.* 2021 Mar 12;84(2):274–83.
25. Ouano, E. A. R. (n.d.). *Principles of wastewater treatment, Vol. 1: Biological processes*. Saulog Press.
26. Vangsgaard AK. *Modeling, Experimentation, and Control of Autotrophic Nitrogen Removal in Granular Sludge Systems*.
27. Henze M, Grady CPL, Gujer W, Marais GVR, Matsuo T. A general model for single-sludge wastewater treatment systems. *Water Res.* 1987 May;21(5):505–15.
28. Mulas, M. (2006). *Modelling and control of activated sludge processes* [Doctoral dissertation, Università degli Studi di Cagliari].
29. Germaey KV, Jeppsson U, Vanrolleghem PA, Copp JB, editors. *Benchmarking of Control Strategies for Wastewater Treatment Plants* [Internet]. IWA Publishing; 2014 [cited 2025 Feb 23]. Available from: <http://iwaponline.com/ebooks/book/421/Benchmarking-of-Control-Strategies-for-Wastewater>

30. Sorour MT, Bahgat LMF. Application of Activated Sludge Models in Traditionally Operated Treatment Plants—A Software Environment Overview. *Water Qual Res J.* 2004 Aug 1;39(3):294–302.
31. Sokolowski JA, Banks CM. *Principles of Modeling and Simulation: A Multidisciplinary Approach.* John Wiley & Sons; 2011. 211 p.
32. ITMO University, Semenova TS, Sergienko OI, ITMO University. Simulation model of treatment facilities for the slaughterhouse of a poultry farm. *Process Food Prod Equip.* 2024;17(2):19–28.
33. Hasan SA, Nile BK, Faris AM. Modeling of the Full-Scale Secondary Sedimentation Basin Using the GPS-X Model. *Civ Eng J.* 2024 Sep 1;10(9):3034–52.
34. Latif EF, Elmolla ES, Mahmoud UF, Saleh MM. Intermittent cycle extended aeration system pilot scale (ICEAS-PS) for wastewater treatment: experimental results and process simulation. *Int J Environ Sci Technol.* 2020 Jun 1;17(6):3261–70.
35. Cao J, Yang E, Xu C, Zhang T, Xu R, Fu B, et al. Model-based strategy for nitrogen removal enhancement in full-scale wastewater treatment plants by GPS-X integrated with response surface methodology. *Sci Total Environ.* 2021 May 15;769:144851.
36. Al-Wardy A, Alquzweeni SS, Al-Saadi R. Modelling and Simulation of Al-muamirah Wastewater Treatment Plant by GPS-X Software. 2021 [cited 2025 Feb 15]; Available from: <https://consensus.app/papers/modelling-and-simulation-of-almuamirah-wastewater-al-wardy-alquzweeni/06fb918c147751ecb2edc675c89a1db1/>
37. Sadri Moghaddam S, Assistant Professor, Department of Civil Engineering, K.N. Toosi University of Technology, Tehran, Iran., Pirali M, MSc, Department of Civil and Environmental Engineering, Amirkabir University of Technology (AUT), Tehran, Iran. Modeling and calibration of a full-scale wastewater treatment plant

- using GPS-X model (A case study of Tehran). *Numer Methods Civ Eng*. 2021 Jun 1;5(4):67–76.
38. Belia E, Benedetti L, Johnson B, Murthy S, Neumann M, Vanrolleghem P, et al., editors. *Uncertainty in Wastewater Treatment Design and Operation: Addressing current practices and future directions* [Internet]. IWA Publishing; 2021 [cited 2025 Feb 15]. Available from: <https://iwaponline.com/ebooks/book/838/Uncertainty-in-Wastewater-Treatment-Design-and>
39. Mikosz J. Determination of permissible industrial pollution load at a municipal wastewater treatment plant. *Int J Environ Sci Technol*. 2015 Mar;12(3):827–36.
40. Messaoud, D., Bachir, A., & Muricee, M. (2013). Determination and analysis of daily reliability level of municipal wastewater treatment plant. *Courier du Savon*, 17, 39–46.
41. Sadri Moghaddam et al. - 2021 - Modeling and calibration of a full-scale wastewater treatment plant using GPS-X model (A case study).
42. Simon-Várhelyi M, Cristea VM, Brehar MA. Efficient calibration methodology of the wastewater treatment plant model based on ASM3 and application to municipal wastewater. *Desalination Water Treat*. 2020 Jun;189:108–18.
43. Varhelyi M, Cristea VM, Brehar M, Nemes ED, Nair A. WWTP MODEL CALIBRATION BASED ON DIFFERENT OPTIMIZATION APPROACHES. *Environ Eng Manag J*. 2019;18(8):1657–70.
44. Chen KL, Hou CW, Liu CW, Wang HY. Improving the operational performance of a wastewater treatment plant by using GPS-X simulations: a case study in northern Taiwan. *Sustain Environ Res*. 2025 Mar 4;35(1):8.
45. Nov. 12, 2017 U. *thewastewaterblog*. 2016 [cited 2025 Mar 7]. Food-to-Mass (F:M) Ratio. Available from: <https://www.thewastewaterblog.com/single-post/2016/12/19/food-to-mass-ratio>

46. Weckenfelder, C. (2008). Factors affecting the activated sludge design for industrial wastewaters. Presented at WEFTEC, The Water Quality Event. AquaAter, Inc., Brentwood, TN.
47. BIOLOGICAL WASTE TREATMENT EXPERT [Internet]. [cited 2025 Mar 7]. Common causes of “toxic” shock and how microbial populations adjust. Available from: <http://www.biologicalwasteexpert.com/1/post/2019/04/common-causes-of-toxic-shock-and-how-microbial-populations-adjust.html>
48. United States Environmental Protection Agency (EPA). (1974). Nitrification and denitrification facilities: Wastewater treatment (EPA-625/4-73-004a Revised). U.S. Government Printing Office.
49. United States Environmental Protection Agency (EPA). (2000). Wastewater technology fact sheet: Trickling filter nitrification (EPA 832-F-00-015). U.S. Environmental Protection Agency, Office of Water.
50. Jiang W, Yao X, Wang F, Li Y, Zhu S, Bian D. Effect of transient organic load and aeration changes to pollutant removal and extracellular polymeric substances. *Environ Technol.* 2023 Jun;44(16):2417–30.
51. Paśmionka IB, Herbut P, Kaczor G, Chmielowski K, Gospodarek J, Boligłowa E, et al. Influence of COD in Toxic Industrial Wastewater from a Chemical Concern on Nitrification Efficiency. *Int J Environ Res Public Health.* 2022 Oct 29;19(21):14124.
52. Jiang W, Yao X, Wang F, Li Y, Zhu S, Bian D. Effect of transient organic load and aeration changes to pollutant removal and extracellular polymeric substances. *Environ Technol.* 2023 Jun;44(16):2417–30.
53. Paśmionka IB, Herbut P, Kaczor G, Chmielowski K, Gospodarek J, Boligłowa E, et al. Influence of COD in Toxic Industrial Wastewater from a Chemical Concern on Nitrification Efficiency. *Int J Environ Res Public Health.* 2022 Oct 29;19(21):14124.

54. Richard, M. (2003, June 8). Activated sludge microbiology problems and their control [Conference presentation]. 20th Annual USEPA National Operator Trainers Conference, Buffalo, NY, United States.
55. Siciliano A, Limonti C, Curcio GM, Molinari R. Advances in Struvite Precipitation Technologies for Nutrients Removal and Recovery from Aqueous Waste and Wastewater. *Sustainability*. 2020 Jan;12(18):7538.
56. Achilleos P, Roberts KR, Williams ID. Struvite precipitation within wastewater treatment: A problem or a circular economy opportunity? *Heliyon*. 2022 Jul 3;8(7):e09862.
57. Tidjma.tn [Internet]. [cited 2025 Mar 7]. shock load. Available from: <https://www.tidjma.tn/en/glenv/shock-load/>
58. Sludge Wasting: An important tool for Activated sludge performance optimization - Levapor [Internet]. 2024 [cited 2025 Mar 7]. Available from: <https://levapor.com/sludge-wasting/>
59. Leu SY, Stenstrom MK. Bioaugmentation to Improve Nitrification in Activated Sludge Treatment. *Water Environ Res*. 2010;82(6):524–35.
60. IFAS Process - Hybrid Process - Levapor [Internet]. 2021 [cited 2025 Mar 7]. Available from: <https://levapor.com/ifas-processes/>
61. Kelly RT, Henriques IDS, Love NG. Chemical inhibition of nitrification in activated sludge. *Biotechnol Bioeng*. 2004 Mar 20;85(6):683–94.
62. Nguyen HD, Yang CC, Dao KC, Le VP, Tsai YP. Comparative Study on Using Various Recovery Stimulation Methods to Boost Nitrification Recovery in SBRs Inhibited by Hazardous Events. *Water*. 2021 Dec 26;14(1):48.
63. Nguyen HD, Yang CC, Dao KC, Le VP, Tsai YP. Comparative Study on Using Various Recovery Stimulation Methods to Boost Nitrification Recovery in SBRs Inhibited by Hazardous Events. *Water*. 2021 Dec 26;14(1):48.

64. Richard, M. (2003, June 8). Activated sludge microbiology problems and their control [Conference presentation]. 20th Annual USEPA National Operator Trainers Conference, Buffalo, NY, United States.
65. Henriques IDS, Kelly RT, Love NG. Deflocculation effects due to chemical perturbations in sequencing batch reactors. *Water Sci Technol J Int Assoc Water Pollut Res.* 2004;50(10):287–94.
66. ECOS. Wastewater Nitrification: How it works [Internet]. ECOS. 2013 [cited 2025 Mar 8]. Available from: <https://www.ecos.ie/wastewater-nitrification-how-it-works/>
67. Sludge Wasting: An important tool for Activated sludge performance optimization - Levapor [Internet]. 2024 [cited 2025 Mar 8]. Available from: <https://levapor.com/sludge-wasting/>
68. Deng J, Huang Z, Wang J, Shan X, Shi W, Ruan W. Wild Heterotrophic Nitrifying Strain *Pseudomonas* BT1 Isolated from Kitchen Waste Sludge Restores Ammonia Nitrogen Removal in a Sewage Treatment Plant Shocked by Thiourea. *Appl Biochem Biotechnol.* 2022 Jul;194(7):2901–18.
69. Jia C, Li J, Li Z, Zhang L. Influence of high-load shocks on achieving mainstream partial nitrification: Microbial community succession. *Water Res X.* 2025 Jan 13;27:100304.
70. (PDF) Rationale For Constant Flow To Optimize Wastewater Treatment And Advanced Water Treatment Performance For Potable Reuse Applications. ResearchGate [Internet]. 2024 Dec 9 [cited 2025 Mar 8]; Available from: https://www.researchgate.net/publication/349077673_Rationale_For_Constant_Flow_To_Optimize_Wastewater_Treatment_And_Advanced_Water_Treatment_Performance_For_Potable_Reuse_Applications
71. Jenkins JC, Chojnacky DC, Heath LS, Birdsey RA. National-Scale Biomass Estimators for United States Tree Species. *For Sci.* 2003 Feb 1;49(1):12–35.
72. Zhang X, Jiang X, Hao Z, Qu K. Advances in online methods for monitoring microbial growth. *Biosens Bioelectron.* 2019 Feb 1;126:433–47.

73. Palestinian Water Authority. (2024). National Water and Wastewater Policy and Strategy for Palestine. Final Version, December 2024.

74. EIA report (2017). Jenin Industrial Free Zone - Jenin. State of Palestine.

Appendices

Appendix A

Jericho WWTP Lab Tests

| Jericho Wastewater Treatment Plant | | | | | |
|------------------------------------|---------|-------------------|--------------------|-----------|------------------|
| Sanitation Lab | | | | | |
| Monthly Report | | | | | |
| Month: November, 2024 | | | | | |
| Treated Water | | | | | |
| Item | | Lower value/month | Higher value/month | Average | Total test/month |
| EC/TDS | uS-mg/l | 1590/874 | 2191/1134 | 1907/1017 | 20/20 |
| pH | - | 6.6 | 7.3 | 6.9 | 20/20 |
| Turbidity | NTU | 1.6 | 5.9 | 3.7 | 20/20 |
| COD | mg/l | 12 | 35 | 26.7 | 9/9 |
| T.N | mg/l | 1 | 11 | 4.7 | 13/13 |
| PO4 | mg/l | 0.2 | 3 | 1.5 | 12/12 |
| DO | mg/l | 0.5 | 2.5 | 1.5 | 19/19 |
| Temp. | c | 25.1 | 29.6 | 27.7 | 20/20 |
| TSS | mg/l | 6 | 15 | 9.3 | 10/10 |
| NH4 | mg/l | 0.27 | 1.35 | 0.95 | 11/11 |
| BOD | mg/l | 8 | 12 | 10.3 | 4/4 |
| Influent | | | | | |
| Item | | Lower value/month | Higher value/month | Average | Total test/month |
| EC/TDS | uS-mg/l | 1707/939 | 2390/1260 | 2051/1107 | 20/20 |
| pH | - | 6.89 | 7.4 | 7.1 | 20/20 |
| Turbidity | NTU | - | - | - | - |
| COD | mg/l | 780 | 1320 | 967 | 10/10 |

| | | | | | |
|-------|------|------|------|-------|-------|
| T.N | mg/l | 43.2 | 72 | 58.6 | 11/11 |
| PO4 | mg/l | 8.76 | 33 | 19 | 12/12 |
| DO | mg/l | - | - | - | - |
| Temp. | c | 25 | 29.9 | 28.2 | 20/20 |
| TSS | mg/l | 300 | 490 | 414 | 9/9 |
| NH4 | mg/l | 36.5 | 66 | 51 | 9/9 |
| BOD | mg/l | 450 | 520 | 482.5 | 10/10 |

Notes:

بلغ إجمالي عدد فحوصات جودة المياه في محطة الصرف الصحي لشهر تشرين ثاني المنصرم حوالي 728 فحص، لمختلف العينات..
حيث أنه اختلفت الجودة اعتماداً على جودة المياه العادمة القادمة للمحطة ونتيجة التغييرات على حالة الطقس السنوية المعتادة، ولكن حافظت المياه المعالجة على جودة ممتازة في تصنيف المواصفة الفلسطينية.

Appendix B

Industrial WW Allowed Concentrations

| Parameter | Maximum Concentration (mg/L) |
|-------------------------------------|------------------------------|
| الحرارة (C°) Temperature | 45 |
| اللون (كوبالت بلاتيني) Colour (PCU) | 150 |
| المواد العالقة الكلية TSS | 500 |
| المواد الذائبة الكلية TDS | 2500 |
| الأس الهيدروجيني pH | 6-9 |
| لأكسجين الممتص حيويًا BOD | 500 |
| الأكسجين الممتص كيميائيًا COD | 2000 |
| النيتروجين الكلي TKN | 60 |
| NH3-N أمونيا | 45 |
| نترات NO3-N | 30 |
| فلوريدات Fluorides | 2 |
| Phosphorus total فوسفور كلي | 15 |
| Sulphides كبريتيد | 1 |
| Phenols الفينول | 3 |
| Fat Oil & Grease الزيوت والشحوم | 100 |
| Mineral Oil زيوت معدنية | 20 |
| Detergent (MBAS) المنظفات | 25 |
| Residual Chlorine الكلور المتبقي | 3 |
| Cyanide سيانيد | 1 |
| Beryllium بيريليوم | 0.5 |
| Boron بورون | 3 |
| Lithium الليثيوم | 0.3 |
| Aluminium الألمنيوم | 10 |
| المعادن الثقيلة | 0.5 |
| Chromium total كروم كلي | 1 |
| Tin قصدير | 1 |
| Nickel نيكيل | 1 |
| Cadmium كادميوم | 0.5 |
| Arsenic زرنيخ | 0.25 |
| Lead رصاص | 1 |
| Manganese منغنيز | 1 |
| Silver فضة | 0.5 |
| Mercury زئبق | 0.05 |
| Iron حديد | 50 |
| Zinc زنك | 5 |
| Cobalt الكوبالت | 1 |
| Selenium السيلينيوم | 0.05 |
| Vanadium الفاناديوم | 0.5 |
| Molybdenum الموليبدنم | 0.15 |
| Copper النحاس | 2 |

Appendix C

Palestinian Specifications for reused treated WW

تصنيف المياه المعالجة حسب جودتها

| جودة المياه المعالجة | | | | الحدود القصوى للخصائص الكيميائية والبيولوجية (ملغم/لتر) ما لم يذكر غير ذلك |
|----------------------|--------------------|------------------|-------------------|---|
| جودة متدنية (D) | جودة متوسطة (C) | جودة جيدة (B) | جودة عالية (A) | |
| 60 | 40 | 20 | 20 | الأوكسجين الممتص حيويًا BOD ₅ |
| 90 | 50 | 30 | 30 | المواد العالقة الكلية TSS |
| 1000 | 1000 | 1000 | 200 | بكتيريا قولونية برازية FC (مستعمرة/100مل) |
| 150 | 100 | 50 | 50 | الأوكسجين الممتص كيميائيًا COD |
| 1< | 1< | 1< | 1< | الأوكسجين المذاب DO |
| 1500 | 1500 | 1500 | 1200 | المواد الذائبة الكلية TDS |
| 9-6 | 9-6 | 9-6 | 9-6 | الرقم الهيدروجيني pH |
| 5 | 5 | 5 | 5 | الدهون والزيوت والشحوم Fat, Oil & Grease |
| 0.002 | 0.002 | 0.002 | 0.002 | الفينول Phenol |
| 25 | 15 | 15 | 15 | المنظفات الصناعية MBAS |
| 40 | 30 | 20 | 20 | النترات- نيتروجين NO ₃ -N |
| 15 | 10 | 5 | 5 | الأمونيوم- نيتروجين NH ₄ -N |
| 60 | 45 | 30 | 30 | النيتروجين الكلي Total-N |
| 400 | 400 | 400 | 400 | الكلوريد Cl |
| 300 | 300 | 300 | 300 | الكبريتات SO ₄ |
| 200 | 200 | 200 | 200 | الصوديوم Na |
| 60 | 60 | 60 | 60 | المغنيسيوم Mg |
| 300 | 300 | 300 | 300 | الكالسيوم Ca |
| 5.83 | 5.83 | 5.83 | 5.83 | نسبة ادمصاص الصوديوم SAR |
| 30 | 30 | 30 | 30 | الفوسفات - فسفور PO ₄ -P |
| 5 | 5 | 5 | 5 | الألمنيوم Al |
| 0.1 | 0.1 | 0.1 | 0.1 | الزرنيخ As |
| 0.2 | 0.2 | 0.2 | 0.2 | النحاس Cu |

| جودة المياه المعالجة | | | | الحدود القصوى للخصائص الكيميائية والبيولوجية (ملغم/لتر) ما لم يذكر غير ذلك |
|----------------------|--------------------|------------------|-------------------|---|
| جودة متدنية (D) | جودة متوسطة (C) | جودة جيدة (B) | جودة عالية (A) | |
| 5 | 5 | 5 | 5 | الحديد Fe |
| 0.2 | 0.2 | 0.2 | 0.2 | المنغنيز Mn |
| 0.2 | 0.2 | 0.2 | 0.2 | النيكل Ni |
| 0.2 | 0.2 | 0.2 | 0.2 | الرصاص Pb |
| 0.02 | 0.02 | 0.02 | 0.02 | السيينيوم Se |
| 0.01 | 0.01 | 0.01 | 0.01 | الكاديوم Cd |
| 2 | 2 | 2 | 2 | الزنك Zn |
| 0.05 | 0.05 | 0.05 | 0.05 | السيانيد CN |
| 0.1 | 0.1 | 0.1 | 0.1 | الكروم Cr |
| 0.001 | 0.001 | 0.001 | 0.001 | الزئبق Hg |
| 0.05 | 0.05 | 0.05 | 0.05 | كوبالت Co |
| 0.7 | 0.7 | 0.7 | 0.7 | البورون B |
| 1000 | 1000 | 1000 | 100 | بكتيريا <i>E. coli</i> (مستعمرة/100مل) |
| 1≥ | 1≥ | 1≥ | 1≥ | بيوض الديدان المعوية Nematodes (Eggs/L) |

Appendix D

Conventional characterization of different industrial wastewaters

| Industrial wastewater | Parameter (mg/l) | | | | | | | | |
|--|------------------|----------|------------------|---------|--------------------|---------|-----|-----|------------|
| | Total COD | Sol. COD | BOD ₅ | Total N | NH ₃ -N | Total P | TSS | VSS | Alkalinity |
| Textile | | | | | | | | | |
| Industrial organized district predominantly textile (Ubay Cokgor <i>et al.</i> , 1998) | 990 | 627 | | 54 | 32 | 7.9 | 226 | 130 | 655 |
| Denim processing (Germirli Babuna <i>et al.</i> , 1998a) | 2400 | 1700 | | 35 | 5.6 | 34 | 500 | 70 | 530 |
| Polyester knit fabrics (Germirli Babuna <i>et al.</i> , 1998a) | 1985 | 1485 | | 27 | 1.7 | 9 | 213 | 22 | 960 |
| Cotton knit fabric (Orhon <i>et al.</i> , 1992) | 981 | 535 | 170 | 40 | | 14 | | | |
| Cotton knit fabric (Germirli Babuna <i>et al.</i> , 1999a) | 2310 | 2185 | | 14 | | 4.5 | 135 | 80 | |
| Cotton knit fabric (Germirli Babuna <i>et al.</i> , 1998a) | 1470 | 1165 | | 110 | 0.5 | 4 | 490 | 160 | 2350 |
| Cotton PES blend knit fabric (Germirli Babuna <i>et al.</i> , 1998a) | 2400 | 1690 | | 20 | 0.2 | 7 | 370 | 180 | 1520 |
| Acrylic processing (Germirli Babuna <i>et al.</i> , 1999a) | 1900 | 1590 | | 72 | | 4.2 | 90 | 43 | |
| Cotton woven fabric (Orhon <i>et al.</i> , 1992) | 1240 | 1176 | 680 | 144 | | 2.2 | | | |

| Industrial wastewater | Parameter (mg/l) | | | | | | | | |
|--|------------------|----------|------------------|---------|--------------------|---------|------|------|------------|
| | Total COD | Sol. COD | BOD ₅ | Total N | NH ₃ -N | Total P | TSS | VSS | Alkalinity |
| Dairy processing | | | | | | | | | |
| Integrated dairy processing (Ubay Cokgor <i>et al.</i> , 1998) | 1745 | 1070 | | 75 | 41 | 9.1 | 400 | 355 | 775 |
| Yogurt&Buttermilk processing (Orhon <i>et al.</i> , 1993) | 1500 | | 1000 | 63 | | 7.2 | 191 | | |
| Tannery (Orhon <i>et al.</i>, 1999b) | | | | | | | | | |
| Raw wastewater | 4180 | 1495 | | 250 | | | 2070 | | |
| Primary effluent | 2255 | 1290 | | 215 | 160 | 5.9 | 770 | 470 | 1420 |
| Chemical effluent | 1090 | 1035 | | 197 | 160 | 1.8 | 150 | 55 | 1140 |
| Meat processing | | | | | | | | | |
| Integrated meat (Ubay Cokgor <i>et al.</i> , 1998) | 2685 | 1000 | | 196 | 85 | 10 | 1152 | 1073 | 520 |
| Integrated meat (del Pozo <i>et al.</i> , 2003) | 7230 | 5500 | 3180 | | 67 | 3.3 | 910 | 850 | |
| Poultry (Eremektar <i>et al.</i> , 1999a) | 2690 | 1700 | 1595 | 343 | 207 | 30 | 418 | | |
| Confectionery (Orhon <i>et al.</i>, 1995) | | | | | | | | | |
| Plant I | 2840 | 2500 | 1840 | 55 | | 65 | 260 | | |
| Plant II | 3630 | 3020 | 2700 | 22 | | 2.5 | 140 | | |
| Plant III | 6220 | 5400 | 4900 | 33 | | 8.6 | 440 | | |
| Corn wet mill (Eremektar <i>et al.</i> , 1999a) | 3800 | 3230 | 2800 | | | 33 | 400 | 315 | |

Conventional wastewater characterization of an industry manufacturing energy drinks

| Parameter | Value |
|--------------------|-------|
| Total COD (mg/l) | 33000 |
| Soluble COD (mg/l) | 27000 |
| TKN (mg/l) | 54 |
| Total P (mg/l) | 2.5 |
| pH | 5.4 |

Appendix E

Aeration Tank Mantis 2 Rates Before the Shock Load

| Variable | Unit | Value |
|--|-------------|-----------|
| [100] adsorption of colloidal COD | mgCOD/(L.d) | 8.275 |
| [100] aerobic hydrolysis of stored/enmeshed COD | mgCOD/(L.d) | 464.7 |
| [100] anoxic hydrolysis of stored/enmeshed COD | mgCOD/(L.d) | 7.234 |
| [100] anaerobic hydrolysis of stored/enmeshed COD | mgCOD/(L.d) | 0.04813 |
| [100] ammonification | mgN/(L.d) | 40.75 |
| [100] aerobic growth of heterotrophs on soluble substrate Sac | mgCOD/(L.d) | 0.00696 |
| [100] aerobic growth of heterotrophs on soluble substrate Spro | mgCOD/(L.d) | 0.0 |
| [100] anoxic growth of heterotrophs on soluble substrate Sac with NO3 | mgCOD/(L.d) | 4.333e-05 |
| [100] anoxic growth of heterotrophs on soluble substrate Spro with NO3 | mgCOD/(L.d) | 0.0 |
| [100] anoxic growth of heterotrophs on soluble substrate Ss with NO2 | mgCOD/(L.d) | 3.303 |
| [100] anoxic growth of heterotrophs on soluble substrate Sac with NO2 | mgCOD/(L.d) | 4.769e-05 |
| [100] anoxic growth of heterotrophs on soluble substrate Spro with NO2 | mgCOD/(L.d) | 0.0 |
| [100] aerobic growth of methylotrophs on methanol | mgCOD/(L.d) | 0.0 |
| [100] anoxic growth of methylotrophs on methanol with NO3 | mgCOD/(L.d) | 0.0 |
| [100] anoxic growth of methylotrophs on methanol with NO2 | mgCOD/(L.d) | 0.0 |
| [100] decay of methylotrophs under | mgCOD/(L.d) | 9.179e-08 |

| | | |
|---|-------------|-----------|
| aerobic, anoxic, and anaerobic conditions | | |
| [100] growth of fermentative biomass at low H ₂ | mgCOD/(L.d) | 0.01082 |
| [100] growth of fermentative biomass at high H ₂ | mgCOD/(L.d) | 1.858e-08 |
| [100] decay of fermentative biomass under aerobic, anoxic, and anaerobic conditions | mgCOD/(L.d) | 7.267e-08 |
| [100] growth of ammonia oxidizer | mgCOD/(L.d) | 4.473 |
| [100] decay of ammonia oxidizer under aerobic, anoxic, and anaerobic conditions | mgCOD/(L.d) | 2.816 |
| [100] growth of nitrite oxidizer | mgCOD/(L.d) | 1.175 |
| [100] decay of nitrite oxidizer under aerobic, anoxic, and anaerobic conditions | mgCOD/(L.d) | 0.7332 |
| [100] growth of anammox biomass | mgCOD/(L.d) | 0.0 |
| [100] decay of anammox biomass under aerobic, anoxic, and anaerobic conditions | mgCOD/(L.d) | 4.435e-09 |
| [100] storage of PHA by PAO using acetate | mgCOD/(L.d) | 3.376e-08 |
| [100] storage of PHA by PAO using propionate | mgCOD/(L.d) | 0.0 |
| [100] aerobic growth of PAO on PHA | mgCOD/(L.d) | 0.0 |
| [100] aerobic storage of XPP | mgP/(L.d) | 1.468e-08 |
| [100] anoxic growth of PAO on PHA using NO ₃ | mgCOD/(L.d) | 0.0 |
| [100] anoxic storage of XPP using NO ₃ | mgP/(L.d) | 0.0 |
| [100] anoxic growth of PAO on PHA using NO ₂ | mgCOD/(L.d) | 0.0 |
| [100] anoxic storage of XPP using NO ₂ | mgP/(L.d) | 0.0 |
| [100] decay of PAO under aerobic, anoxic, and anaerobic conditions | mgCOD/(L.d) | 9.181e-08 |
| [100] Xpp lysis under aerobic, anoxic, and | mgP/(L.d) | 3.428e-08 |

| | | |
|--|--|------------|
| anaerobic conditions | | |
| [100] PHA lysis under aerobic, anoxic, and anaerobic conditions | mgCOD/(L.d) | 1.076e-07 |
| [100] growth of acetogens by conversion of propionate to acetate and hydrogen | mgCOD/(L.d) | 0.0 |
| [100] decay of acetogens under aerobic, anoxic, and anaerobic conditions | mgCOD/(L.d) | 4.35e-08 |
| [100] growth of hydrogenotrophic methanogens (production of methane from H ₂) | mgCOD/(L.d) | 0.0 |
| [100] decay of hydrogenotrophic methanogens under aerobic, anoxic, and anaerobic conditions | mgCOD/(L.d) | 2.346e-08 |
| [100] growth of methanogens (production of methane from acetate) | mgCOD/(L.d) | 0.0 |
| [100] decay of acetoclastic methanogens under aerobic, anoxic, and anaerobic conditions | mgCOD/(L.d) | 4.35e-08 |
| [100] precipitation of CaCO ₃ | g CaCO ₃ /m ³ /d | 0.0004241 |
| [100] precipitation of MgNH ₄ PO ₄ (struvite) | g MgNH ₄ PO ₄ .6H ₂ O/m ³ /d | 3.614e-07 |
| [100] precipitation of MgHPO ₄ (newberyite) | g MgHPO ₄ .3H ₂ O/m ³ /d | 1.177e-05 |
| [100] precipitation of Ca ₃ (PO ₄) ₂ (amorphous calcium phosphate) | g Ca ₃ (PO ₄) ₂ /m ³ /d | -2.084e-08 |
| [100] precipitation of MgCO ₃ | g MgCO ₃ /m ³ /d | 0.0007522 |
| [100] precipitation of AlPO ₄ | g AlPO ₄ /m ³ /d | 0.0 |
| [100] precipitation of FePO ₄ | g FePO ₄ /m ³ /d | 0.0 |
| [100] gas transfer of CO ₂ | gC/m ³ /d | -109.4 |
| [100] gas transfer of N ₂ | mgN/(L.d) | -1.931 |
| [100] gas transfer of CH ₄ | mgCOD/(L.d) | 8.988e-05 |
| [100] gas transfer of H ₂ | mgCOD/(L.d) | -0.01641 |

| | | |
|--|-------------------------|------------|
| [100] gas transfer of NH ₃ | mgN/(L.d) | 0.0 |
| [100] hydrolysis of unbiodegradable residue | mgCOD/(L.d) | 6.01 |
| [100] hydrolysis of inert particulate | mgCOD/(L.d) | 4.497 |
| [100] rate for dissolved oxygen | mgO ₂ /(L.d) | -343.7 |
| [100] rate for dissolved hydrogen | mgCOD/(L.d) | 6.989e-06 |
| [100] rate for dissolved dinitrogen gas | mgN/(L.d) | -0.2428 |
| [100] rate for dissolved methane | mgCOD/(L.d) | 8.988e-05 |
| [100] rate for soluble inert material | mgCOD/(L.d) | 0.0 |
| [100] rate for colloidal substrate | mgCOD/(L.d) | -8.275 |
| [100] rate for readily degradable substrate | mgCOD/(L.d) | -281.7 |
| [100] rate for acetate | mgCOD/(L.d) | 0.02186 |
| [100] rate for propionate | mgCOD/(L.d) | 4.934e-08 |
| [100] rate for methanol | mgCOD/(L.d) | 0.0 |
| [100] rate for particulate inert material | mgCOD/(L.d) | -4.497 |
| [100] rate for unbiodegradable cell products | mgCOD/(L.d) | 27.97 |
| [100] rate for slowly biodegradable substrate | mgCOD/(L.d) | -73.01 |
| [100] rate for poly-hydroxy alkoates in PAO | mgCOD/(L.d) | -7.685e-08 |
| [100] rate for total ammonia | mgN/(L.d) | -10.17 |
| [100] rate for soluble organic nitrogen | mgN/(L.d) | 0.2525 |
| [100] rate for nitrite | mgN/(L.d) | 0.1088 |
| [100] rate for nitrate | mgN/(L.d) | 15.38 |
| [100] rate for nitrogen in slowly degradable substrate | mgN/(L.d) | -13.68 |
| [100] rate for ortho-phosphate | mgP/(L.d) | -1.235 |

| | | |
|--|-----------------------|------------|
| [100] rate for phosphorus in slowly degradable substrate | mgP/(L.d) | -0.5692 |
| [100] rate for polyphosphate in PAO | mgP/(L.d) | -3.3e-08 |
| [100] rate for heterotrophic biomass | mgCOD/(L.d) | 67.25 |
| [100] rate for fermenting biomass | mgCOD/(L.d) | -7.266e-08 |
| [100] rate for ammonia oxidizer biomass | mgCOD/(L.d) | 1.657 |
| [100] rate for nitrite oxidizer biomass | mgCOD/(L.d) | 0.4413 |
| [100] rate for phosphate accumulating biomass | mgCOD/(L.d) | -9.178e-08 |
| [100] rate for acetogenic biomass | mgCOD/(L.d) | -4.35e-08 |
| [100] rate for acetoclastic methanogenic biomass | mgCOD/(L.d) | -4.35e-08 |
| [100] rate for hydrogenotrophic methanogenic biomass | mgCOD/(L.d) | -2.346e-08 |
| [100] rate for methylotrophic biomass | mgCOD/(L.d) | -9.179e-08 |
| [100] rate for anammox biomass | mgCOD/(L.d) | -4.42e-09 |
| [100] rate for total soluble inorganic carbon | gC/m ³ /d | -24.04 |
| [100] rate for total calcium | gCa/m ³ /d | -0.2337 |
| [100] rate for total magnesium | gMg/m ³ /d | -0.2887 |
| [100] rate for total inorganic potassium | gK/m ³ /d | -0.464 |
| [100] rate for other cation | eq/m ³ /d | -0.04276 |
| [100] rate for other anion | eq/m ³ /d | -0.03572 |
| [100] rate for inorganic inert particulate | mg/(L.d) | 0.0 |
| [100] rate for aluminum hydroxide | mg/(L.d) | 0.0 |
| [100] rate for aluminum phosphate | mg/(L.d) | 0.0 |
| [100] rate for iron hydroxide | mg/(L.d) | 0.0 |
| [100] rate for iron phosphate | mg/(L.d) | 0.0 |

| | | |
|--|-------------|------------|
| [100] rate for calcium carbonate | mg/(L.d) | 0.0004241 |
| [100] rate for calcium phosphate | mg/(L.d) | -2.084e-08 |
| [100] rate for magnesium carbonate | mg/(L.d) | 0.0007522 |
| [100] rate for magnesium hydrogen phosphate (newberyite) | mg/(L.d) | 1.177e-05 |
| [100] rate for magnesium ammonium phosphate (struvite) | mg/(L.d) | 3.614e-07 |
| [100] rate for soluble component "a" | notset/d | 0.0 |
| [100] rate for soluble component "b" | notset/d | 0.0 |
| [100] rate for particulate component "a" | notset/d | 0.0 |
| [100] rate for particulate component "b" | notset/d | 0.0 |
| [100] derivative of dissolved oxygen | mgO2/(L.d) | -0.0002153 |
| [100] derivative of dissolved hydrogen | mgCOD/(L.d) | -5.846e-08 |
| [100] derivative of dissolved dinitrogen gas | mgN/(L.d) | -2.16e-06 |
| [100] derivative of dissolved methane | mgCOD/(L.d) | 0.0 |
| [100] derivative of soluble inert material | mgCOD/(L.d) | 0.0 |
| [100] derivative of colloidal substrate | mgCOD/(L.d) | 4.697e-06 |
| [100] derivative of readily degradable substrate | mgCOD/(L.d) | 0.004185 |
| [100] derivative of acetate | mgCOD/(L.d) | 9.609e-07 |
| [100] derivative of propionate | mgCOD/(L.d) | -1.053e-07 |
| [100] derivative of methanol | mgCOD/(L.d) | -1.197e-07 |
| [100] derivative of particulate inert material | mgCOD/(L.d) | 6.199e-05 |
| [100] derivative of unbiodegradable cell products | mgCOD/(L.d) | -0.0002017 |
| [100] derivative of slowly biodegradable substrate | mgCOD/(L.d) | -0.00289 |

| | | |
|---|-----------------------|------------|
| [100] derivative of poly-hydroxy alkoates in PAO | mgCOD/(L.d) | -1.019e-07 |
| [100] derivative of total ammonia | mgN/(L.d) | 6.251e-05 |
| [100] derivative of soluble organic nitrogen | mgN/(L.d) | -0.0001971 |
| [100] derivative of nitrite | mgN/(L.d) | 1.564e-05 |
| [100] derivative of nitrate | mgN/(L.d) | -0.0001221 |
| [100] derivative of nitrogen in slowly degradable substrate | mgN/(L.d) | -8.202e-05 |
| [100] derivative of ortho-phosphate | mgP/(L.d) | -3.131e-05 |
| [100] derivative of phosphorus in slowly degradable substrate | mgP/(L.d) | -3.412e-06 |
| [100] derivative of polyphosphate in PAO | mgP/(L.d) | -7.667e-08 |
| [100] derivative of heterotrophic biomass | mgCOD/(L.d) | -0.000375 |
| [100] derivative of fermenting biomass | mgCOD/(L.d) | -9.859e-08 |
| [100] derivative of ammonia oxidizer biomass | mgCOD/(L.d) | -9.673e-05 |
| [100] derivative of nitrite oxidizer biomass | mgCOD/(L.d) | -1.912e-05 |
| [100] derivative of phosphate accumulating biomass | mgCOD/(L.d) | -1.065e-07 |
| [100] derivative of acetogenic biomass | mgCOD/(L.d) | -8.291e-08 |
| [100] derivative of acetoclastic methanogenic biomass | mgCOD/(L.d) | -8.291e-08 |
| [100] derivative of hydrogenotrophic methanogenic biomass | mgCOD/(L.d) | -7.086e-08 |
| [100] derivative of methylotrophic biomass | mgCOD/(L.d) | -1.065e-07 |
| [100] derivative of anammox biomass | mgCOD/(L.d) | -5.883e-08 |
| [100] derivative of total soluble inorganic carbon | gC/m ³ /d | -0.02233 |
| [100] derivative of total calcium | gCa/m ³ /d | 0.000992 |

| | | |
|---|-----------------------|------------|
| [100] derivative of total magnesium | gMg/m ³ /d | 0.002365 |
| [100] derivative of total inorganic potassium | gK/m ³ /d | -8.713e-07 |
| [100] derivative of other cation | eq/m ³ /d | -2.947e-07 |
| [100] derivative of other anion | eq/m ³ /d | -5.961e-08 |
| [100] derivative of inorganic inert particulate | mg/(L.d) | 5.483e-05 |
| [100] derivative of aluminum hydroxide | mg/(L.d) | -5.598e-08 |
| [100] derivative of aluminum phosphate | mg/(L.d) | -5.598e-08 |
| [100] derivative of iron hydroxide | mg/(L.d) | -5.598e-08 |
| [100] derivative of iron phosphate | mg/(L.d) | -5.598e-08 |
| [100] derivative of calcium carbonate | mg/(L.d) | -0.001003 |
| [100] derivative of calcium phosphate | mg/(L.d) | -2.533e-09 |
| [100] derivative of magnesium carbonate | mg/(L.d) | -0.002239 |
| [100] derivative of magnesium hydrogen phosphate (newberyite) | mg/(L.d) | -1.016e-07 |
| [100] derivative of magnesium ammonium phosphate (struvite) | mg/(L.d) | -8.415e-08 |
| [100] derivative of soluble component "a" | notset/d | 0.0 |
| [100] derivative of soluble component "b" | notset/d | 0.0 |

Appendix F

Aeration Tank Mantis 2 Rates During the Shock Load

| Variable | Unit | Value |
|--|-------------|-----------|
| [100] adsorption of colloidal COD | mgCOD/(L.d) | 21.23 |
| [100] aerobic hydrolysis of stored/enmeshed COD | mgCOD/(L.d) | 931.4 |
| [100] anoxic hydrolysis of stored/enmeshed COD | mgCOD/(L.d) | 14.66 |
| [100] anaerobic hydrolysis of stored/enmeshed COD | mgCOD/(L.d) | 0.04489 |
| [100] ammonification | mgN/(L.d) | 56.13 |
| [100] aerobic growth of heterotrophs on soluble substrate Sac | mgCOD/(L.d) | 3.332e-05 |
| [100] aerobic growth of heterotrophs on soluble substrate Spro | mgCOD/(L.d) | 0.0 |
| [100] anoxic growth of heterotrophs on soluble substrate Sac with NO3 | mgCOD/(L.d) | 2.098e-07 |
| [100] anoxic growth of heterotrophs on soluble substrate Spro with NO3 | mgCOD/(L.d) | 0.0 |
| [100] anoxic growth of heterotrophs on soluble substrate Ss with NO2 | mgCOD/(L.d) | 3.964 |
| [100] anoxic growth of heterotrophs on soluble substrate Sac with NO2 | mgCOD/(L.d) | 2.921e-07 |
| [100] anoxic growth of heterotrophs on soluble substrate Spro with NO2 | mgCOD/(L.d) | 0.0 |
| [100] aerobic growth of methylotrophs on methanol | mgCOD/(L.d) | 0.0 |
| [100] anoxic growth of methylotrophs on methanol with NO3 | mgCOD/(L.d) | 0.0 |
| [100] anoxic growth of methylotrophs on methanol with NO2 | mgCOD/(L.d) | 0.0 |
| [100] decay of methylotrophs under aerobic, | mgCOD/(L.d) | 1.339e-09 |

| | | |
|---|-------------|-----------|
| anoxic, and anaerobic conditions | | |
| [100] growth of fermentative biomass at low H ₂ | mgCOD/(L.d) | 0.005134 |
| [100] growth of fermentative biomass at high H ₂ | mgCOD/(L.d) | 6.216e-09 |
| [100] decay of fermentative biomass under aerobic, anoxic, and anaerobic conditions | mgCOD/(L.d) | 1.929e-09 |
| [100] growth of ammonia oxidizer | mgCOD/(L.d) | 6.861 |
| [100] decay of ammonia oxidizer under aerobic, anoxic, and anaerobic conditions | mgCOD/(L.d) | 2.589 |
| [100] growth of nitrite oxidizer | mgCOD/(L.d) | 2.135 |
| [100] decay of nitrite oxidizer under aerobic, anoxic, and anaerobic conditions | mgCOD/(L.d) | 0.7898 |
| [100] growth of anammox biomass | mgCOD/(L.d) | 0.0 |
| [100] decay of anammox biomass under aerobic, anoxic, and anaerobic conditions | mgCOD/(L.d) | 3.794e-10 |
| [100] storage of PHA by PAO using acetate | mgCOD/(L.d) | 3.227e-10 |
| [100] storage of PHA by PAO using propionate | mgCOD/(L.d) | 0.0 |
| [100] aerobic growth of PAO on PHA | mgCOD/(L.d) | 0.0 |
| [100] aerobic storage of XPP | mgP/(L.d) | 2.725e-10 |
| [100] anoxic growth of PAO on PHA using NO ₃ | mgCOD/(L.d) | 0.0 |
| [100] anoxic storage of XPP using NO ₃ | mgP/(L.d) | 0.0 |
| [100] anoxic growth of PAO on PHA using NO ₂ | mgCOD/(L.d) | 0.0 |
| [100] anoxic storage of XPP using NO ₂ | mgP/(L.d) | 0.0 |
| [100] decay of PAO under aerobic, anoxic, and anaerobic conditions | mgCOD/(L.d) | 1.339e-09 |
| [100] Xpp lysis under aerobic, anoxic, and anaerobic conditions | mgP/(L.d) | 2.01e-09 |

| | | |
|--|--|-----------|
| [100] PHA lysis under aerobic, anoxic, and anaerobic conditions | mgCOD/(L.d) | 2.22e-09 |
| [100] growth of acetogens by conversion of propionate to acetate and hydrogen | mgCOD/(L.d) | 0.0 |
| [100] decay of acetogens under aerobic, anoxic, and anaerobic conditions | mgCOD/(L.d) | 2.111e-09 |
| [100] growth of hydrogenotrophic methanogens (production of methane from H ₂) | mgCOD/(L.d) | 0.0 |
| [100] decay of hydrogenotrophic methanogens under aerobic, anoxic, and anaerobic conditions | mgCOD/(L.d) | 1.558e-09 |
| [100] growth of methanogens (production of methane from acetate) | mgCOD/(L.d) | 0.0 |
| [100] decay of acetoclastic methanogens under aerobic, anoxic, and anaerobic conditions | mgCOD/(L.d) | 2.111e-09 |
| [100] precipitation of CaCO ₃ | g CaCO ₃ /m ³ /d | 0.3673 |
| [100] precipitation of MgNH ₄ PO ₄ (struvite) | g MgNH ₄ PO ₄ .6H ₂ O/m ³ /d | 3.606e-05 |
| [100] precipitation of MgHPO ₄ (newberyite) | g MgHPO ₄ .3H ₂ O/m ³ /d | 5.873e-05 |
| [100] precipitation of Ca ₃ (PO ₄) ₂ (amorphous calcium phosphate) | g Ca ₃ (PO ₄) ₂ /m ³ /d | 3.57e-06 |
| [100] precipitation of MgCO ₃ | g MgCO ₃ /m ³ /d | 9.139 |
| [100] precipitation of AlPO ₄ | g AlPO ₄ /m ³ /d | 0.0 |
| [100] precipitation of FePO ₄ | g FePO ₄ /m ³ /d | 0.0 |
| [100] gas transfer of CO ₂ | gC/m ³ /d | -247.9 |
| [100] gas transfer of N ₂ | mgN/(L.d) | -2.269 |
| [100] gas transfer of CH ₄ | mgCOD/(L.d) | 8.988e-05 |
| [100] gas transfer of H ₂ | mgCOD/(L.d) | -0.007783 |
| [100] gas transfer of NH ₃ | mgN/(L.d) | 0.0 |
| [100] hydrolysis of unbiodegradable residue | mgCOD/(L.d) | 2.628 |

| | | |
|--|-------------------------|------------|
| [100] hydrolysis of inert particulate | mgCOD/(L.d) | 9.494 |
| [100] rate for dissolved oxygen | mgO ₂ /(L.d) | -389.1 |
| [100] rate for dissolved hydrogen | mgCOD/(L.d) | 4.949e-06 |
| [100] rate for dissolved dinitrogen gas | mgN/(L.d) | -0.2426 |
| [100] rate for dissolved methane | mgCOD/(L.d) | 8.988e-05 |
| [100] rate for soluble inert material | mgCOD/(L.d) | 0.0 |
| [100] rate for colloidal substrate | mgCOD/(L.d) | -21.23 |
| [100] rate for readily degradable substrate | mgCOD/(L.d) | 258.2 |
| [100] rate for acetate | mgCOD/(L.d) | 0.01555 |
| [100] rate for propionate | mgCOD/(L.d) | 1.651e-08 |
| [100] rate for methanol | mgCOD/(L.d) | 0.0 |
| [100] rate for particulate inert material | mgCOD/(L.d) | -9.494 |
| [100] rate for unbiodegradable cell products | mgCOD/(L.d) | 23.13 |
| [100] rate for slowly biodegradable substrate | mgCOD/(L.d) | -628.6 |
| [100] rate for poly-hydroxy alkoates in PAO | mgCOD/(L.d) | -1.952e-09 |
| [100] rate for total ammonia | mgN/(L.d) | -11.64 |
| [100] rate for soluble organic nitrogen | mgN/(L.d) | 0.2575 |
| [100] rate for nitrite | mgN/(L.d) | 0.5418 |
| [100] rate for nitrate | mgN/(L.d) | 33.24 |
| [100] rate for nitrogen in slowly degradable substrate | mgN/(L.d) | -35.8 |
| [100] rate for ortho-phosphate | mgP/(L.d) | -2.602 |
| [100] rate for phosphorus in slowly degradable substrate | mgP/(L.d) | -0.6118 |
| [100] rate for polyphosphate in PAO | mgP/(L.d) | -1.863e-09 |
| [100] rate for heterotrophic biomass | mgCOD/(L.d) | 140.4 |
| [100] rate for fermenting biomass | mgCOD/(L.d) | -1.928e-09 |

| | | |
|--|-------------|------------|
| [100] rate for ammonia oxidizer biomass | mgCOD/(L.d) | 4.272 |
| [100] rate for nitrite oxidizer biomass | mgCOD/(L.d) | 1.346 |
| [100] rate for phosphate accumulating biomass | mgCOD/(L.d) | -1.339e-09 |
| [100] rate for acetogenic biomass | mgCOD/(L.d) | -2.111e-09 |
| [100] rate for acetoclastic methanogenic biomass | mgCOD/(L.d) | -2.111e-09 |
| [100] rate for hydrogenotrophic methanogenic biomass | mgCOD/(L.d) | -1.558e-09 |
| [100] rate for methylotrophic biomass | mgCOD/(L.d) | -1.339e-09 |
| [100] rate for anammox biomass | mgCOD/(L.d) | -3.752e-10 |
| [100] rate for total soluble inorganic carbon | gC/m3/d | -179.0 |
| [100] rate for total calcium | gCa/m3/d | -0.5529 |
| [100] rate for total magnesium | gMg/m3/d | -3.136 |
| [100] rate for total inorganic potassium | gK/m3/d | -0.8065 |
| [100] rate for other cation | eq/m3/d | -0.1036 |
| [100] rate for other anion | eq/m3/d | -0.06208 |
| [100] rate for inorganic inert particulate | mg/(L.d) | 0.0 |
| [100] rate for aluminum hydroxide | mg/(L.d) | 0.0 |
| [100] rate for aluminum phosphate | mg/(L.d) | 0.0 |
| [100] rate for iron hydroxide | mg/(L.d) | 0.0 |
| [100] rate for iron phosphate | mg/(L.d) | 0.0 |
| [100] rate for calcium carbonate | mg/(L.d) | 0.3673 |
| [100] rate for calcium phosphate | mg/(L.d) | 3.57e-06 |
| [100] rate for magnesium carbonate | mg/(L.d) | 9.139 |
| [100] rate for magnesium hydrogen phosphate (newberyite) | mg/(L.d) | 5.873e-05 |
| [100] rate for magnesium ammonium | mg/(L.d) | 3.606e-05 |

| | | |
|--|-------------------------|------------|
| phosphate (struvite) | | |
| [100] rate for soluble component "a" | notset/d | 0.0 |
| [100] rate for soluble component "b" | notset/d | 0.0 |
| [100] rate for particulate component "a" | notset/d | 0.0 |
| [100] rate for particulate component "b" | notset/d | 0.0 |
| [100] derivative of dissolved oxygen | mgO ₂ /(L.d) | 0.002322 |
| [100] derivative of dissolved hydrogen | mgCOD/(L.d) | -3.202e-08 |
| [100] derivative of dissolved dinitrogen gas | mgN/(L.d) | -1.548e-05 |
| [100] derivative of dissolved methane | mgCOD/(L.d) | 0.0 |
| [100] derivative of soluble inert material | mgCOD/(L.d) | 20.39 |
| [100] derivative of colloidal substrate | mgCOD/(L.d) | 0.19 |
| [100] derivative of readily degradable substrate | mgCOD/(L.d) | 38.38 |
| [100] derivative of acetate | mgCOD/(L.d) | -0.001301 |
| [100] derivative of propionate | mgCOD/(L.d) | -4.269e-09 |
| [100] derivative of methanol | mgCOD/(L.d) | -1.952e-09 |
| [100] derivative of particulate inert material | mgCOD/(L.d) | 5.895 |
| [100] derivative of unbiodegradable cell products | mgCOD/(L.d) | -7.255 |
| [100] derivative of slowly biodegradable substrate | mgCOD/(L.d) | 5.909 |
| [100] derivative of poly-hydroxy alkoates in PAO | mgCOD/(L.d) | -5.037e-09 |
| [100] derivative of total ammonia | mgN/(L.d) | 0.03269 |
| [100] derivative of soluble organic nitrogen | mgN/(L.d) | 0.01804 |
| [100] derivative of nitrite | mgN/(L.d) | 0.03942 |
| [100] derivative of nitrate | mgN/(L.d) | 0.1494 |
| [100] derivative of nitrogen in slowly | mgN/(L.d) | 0.2588 |

| | | |
|---|-------------|------------|
| degradable substrate | | |
| [100] derivative of ortho-phosphate | mgP/(L.d) | 6.025e-05 |
| [100] derivative of phosphorus in slowly degradable substrate | mgP/(L.d) | 0.004422 |
| [100] derivative of polyphosphate in PAO | mgP/(L.d) | -1.319e-08 |
| [100] derivative of heterotrophic biomass | mgCOD/(L.d) | -8.667 |
| [100] derivative of fermenting biomass | mgCOD/(L.d) | -5.982e-09 |
| [100] derivative of ammonia oxidizer biomass | mgCOD/(L.d) | -0.1865 |
| [100] derivative of nitrite oxidizer biomass | mgCOD/(L.d) | -0.0421 |
| [100] derivative of phosphate accumulating biomass | mgCOD/(L.d) | -3.194e-09 |
| [100] derivative of acetogenic biomass | mgCOD/(L.d) | -1.099e-08 |
| [100] derivative of acetoclastic methanogenic biomass | mgCOD/(L.d) | -1.099e-08 |
| [100] derivative of hydrogenotrophic methanogenic biomass | mgCOD/(L.d) | -1.491e-08 |
| [100] derivative of methylotrophic biomass | mgCOD/(L.d) | -3.193e-09 |
| [100] derivative of anammox biomass | mgCOD/(L.d) | -1.891e-08 |
| [100] derivative of total soluble inorganic carbon | gC/m3/d | 0.1999 |
| [100] derivative of total calcium | gCa/m3/d | -0.008694 |
| [100] derivative of total magnesium | gMg/m3/d | -0.2944 |
| [100] derivative of total inorganic potassium | gK/m3/d | -0.004886 |
| [100] derivative of other cation | eq/m3/d | 0.0514 |
| [100] derivative of other anion | eq/m3/d | -0.0003761 |
| [100] derivative of inorganic inert particulate | mg/(L.d) | 14.66 |
| [100] derivative of aluminum hydroxide | mg/(L.d) | -1.987e-08 |

| | | |
|---|----------|------------|
| [100] derivative of aluminum phosphate | mg/(L.d) | -1.987e-08 |
| [100] derivative of iron hydroxide | mg/(L.d) | -1.987e-08 |
| [100] derivative of iron phosphate | mg/(L.d) | -1.987e-08 |
| [100] derivative of calcium carbonate | mg/(L.d) | 0.02907 |
| [100] derivative of calcium phosphate | mg/(L.d) | 3.73e-07 |
| [100] derivative of magnesium carbonate | mg/(L.d) | 1.747 |
| [100] derivative of magnesium hydrogen phosphate (newberyite) | mg/(L.d) | 7.405e-07 |
| [100] derivative of magnesium ammonium phosphate (struvite) | mg/(L.d) | 4.154e-06 |
| [100] derivative of soluble component "a" | notset/d | 0.0 |
| [100] derivative of soluble component "b" | notset/d | 0.0 |
| [100] derivative of particulate component "a" | notset/d | 0.0 |
| [100] derivative of particulate component "b" | notset/d | 0.0 |

Appendix G

JIFZ-WWTP's Influent Concentration

| Parameter | Concentration |
|----------------------------------|---------------------------|
| Total COD | 1040 gCOD/m ³ |
| Total TKN | 64 gN/m ³ |
| Total Phosphorus (TP) | 4.0 gP/m ³ |
| Ammonia Nitrogen (S_NH3) | 25.0 gN/m ³ |
| Nitrate (S_NO3) | 0.0 gN/m ³ |
| Orthophosphate (S_PO4) | 3.0 gP/m ³ |
| Total Suspended Solids (TSS) | 284.7 g/m ³ |
| Volatile Suspended Solids (VSS) | 173.7 g/m ³ |
| Total Inorganic Suspended Solids | 111.0 g/m ³ |
| Total Soluble Inorganic Carbon | 65.7 gC/m ³ |
| pH | 7.4 |
| Alkalinity | 250 gCaCO3/m ³ |
| Calcium | 140.0 gCa/m ³ |
| Magnesium | 50.0 gMg/m ³ |
| Potassium | 28.0 gK/m ³ |

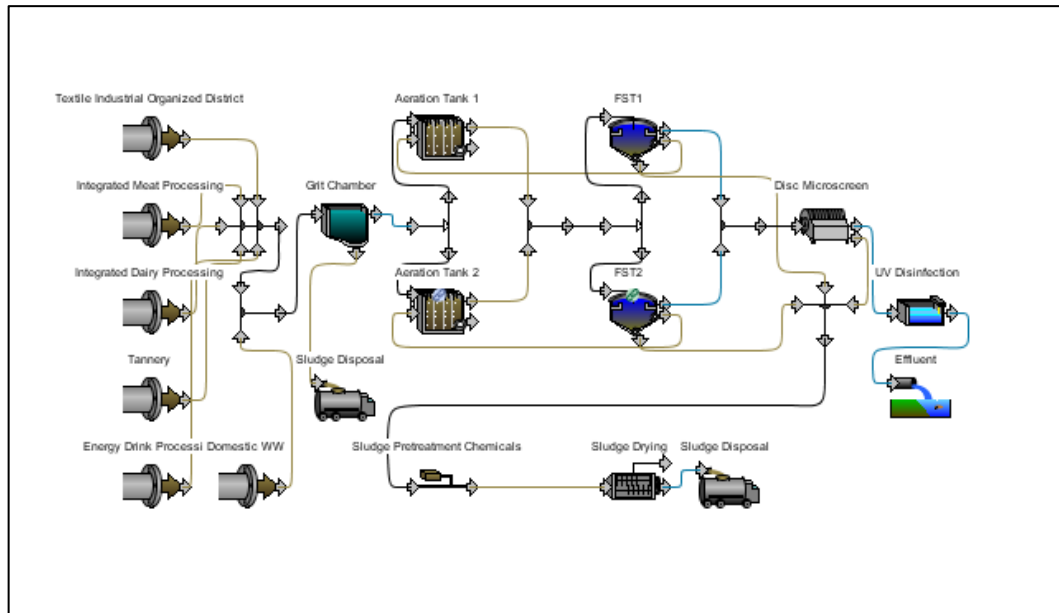
Appendix H

JIFZ-WWTP's Effluent Concentration

| | | |
|------------------|-----------|----------|
| TSS | mg/L | 13.72 |
| VSS | mg/L | 11.09 |
| cBOD5 | mg/L | 36.51 |
| COD | mg/L | 109.2 |
| Ammonia N | mgN/L | 0.3272 |
| Nitrite N | mgN/L | 0.2601 |
| Nitrate N | mgN/L | 37.31 |
| TKN | mgN/L | 4.816 |
| TN | mgN/L | 42.39 |
| Soluble PO4-P | mgP/L | 0.003748 |
| TP | mgP/L | 1.342 |
| Total Alkalinity | mgCaCO3/L | 30.72 |
| pH | - | 7.729 |
| DO | mgO2/L | 10.13 |

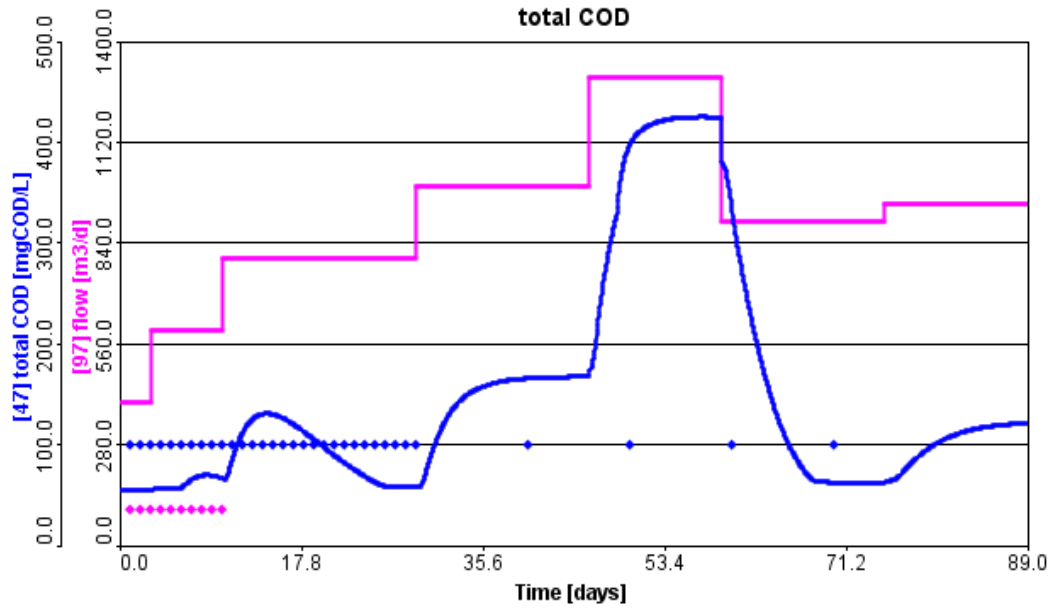
Appendix I

Diagram of the simulation model used during the research.

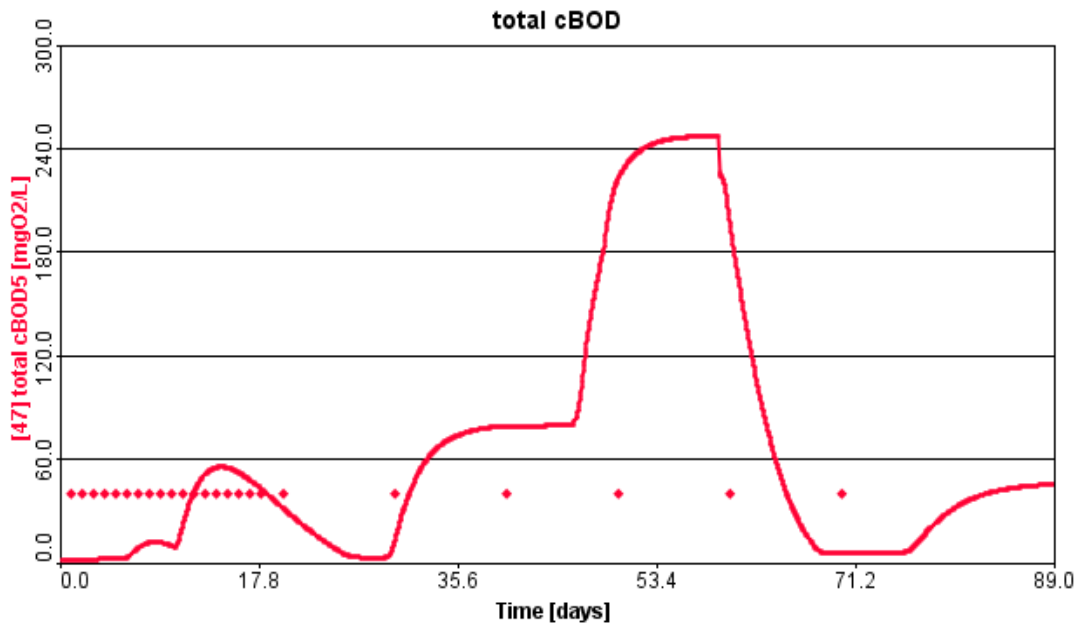


Appendix J

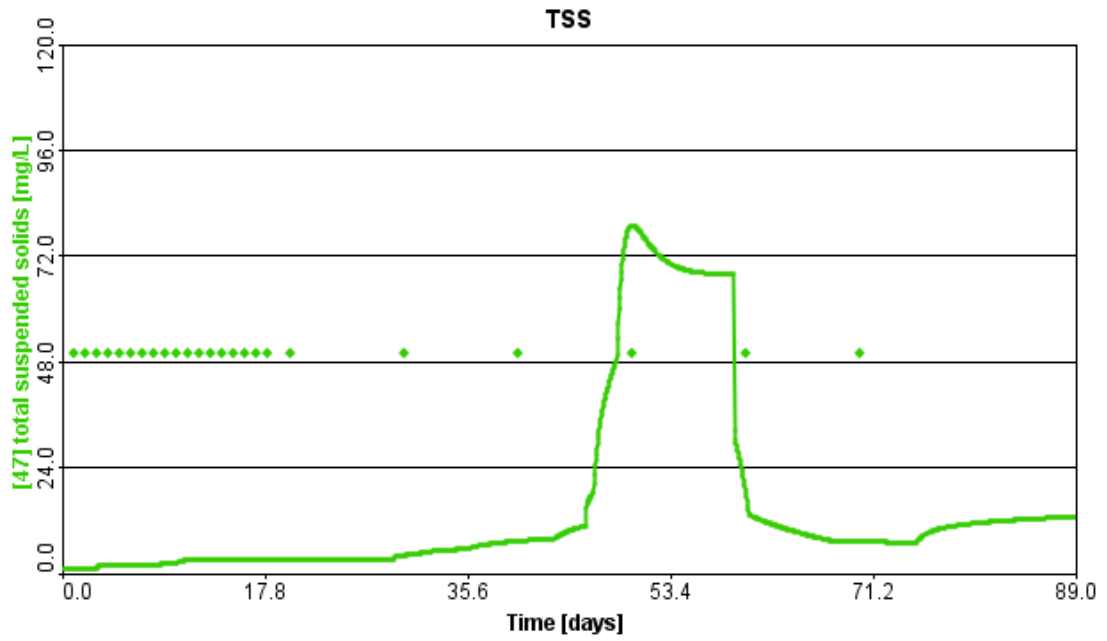
Effluent total COD, BoD, TSS and TN Vs. Influent Flow



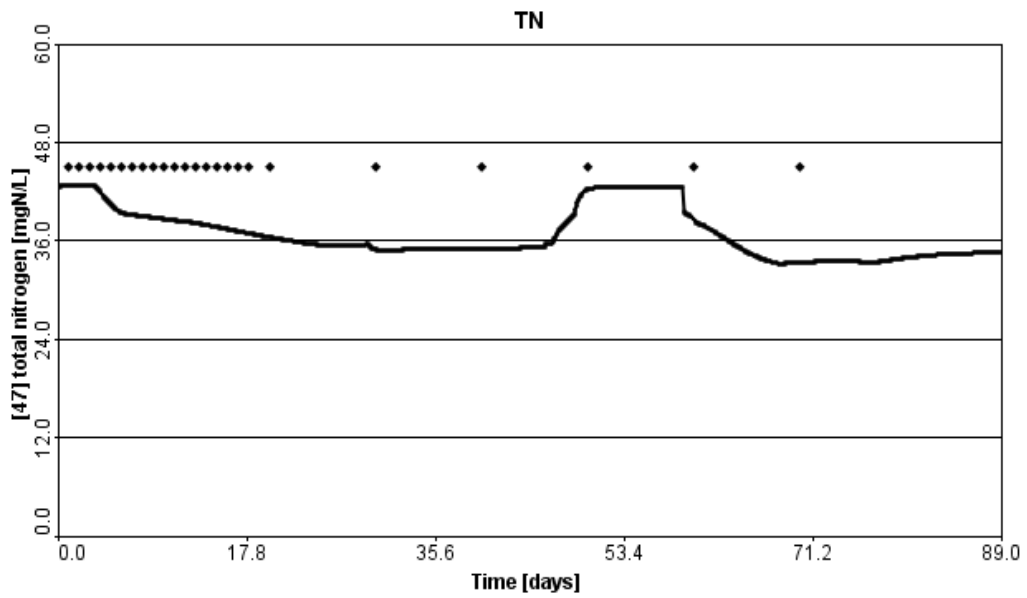
Effluent total cBOD Vs. Influent Flow



Effluent TSS Vs. Influent Flow

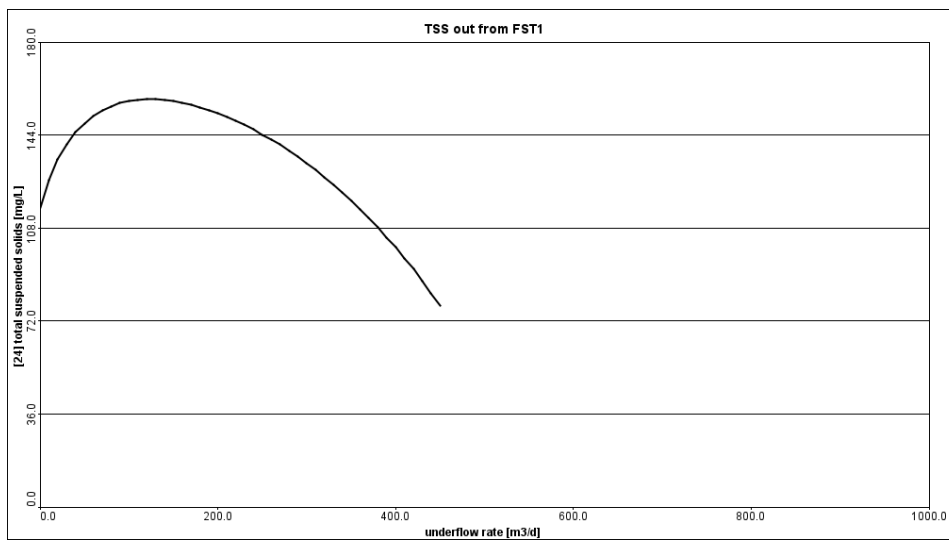
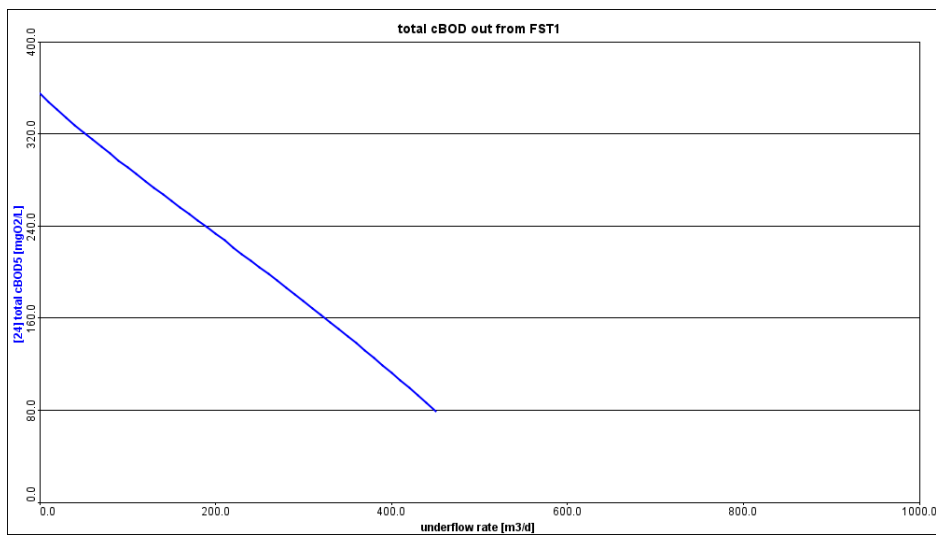
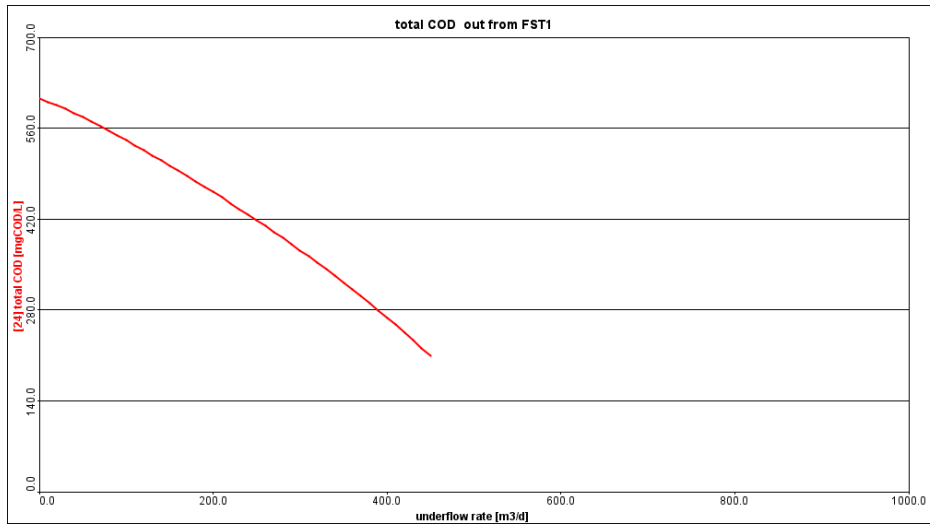


Effluent total TN Vs. Influent Flow



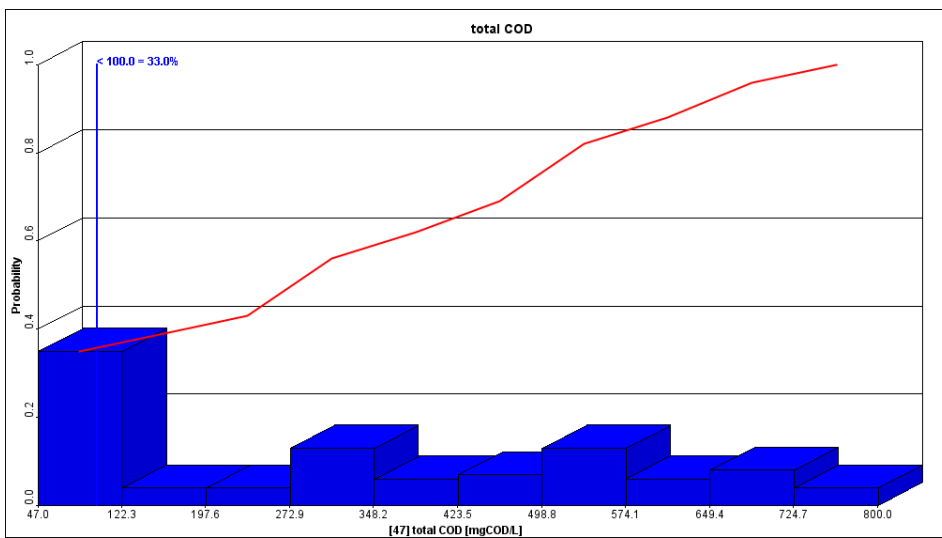
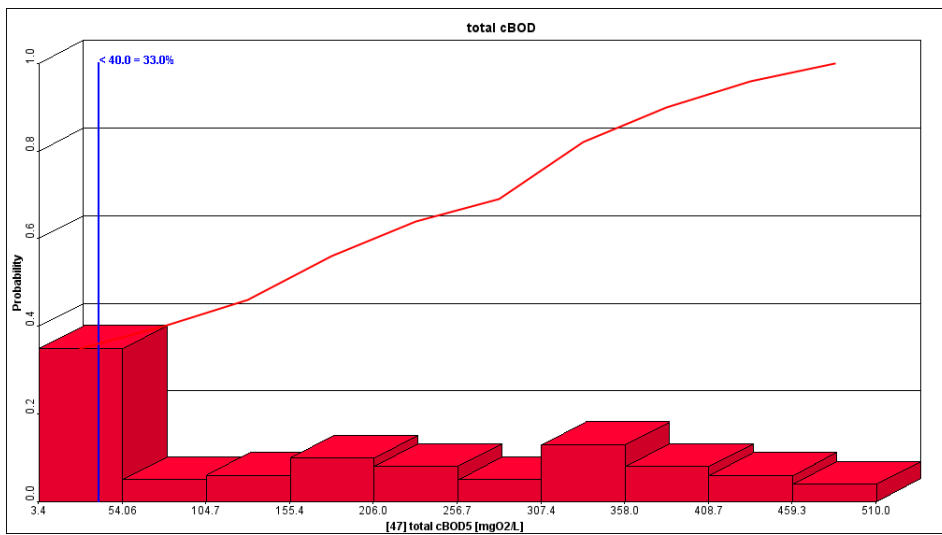
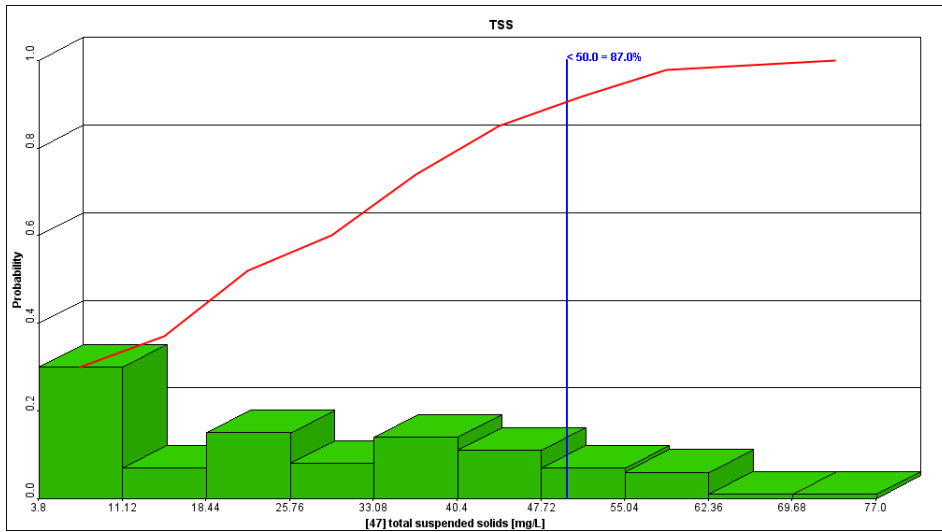
Appendix K

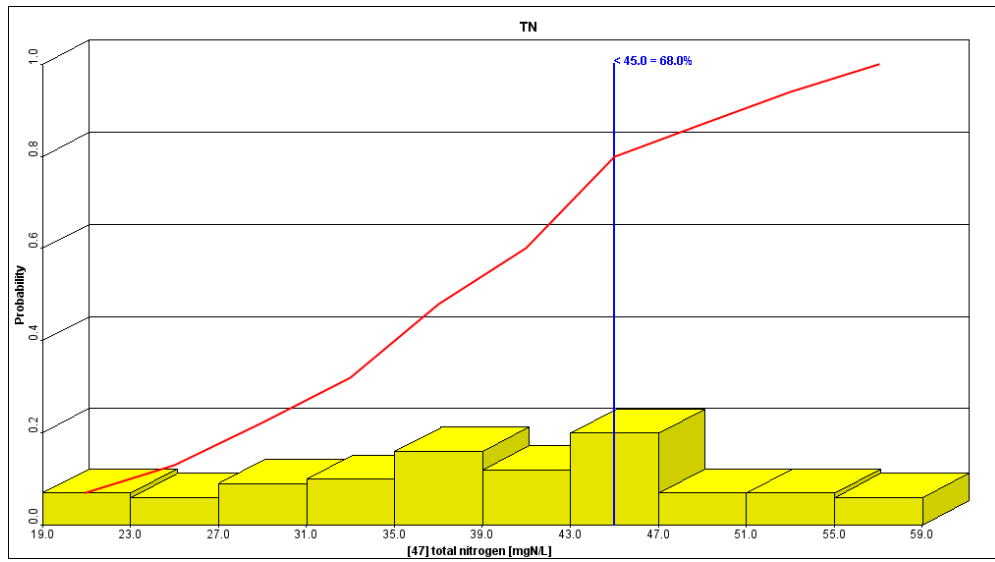
Optimizing the RAS Vs. Effluent pollutants



Appendix L

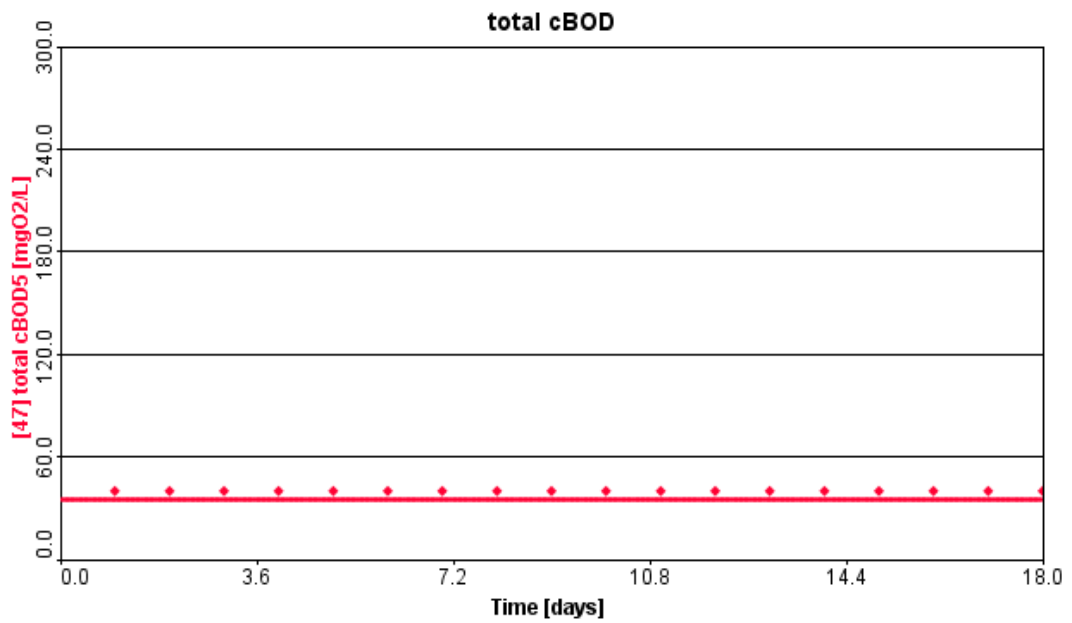
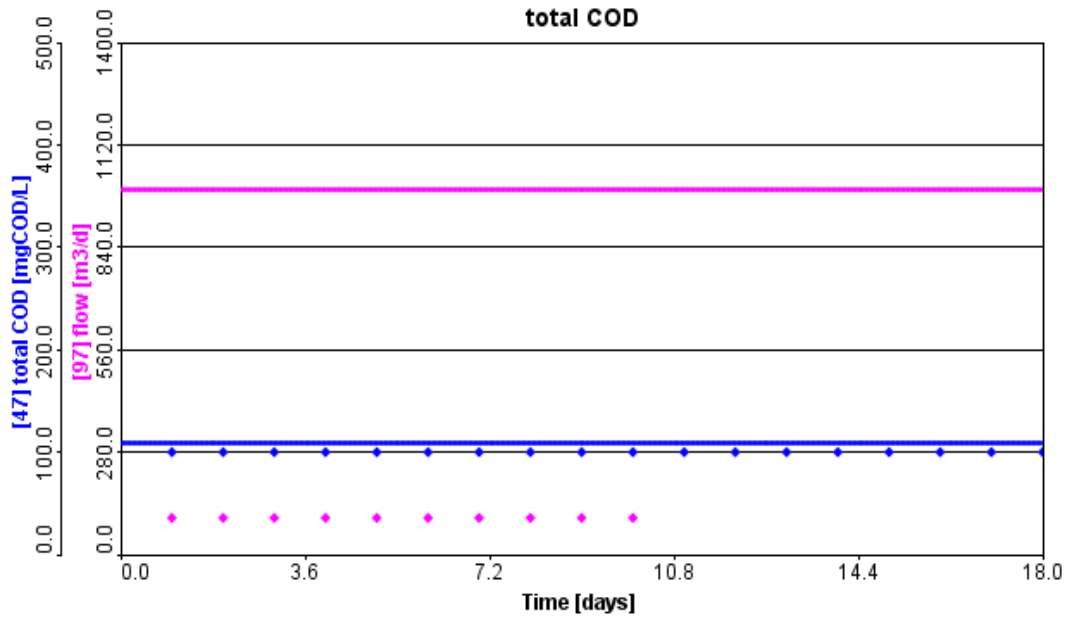
Monte Carlo probability Distribution of Effluent pollutants

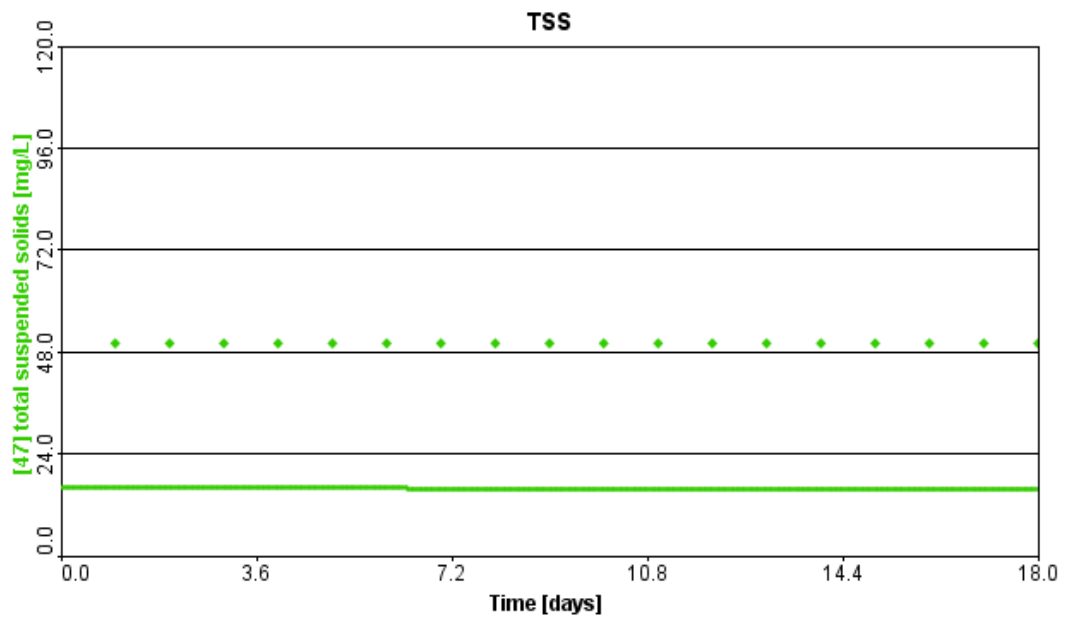
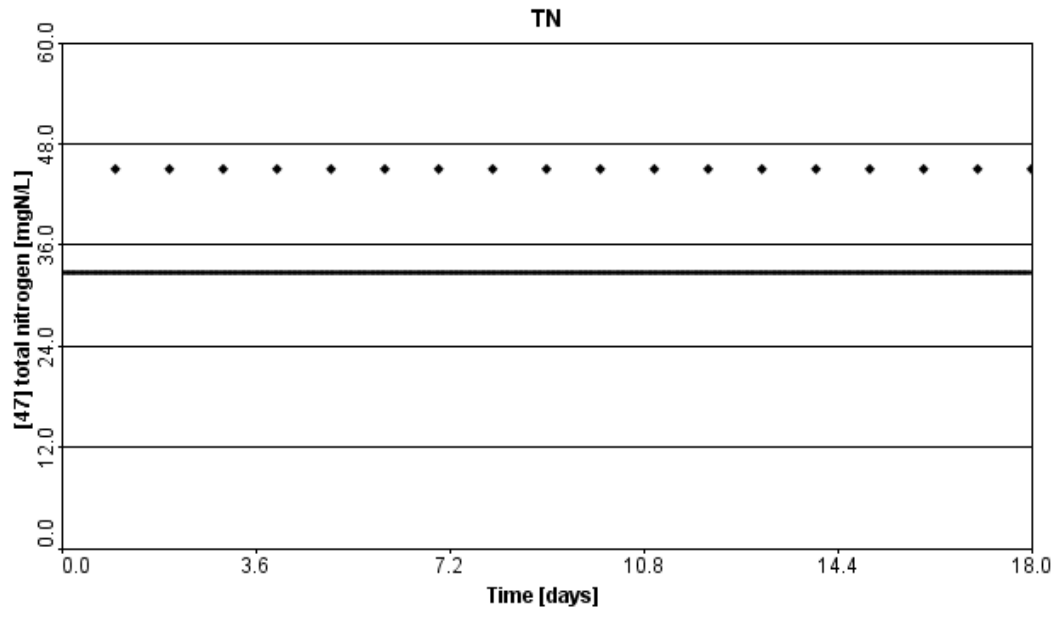




Appendix M

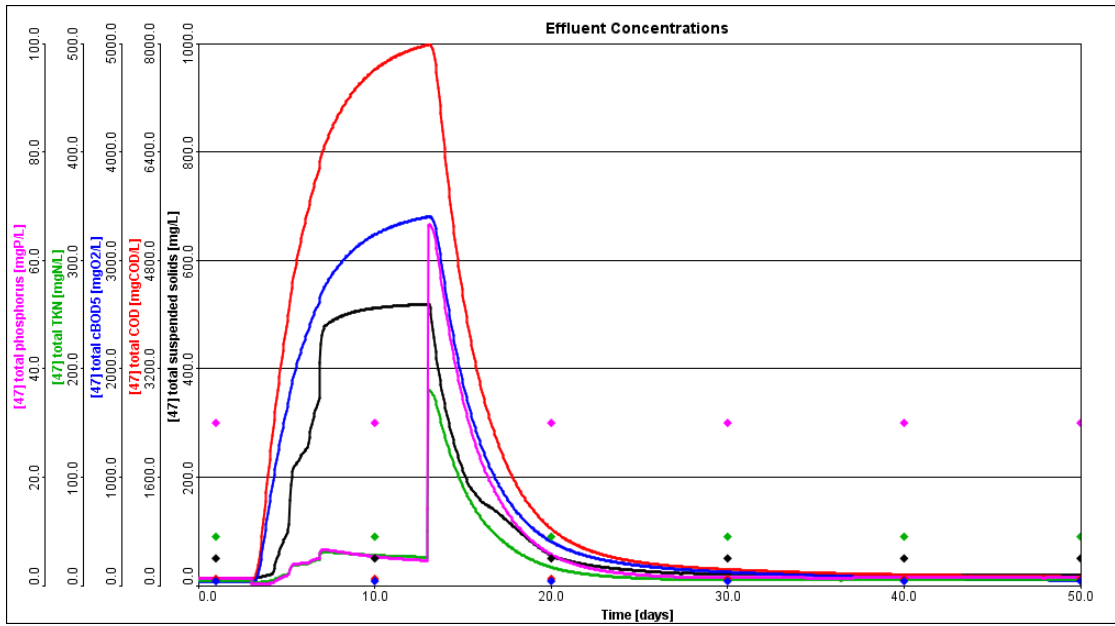
Optimized RAS and WAS Vs. Effluent pollutants





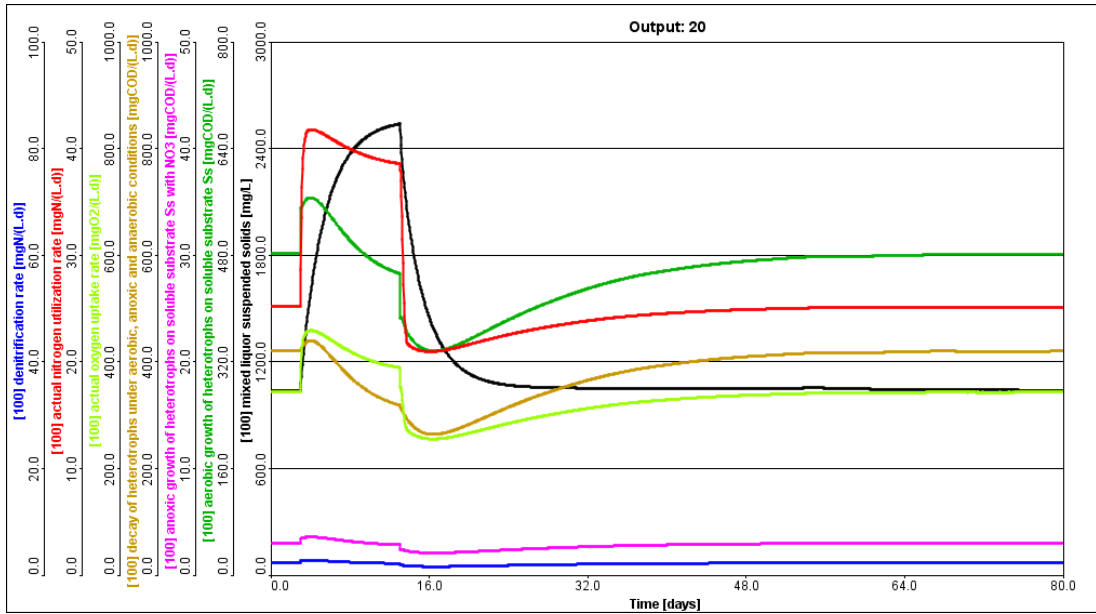
Appendix N

Effluent Concentrations during the Shock Load Scenario

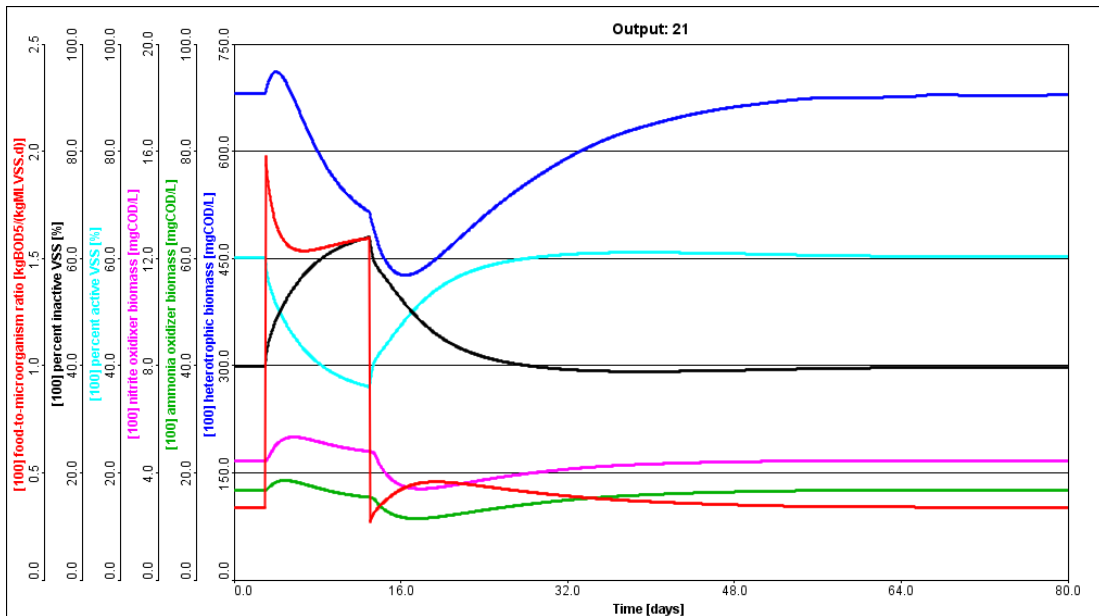


Appendix O

Time-Series Simulation of Biological Processes in an Extended Aeration Wastewater Treatment Plant

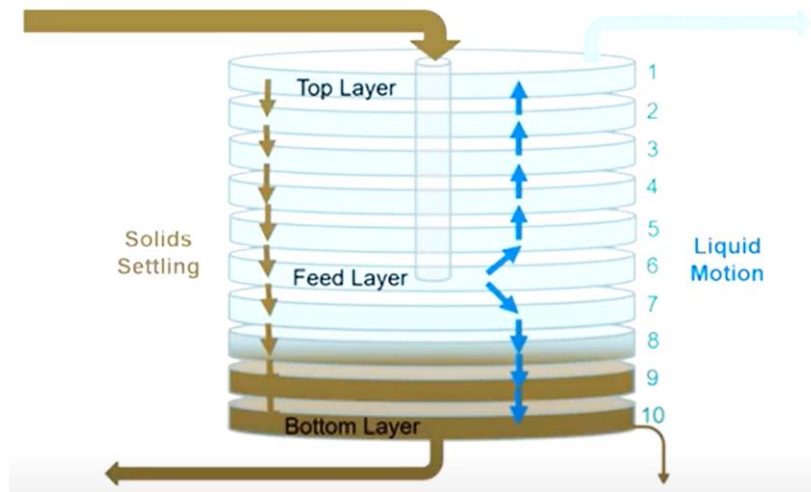


Dynamics of Biomass Fractions and Food-to-Microorganism Ratio in an Extended Aeration Wastewater Treatment System



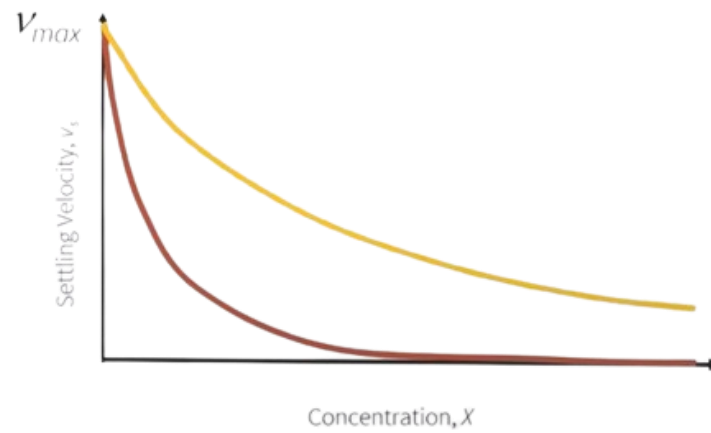
Appendix P

Mechanistic Clarifier Model - The 1-D Flux Model



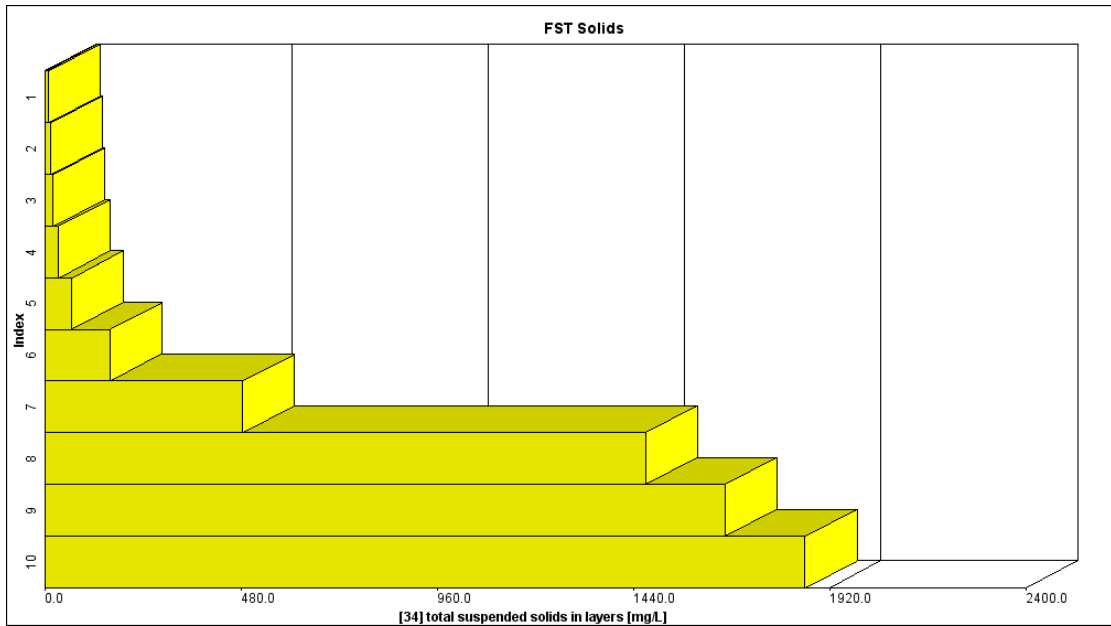
Double Exponential Model (Takacs et al., 1991)

$$v_s = v_{\{max\}} e^{\{-r_{\{hin\}} \cdot x\}} - v_{\{max\}} e^{\{-r_{\{floc\}} \cdot x\}} \quad \text{Equation 1}$$

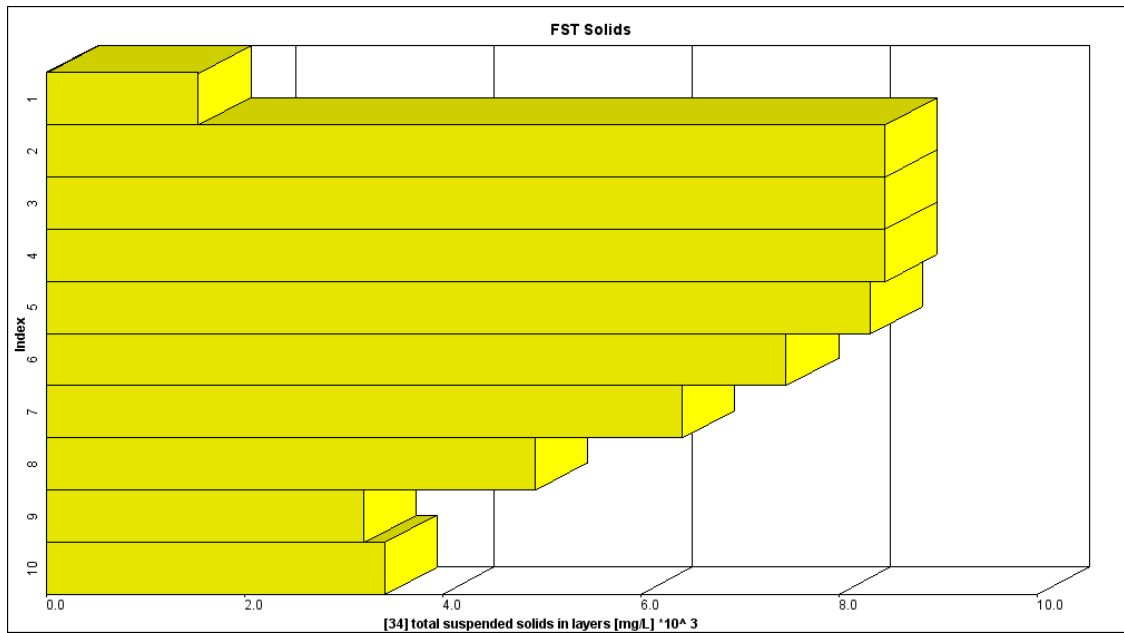


Appendix Q

Final Sedimentation Tank Solids Prior to and during the Shock Load

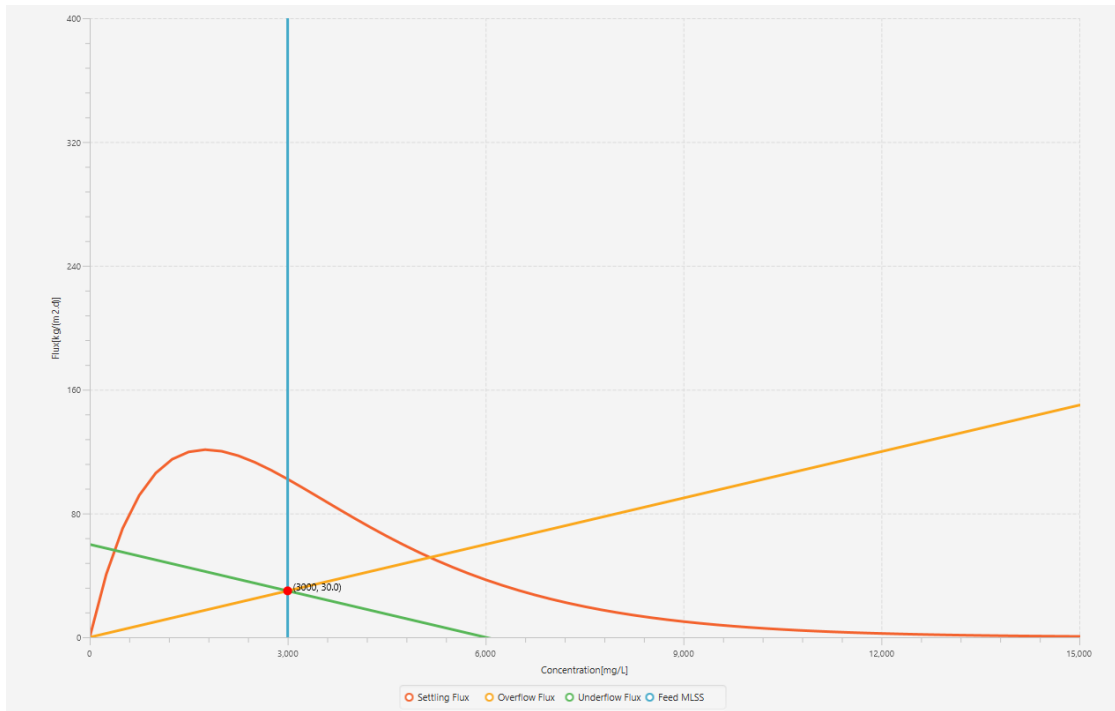


Final Sedimentation Tank Solids During the Shock Load

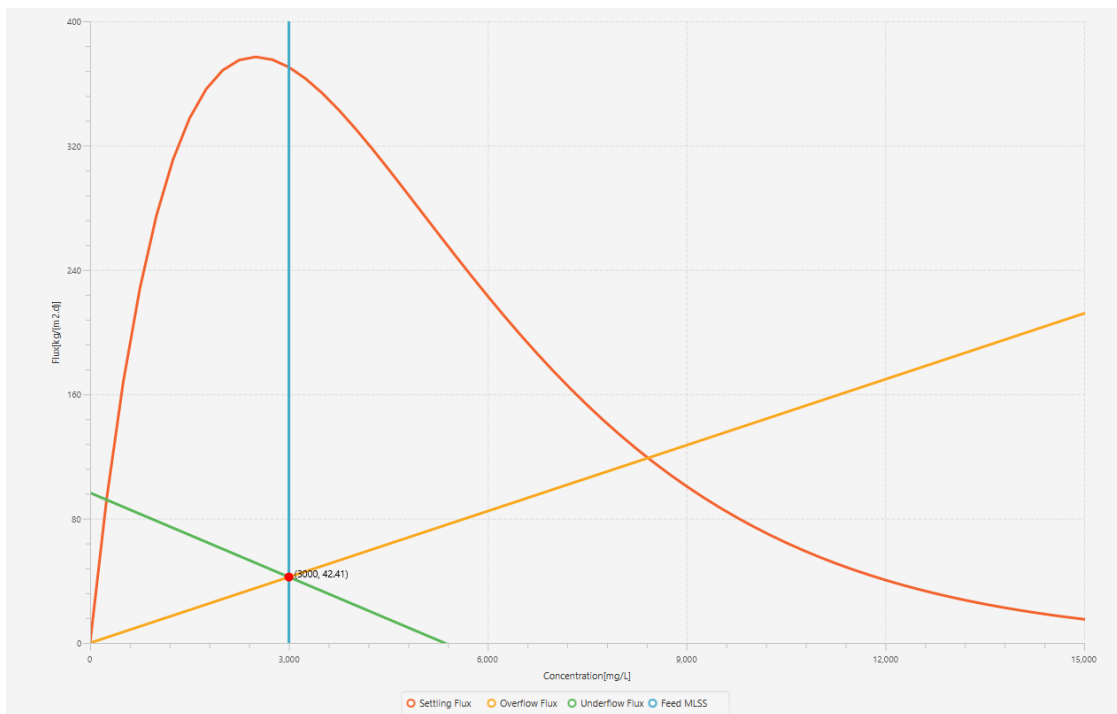


Appendix R

FST State Point Analysis prior to and during the Shock Load

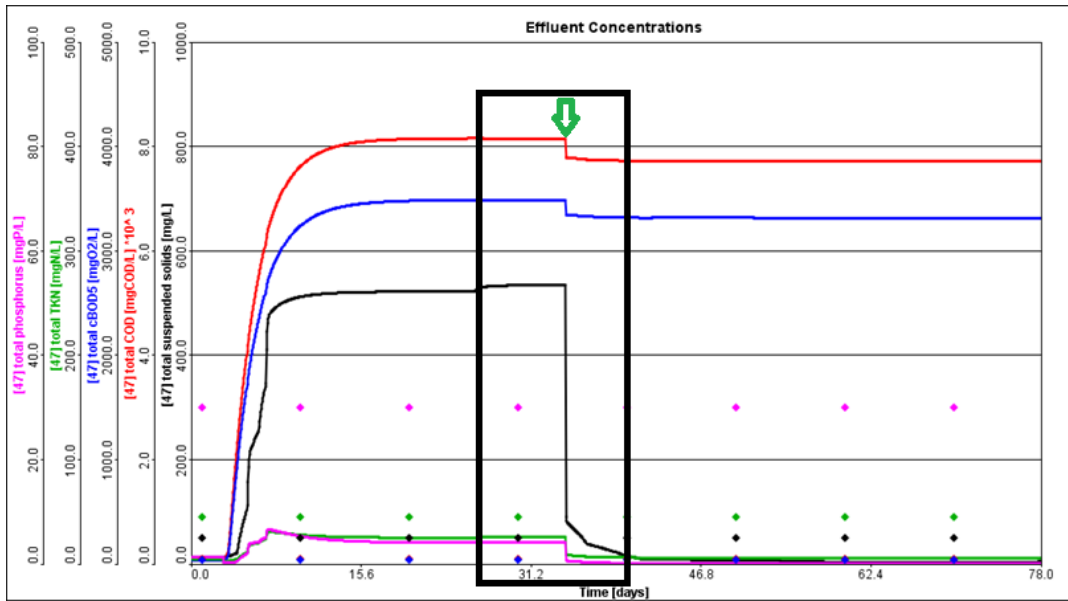


FST State Point Analysis During the Shock Load



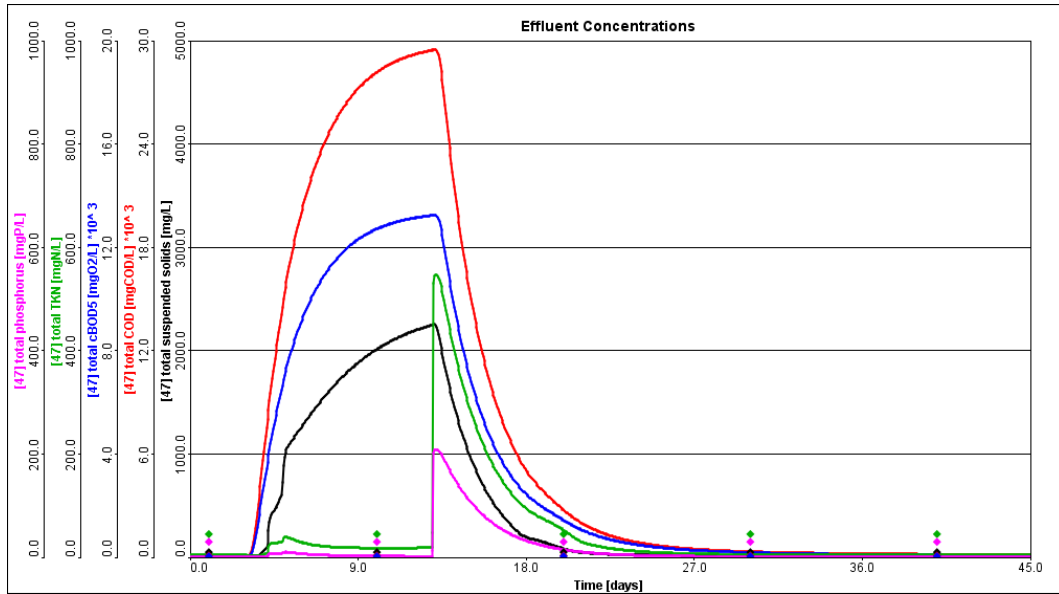
Appendix S

Effluent Concentration

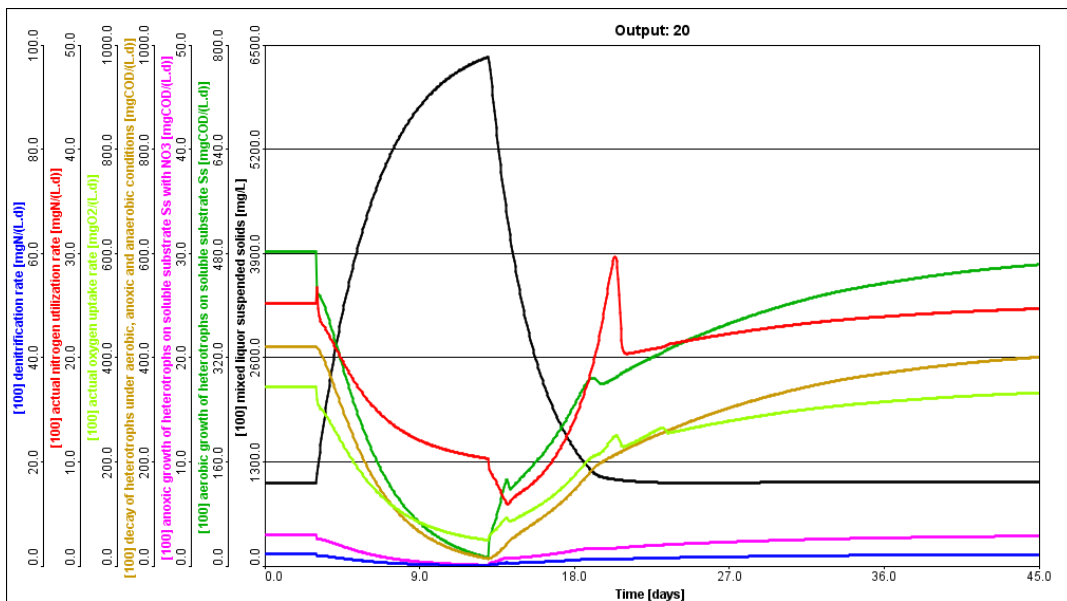


Appendix T

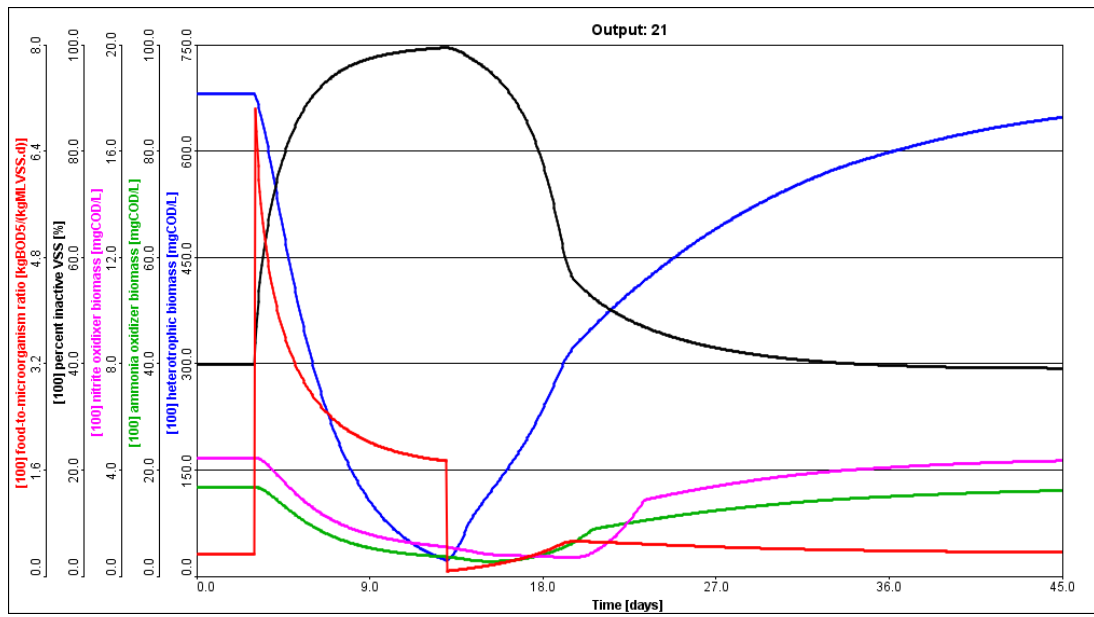
Effluent Concentration Analysis and WWTP's Recovery Scheme During the Shock load



Time-Series Simulation of Biological Processes During the Shock load

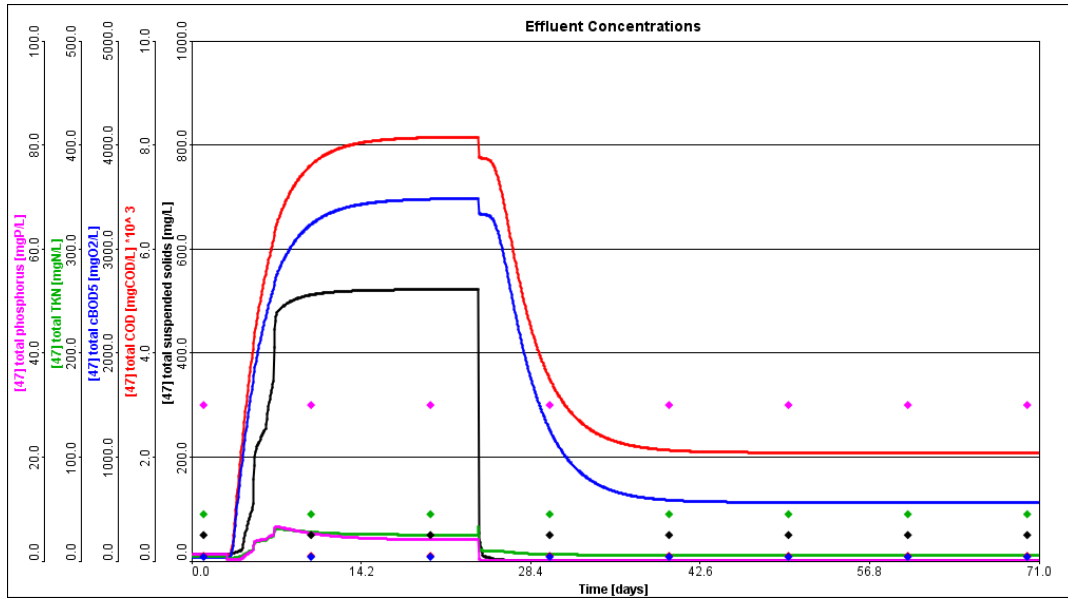


Dynamics of Biomass Fractions and Food-to-Microorganism Ratio during the shock load



Appendix U

Effluent Concentration Analysis and WWTP's Recovery Scheme During the Shock after removing the Energy Drink Process



Appendix V

Changes in Key Variables (Before vs. During Shock Load)

| Parameter | Before Shock Load | During Shock Load | Change |
|---|--------------------------|--------------------------|---------------|
| Influent TSS (mg/L) | 1047 | 2582 | 146% |
| Overflow TSS (mg/L) | 50.98 | 1659 | 3156% |
| Influent COD (mg/L) | 1305 | 9374 | 618% |
| Effluent COD (mg/L) | 151.6 | 8788 | 5700% |
| Ammonia-N (mg/L) | 0.3278 | 1.355 | 313% |
| Nitrite-N (mg/L) | 0.2605 | 81.9 | 31300% |
| Nitrate-N (mg/L) | 37.32 | 0.004 | -99.99% |
| Total Phosphorus (mg/L) | 21.92 | 11.31 | -48.40% |
| Total Alkalinity (mg CaCO₃/L) | 30.7 | 524.4 | 1600% |
| pH | 7.736 | 8.461 | 0.725 |

Appendix W

FST Variables Prior to the Occurrence of the Shock Load

| | Unit | FST Input | FST Overflow | WAS | RAS |
|---------------------|-------------------|----------------------|-------------------------|------------|------------|
| Flow | m ³ /d | 998.3 | 438.3 | 60.0 | 500.0 |
| TSS | mg/L | 1047 | 50.98 | 1827 | 1827 |
| VSS | mg/L | 792.0 | 38.56 | 1382 | 1382 |
| cBOD5 | mg/L | 442.2 | 49.22 | 749.7 | 749.7 |
| COD | mg/L | 1305 | 151.6 | 2207 | 2207 |
| Ammonia N | mgN/L | 0.3278 | 0.3278 | 0.3278 | 0.3278 |
| Nitrite N | mgN/L | 0.2605 | 0.2605 | 0.2605 | 0.2605 |
| Nitrate N | mgN/L | 37.32 | 37.32 | 37.32 | 37.32 |
| TKN | mgN/L | 82.05 | 7.529 | 140.4 | 140.4 |
| TN | mgN/L | 119.6 | 45.11 | 177.9 | 177.9 |
| Soluble PO4-P | mgP/L | 0.003754 | 0.003754 | 0.003754 | 0.003754 |
| TP | mgP/L | 21.92 | 2.06 | 37.47 | 37.47 |
| Total Alkalinity | mgCaCO3/L | 30.7 | 30.69 | 30.7 | 30.7 |
| pH | - | 7.736 | 7.736 | 7.736 | 7.736 |
| DO | mgO2/L | 10.14 | 10.14 | 0.0 | 0.0 |

FST Variables During the Occurrence of the Shock Load

| | Unit | FST Input | FST Overflow | WAS | RAS |
|---------------------|-------------------|-----------|-----------------|----------|----------|
| Flow | m ³ /d | 998.3 | 438.3 | 60.0 | 500.0 |
| TSS | mg/L | 2582 | 1659 | 3304 | 3304 |
| VSS | mg/L | 991.7 | 637.9 | 1269 | 1269 |
| cBOD5 | mg/L | 3730 | 3586 | 3843 | 3843 |
| COD | mg/L | 9374 | 8788 | 9833 | 9833 |
| Ammonia N | mgN/L | 1.355 | 1.353 | 1.355 | 1.355 |
| Nitrite N | mgN/L | 81.89 | 81.9 | 81.89 | 81.89 |
| Nitrate N | mgN/L | 0.004276 | 0.004017 | 0.004274 | 0.004274 |
| TKN | mgN/L | 68.55 | 45.97 | 86.25 | 86.25 |
| TN | mgN/L | 150.4 | 127.9 | 168.1 | 168.1 |
| Soluble PO4-P | mgP/L | 0.005745 | 0.005742 | 0.005745 | 0.005745 |
| TP | mgP/L | 11.31 | 7.281 | 14.47 | 14.47 |
| Total Alkalinity | mgCaCO3/L | 524.4 | 524.0 | 524.4 | 524.4 |
| pH | - | 8.461 | 8.46 | 8.461 | 8.461 |
| DO | mgO2/L | 10.14 | 10.14 | 0.0 | 0.0 |

Appendix X

Recommended Pre-treatment Processes for Various Industries

| Industry | Screening | Equalization | pH Adjustment | DAF | Anaerobic Digestion | Coagulation /Flocculation | Precipitation | Filtration |
|---------------------------|-----------|--------------|---------------|----------|---------------------|---------------------------|---------------|------------|
| Energy Drink Processing | Yes | Yes | Yes | Yes | Yes | No | No | No |
| Meat and Dairy Processing | Yes | Yes | Yes | Yes | Yes | No | No | No |
| Textile Industry | No | Yes | Yes | Optional | No | Yes | Optional | Yes |
| Tannery Industry | Yes | Yes | Yes | Optional | No | Yes | Yes | Optional |

Appendix Y

JIFZ-WWTP designed process

The wastewater treatment process is intermittent denitrification single sludge activated sludge process. The simultaneous aerobic sludge stabilization is performed inside the aeration tanks with a sludge age of 20 days .

The implementation of the WWTP is divided into two stages:

Stage 1: Mechanical and biological wastewater treatment, filtration, and sludge treatment.

Stage 2: Extension of biological treatment and addition of disinfection unit.

Stage one of the WWTP is currently implemented. The Stage-1 design allows and demonstrates possible future extension to the full Stage-2 capacity by logical special reservations.

The wastewater flows to Inlet Pumping Station, where it is lifted to obtain a free flow by gravity through the wastewater treatment plant. A manual basket screen is provided at the outlet of sewer to protect the inlet pumps.

The wastewater is initially conveyed to the Compact Mechanical Pre-Cleaning Unit (MPCU), which integrates components for fine screening, as well as grit and grease removal. Within this unit, fine solids are automatically extracted, cleansed, dewatered, and then discharged into a designated collection container. Grit is separated at this stage to minimize potential abrasion or damage to subsequent mechanical systems. Additionally, grease is skimmed from the surface to prevent operational issues and to mitigate the formation of foul odors associated with floating organic matter .

Separated grit will be transported to a container. Floating materials will be scrapped to an oil separation tank and then discharged to a container.

The design of mechanical pre-treatment unit has already been performed for Stage 2 design flow. After Compact Mechanical Pre-Cleaning Unit (MPCU), the wastewater is distributed into biological treatment units, which belong to Stage 1 and Stage 2. An automatic sampling device is installed in the distribution chamber.

Following its passage through the distribution chamber, the wastewater enters the activated sludge reactors. Within these aeration basins, the biodegradation of organic pollutants is facilitated by microbial populations that remain suspended in the liquid medium. These biological processes rely heavily on the continuous provision of oxygen to sustain microbial activity. The aeration tanks are designed to support multiple treatment functions simultaneously, including nitrification, denitrification, and the removal of organic carbon, all occurring within a single integrated reactor environment.

The aeration basins are engineered to facilitate both biological nitrogen removal and concurrent aerobic stabilization of the sludge. Oxygen required for these processes is introduced via membrane diffusers mounted at the base of the tanks, with air supplied by blowers. These blowers are regulated automatically using dissolved oxygen sensors, motorized control valves installed along the aeration pipelines, and oxidation-reduction potential (ORP) measurements. In scenarios where aeration is temporarily suspended, submersible mixers are utilized to maintain the suspension of activated sludge.

The mixture of activated sludge and treated water—referred to as mixed liquor—is then conveyed from the aeration tanks to the secondary clarifiers. Within these units, the solid-liquid separation process occurs through gravity-driven sedimentation. Treated effluent is collected from the upper surface through perforated weir pipes, while the settled sludge accumulates in conical hoppers at the bottom of the clarifiers. A portion of this concentrated sludge is recirculated to the aeration tanks to maintain an optimal biomass concentration essential for continued treatment efficiency. The rate of return sludge flow is adjusted proportionally to the influent wastewater rate. Any surface scum that forms during clarification is retained and subsequently transferred to the Sludge Storage Tank for further handling.

The clarified effluent flow is measured by an electromagnetic type flow measurement. The biologically treated wastewater is directed to the disc filter unit to apply post treatment to achieve discharge standards.

Treated effluent is used for service water and fire-fighting water needs. Inline UV disinfection is applied for service water disinfection.

Treated water is discharged to Wadi in Stage 1. In Stage 2, UV disinfection will be installed in already constructed concrete channels and disinfected effluent will be stored and used as irrigation purposes.

During the biological treatment process, microorganisms proliferate continuously, resulting in the generation of surplus biomass. This excess is referred to as waste activated sludge, which is extracted from the system once it exceeds the required concentration for process stability. The biologically stabilized sludge, treated aerobically within the aeration basins, is conveyed to the sludge storage tank through dedicated excess sludge pumps.

Within the sludge storage facility, the surplus sludge is temporarily held before undergoing a dewatering phase using a centrifugal decanter. Prior to dewatering, chemical conditioning is performed by adding cationic polyelectrolytes to enhance the separation efficiency. The resulting dewatered sludge is then transported to designated sludge containers via a screw conveyor. Meanwhile, the liquid by-product—known as centrate—produced during the dewatering process is redirected back to the plant's inlet pumping station for reprocessing.

This project is designed and executed for Stage 1 requirements with daily average wastewater flow of 1,000 m³/d. The final capacity of Stage 2 will be 2,000 m³/d and the design of WWTP lets this extension easily.

Wastewater treatment plant consists of following treatment units:

- Inlet pumping station,
- Compact Mechanical Pre-Cleaning Unit, including fine screen and grit and grease removal unit,
- Distribution Chamber for Stage 2 connection,
- Activated sludge tanks for carbon and nitrogen removal,
- Final sedimentation tanks,
- Disc filtration,

- Return and surplus sludge pumping station,
- Outflow measurement station,
- Service water storage tank,
- Service water station (including service water and fire-fighting water booster pumps and inline UV disinfection for service water),
- Sludge storage tank and pumping station,
- Sludge dewatering,
- Odour treatment plant.

Minimum wastewater design temperature is 15°C, while the maximum design temperature is 25°C.

Treatment Stages

Inlet Pumping Station

The inlet pumping station ensures gravity flow through the wastewater treatment plant (WWTP). It is equipped with two submersible centrifugal pumps (one duty, one standby) with frequency converters (capacity: 75 m³/h). A manual basket screen is installed for coarse material separation, and pump operation is controlled via water level measurements to minimize wear.

Mechanical Pre-Cleaning Unit (MPCU)

This unit removes fine particles, grit, and grease using a 6 mm perforated fine screen and a grit and grease chamber (capacity: 150 m³/h). The fine screen and aerated grit removal function as a compact unit, separating screenings, sand, and grease into different containers. A bypass pipe ensures flow continuity in case of failure.

Distribution Chamber (Stage 2 Connection)

Designed for equal distribution of wastewater between biological treatment units of both Stage 1 and Stage 2. No isolation equipment is needed for Stage 1, as a temporary wall extends the free fall weir for Stage 2.

Activated Sludge Tanks

Used for biological degradation of organic carbon and nitrogen, following an intermittent denitrification single sludge process. The system consists of two carousel-shaped activated sludge tanks with fine bubble aeration systems and air blowers, which operate in a duty/duty/standby configuration. Oxygen intake is automatically controlled via air control valves, O₂ meters, and ORP meters. The mixed liquor flows directly to the final sedimentation tanks.

Blower Building

Houses three root blowers (two duty, one standby) that supply oxygen for biological treatment. The fine bubble air diffusers maintain a minimum dissolved oxygen level of 2 mg/L. The intermittent denitrification process achieves nitrification and denitrification through alternating aeration and non-aeration cycles, allowing flexible operational control.

Final Sedimentation Tanks

This vertical flow (inverse cone) concrete tanks separate activated sludge from treated wastewater. Scum is collected and directed to sludge storage tanks. A center-feed well gently releases the mixed liquor for effective settling. The settled sludge is transferred to the return activated sludge and excess sludge pumping station, while the clarified effluent is filtered before discharge.

Return Activated and Surplus Sludge Pumping Station

Manages recirculation of return activated sludge to the aeration tanks and pumping excess sludge to sludge treatment units. Submersible centrifugal pumps (with frequency converters) operate in an automated sequence based on wastewater flow. An ultrasonic level measurement prevents dry running.

Outlet Flow Measurement

Treated water flow is monitored using an electromagnetic flow meter connected to a SCADA system for automated control. Automatic sampling devices ensure compliance with effluent quality standards.

Disc Filter

Used for micro-screening (10-micron filter size) to enhance water quality before UV disinfection. High- and low-level sensors prevent clogging, and a backwash system ensures continuous operation.

Disinfection (Stage 2)

A UV disinfection unit will be implemented in Stage 2 for treated wastewater effluent. Infrastructure is already prepared for future installation.

Effluent Quality Control

Includes automatic sampling, pH, and temperature measurements to monitor treatment efficiency. Composite 24-hour samples are collected downstream of the discharge point.

Sludge Storage Tank

Balances sludge withdrawal and dewatering operations. A circular concrete tank with a submersible mixer prevents sludge settling. The sludge retention time is five days, and dewatering is performed five days per week, six hours per day.

Sludge Dewatering

A centrifugal decanter increases sludge solids content. The system includes:

- Dewatering centrifuge feed pumps
- Polyelectrolyte preparation and dosing units
- Sludge conveyor with a reversible screw mechanism for sequential container filling
- Polyelectrolyte preparation can be adjusted for Stage 2 if needed.

Odor Treatment Unit

A biofilter system removes odors from the inlet pumping station, pre-cleaning unit, and sludge dewatering process. The air is first pre-scrubbed and then treated using biological degradation before being discharged into the atmosphere.

Treated Effluent Storage Tank and Pumping Station (Stage 2)

This unit will temporarily store water treated for irrigation. It includes submersible effluent pumps and an above-ground storage tank (500 m³ capacity).

Chemical Dosing for PO₄ Precipitation (Stage 2)

Phosphorus removal through chemical precipitation will be implemented in Stage 2, with automatic control based on real-time phosphorus measurements.

Appendix Z

Types of Clarifiers in GPS-X

| Model Name | Volume | Model Details |
|------------------------------|----------------------------|---|
| Point | Zero-volume | "Perfect" settler model |
| Empiric | Zero-volume | User sets capture rate (%) |
| WEF-TSS-SOR / TSS-SOR-SLR | Zero-volume | Capture rates (%) determined from empirical model based on flow rate and/or loading |
| Simple1d (Noreact1d) | User sets shape and volume | Full 1-dimensional flux settling model (default model choice) |
| Mantis2 | User sets shape and volume | Simple1d Model + biological and chemical reactions |



جامعة النجاح الوطنية
كلية الدراسات العليا

نمذجة وتقييم تأثيرات المياه العادمة الصناعية على محطة معالجة المياه
العادمة في منطقة جنين الصناعية الحرة

اعداد

أسامة حربي مصطفى عمران

اشراف

د. عبد الحليم خضر

قدمت هذه الأطروحة استكمالاً لمتطلبات الحصول على درجة الماجستير في هندسة المياه والبيئة، من كلية الدراسات العليا في جامعة النجاح الوطنية في نابلس، فلسطين

2025

نمذجة وتقييم تأثيرات المياه العادمة الصناعية على محطة معالجة المياه العادمة في منطقة جنين الصناعية الحرة

اعداد

أسامة حربي مصطفى عمران

اشراف

د. عبد الحلیم خضر

المخلص

محطة معالجة مياه الصرف الصحي في المنطقة الصناعية الحرة في جنين (JIFZ-WWTP)، المصممة أساساً لمعالجة مياه الصرف المنزلي، قد تواجه تحديات بسبب التدفقات الصناعية غير المنتظمة، مما يؤثر على عمليات المعالجة البيولوجية وجودة المياه المعالجة. تقيم هذه الدراسة أداء المحطة باستخدام نموذج محاكاة ديناميكي في برنامج GPS-X (الإصدار 8.5) مع إطار عمل MANTIS المعتمد على ASMI تمت معايرة النموذج ببيانات 2024 من محطة معالجة مياه الصرف في أريحا، مع تعديلات لدرجة الحرارة المحلية، الارتفاع، وخصائص التدفق الوارد لتعكس سلوك الكائنات الحية الدقيقة وديناميكيات الأكسجين في جنين.

شملت المحاكاة العمليات العادية، السيناريوهات عالية التحميل، وحدث صدمة بتدفق 1000 م³ من مياه الصرف الصناعي غير المعالجة. في الظروف المثلى، حققت المحطة كفاءة إزالة عالية TSS (95.18%)، VSS (93.62%)، COD (89.5%)، cBOD₅ (94.32%)، PO₄³⁻ (99.88%)، وTP (66.45%)، مع قيود بسبب الفوسفور المرتبط بالجسيمات. كانت إزالة النيتروجين الكلي (TN) أقل (33.8%) بسبب نقص الظروف اللاهوائية ومحدودية توافر الكربون. تشمل التوصيات إضافة مفاعل لاهوائي، جرعات كربون خارجية (مثل الميثانول)، وتحسين زمن احتجاز المواد الصلبة.

حافظت المحطة على جودة مياه معالجة القابلة لاعادة الاستخدام الزراعي من الفئة C عند تدفقات تصل إلى 1000 م³/يوم من مياه الصرف الصناعي من خلال تنظيم تدفق الحمأة المعادة (RAS) بمعدل 460 م³/يوم والحمأة المهذرة (WAS) بمعدل 60 م³/يوم، مما يضمن الاستقرار تحت الأحمال القصوى. أظهرت محاكاة مونت كارلو أن 68% من السيناريوهات حققت ازالة النيتروجين، 33% حققت معايير cBOD_s و COD، و87% حققت معايير TSS، مما يشير إلى حساسية لتغيرات التدفقات الصناعية.

كشف سيناريو الحمل الصدمي عن نقاط ضعف، حيث تجاوزت تركيزات المياه المعالجة (COD: 8000 ملغ/لتر، BOD_s: 3500 ملغ/لتر، TP: 63 ملغ/لتر، TKN: 37 ملغ/لتر، TSS: 510 ملغ/لتر) الحدود التنظيمية الفلسطينية. انخفضت نشاط الكتلة الحيوية، توقفت النتجة، وتراكمت المواد الصلبة، مع تعافي تدريجي لاحقاً. توصي الدراسة بمعايير معالجة مسبقة صارمة (الفرز، تصحيح الأس الهيدروجيني، التسوية، التعويم بالهواء المذاب، الهضم اللاهوائي، التخثر، التلبد، الترسيب، الترشيح) ومراقبة التدفقات الواردة لحماية المحطة. تدعم المحطة إدارة المياه المستدامة في جنين من خلال إعادة استخدام المياه المعالجة للري الزراعي، كذلك التحديات المالية، بما في ذلك خصم إسرائيل السنوي بحوالي 100 مليون شيكل من إيرادات السلطة الفلسطينية بسبب المياه العادمة.

الكلمات المفتاحية: منطقة جنين الصناعية الحرة (JIFZ)، المياه العادمة الصناعية، برنامج محاكاة GPS-X، تحليل الحساسية مونت كارلو، الكتلة الحيوية الهيتروتروفية.